ANL/ES-CEN-1018
and
FE-1780-6

ANL/ES-CEN-1018
and
FE-1780-6

SUPPORTIVE STUDIES IN FLUIDIZED-BED COMBUSTION

Quarterly Report
October–December 1976

by

G. J. Vogel, I. Johnson, S. H. Lee, J. F. Lenc,
A. S. Lescarret, J. Montagna, F. F. Nunes, J. A. Shearer,
R. B. Snyder, G. W. Smith, W. M. Swift, F. G. Teats
C. B. Turner, W. I. Wilson, and A. A. Jonke

U of C-AUA-USERDA

ARGONNE NATIONAL LABORATORY, ARGONNE, ILLINOIS

Prepared for the U. S. ENERGY RESEARCH
AND DEVELOPMENT ADMINISTRATION
under Contract W-31-109-Eng-38

DISCLAIMER

The facilities of Argonne National Laboratory are owned by the United States Government. Under the terms of a contract (W-31-109-Eng-38) between the U. S. Energy Research and Development Administration, Argonne Universities Association and The University of Chicago, the University employs the staff and operates the Laboratory in accordance with policies and programs formulated, approved and reviewed by the Association.

MEMBERS OF ARGONNE UNIVERSITIES ASSOCIATION

The University of Arizona
Carnegie-Mellon University
Case Western Reserve University
The University of Chicago
University of Cincinnati
Illinois Institute of Technology
University of Illinois
Indiana University
Iowa State University
The University of Iowa
Kansas State University
The University of Kansas
Loyola University
Marquette University
Michigan State University
The University of Michigan
University of Minnesota
University of Missouri
Northwestern University
University of Notre Dame
The Ohio State University
Ohio University
The Pennsylvania State University
Purdue University
Saint Louis University
Southern Illinois University
The University of Texas at Austin
Washington University
Wayne State University
The University of Wisconsin

Printed in the United States of America
Available from
National Technical Information Service
U. S. Department of Commerce
5285 Port Royal Road
Springfield, Virginia 22161
Price: Printed Copy $5.00; Microfiche $3.00

ANL/ES-CEN-1018 and
FE-1780-6
Coal Conversion and Utilization—
Direct Combustion of Coal
(UC-90e)

ARGONNE NATIONAL LABORATORY
9700 South Cass Avenue
Argonne, Illinois 60439

SUPPORTIVE STUDIES IN FLUIDIZED-BED COMBUSTION

Quarterly Report
October—December 1976

by

G. J. Vogel, I. Johnson, S. H. Lee, J. F. Lenc,
A. S. Lescarret, J. Montagna, F. F. Nunes, J. A. Shearer,
R. B. Snyder, G. W. Smith, W. M. Swift, F. G. Teats,
C. B. Turner, W. I. Wilson, and A. A. Jonke

Chemical Engineering Division

Prepared for the
U. S. Energy Research and Development Administration
under Contract No. W-31-109-Eng-38

and the

U. S. Environmental Protection Agency
under Agreement IAG-D5-E681

Preceding Reports in This Series

ANL/ES-CEN-1016
ANL/ES-CEN-1017

BIBLIOGRAPHIC DATA SHEET	1. Report No. ANL/ES-CEN-1018	2.	3. Recipient's Accession No. FE-1780-6
4. Title and Subtitle Supportive Studies in Fluidized Bed Combustion			5. Report Date February 1977 6.
7. Author(s) G. J. Vogel et al.			8. Performing Organization Rept. No. ANL/ES-CEN-1018
9. Performing Organization Name and Address Argonne National Laboratory 9700 South Cass Avenue Argonne, Illinois 60439			10. Project/Task/Work Unit No. 11. Contract/Grant No. W31-109-ENG-38 (ERDA) IAG-D5-E681 (EPA)
12. Sponsoring Organization Name and Address U.S. Energy Research and Development Administration and the U.S. Environmental Protection Agency			13. Type of Report & Period Covered Quarterly Oct. 1 - Dec. 31, 1976 14.
15. Supplementary Notes			

16. Abstracts A development program on pressurized fluidized-bed combustion is being carried out in a bench-scale pilot plant capable of operating at 10-atm pressure. The concept involves burning fuels such as coal in a fluidized bed of particulate lime additive that reacts with the sulfur compounds formed during combustion to reduce air pollution. Nitrogen oxide emissions are also reduced at the combustion temperatures used, which are lower than those used in a conventional coal combustor. The $CaSO_4$ produced in the combustor is regenerated to CaO that is recycled to the combustor for further removal of sulfur compounds.

This report presents information on: a 10-cycle combustion-regeneration experiment, an alternative regeneration process, preparation of synthetic SO_2-sorbents containing metal oxides, limestone characterization, studies of the enhancement of the sulfation of limestone by NaCl, and flue-gas-particulate cleaning studies.

17. Key Words and Document Analysis. 17a. Descriptors

Additives
Air Pollution
Aluminum Oxide
Bauxite
Calcite
Calcium Carbonate
Calcium Chloride
Calcium Oxide
Calcium Sulfate
Calcium Sulfide
Coal
Cold Traps
Combustion
Desulfurization
Dolomite
Flue Gas
Fluidized-Bed Processing
Fossil Fuel
Fragmentation
Limestone
Roasting
Sodium Carbonate
Sodium Chloride
Sodium Sulfate
Sorbents
Sulfur Oxide
X-Ray Diffraction

17b. Identifiers/Open-Ended Terms

Air Pollution
Flue Gas Cleaning
Fluidized-Bed Combustion
Sorbent Regeneration
Stationary Sources
Supported Additives

17c. COSATI Field/Group 13B

18. Availability Statement	19. Security Class (This Report) UNCLASSIFIED	21. No. of Pages
	20. Security Class (This Page UNCLASSIFIED	22. Price

TABLE OF CONTENTS

LIST OF FIGURES

LIST OF FIGURES (Contd.)

LIST OF FIGURES (Contd.)

LIST OF TABLES

SUPPORTIVE STUDIES IN FLUIDIZED BED COMBUSTION

Quarterly Report

G. J. Vogel, I. Johnson, S. Lee, J. Lenc, A. Lescarret, J. Montagna, F. Nunes, J. Shearer, R. Snyder, G. Smith, W. Swift, F. G. Teats, C. Turner, I. Wilson, and A. A. Jonke

ABSTRACT

A development program on pressurized fluidized-bed combustion is being carried out in a process demonstration unit capable of operating at 10-atm pressure. The concept involves burning fuels such as coal in a fluidized bed of particulate lime additive that reacts with the sulfur compounds formed during combustion to reduce air pollution. The $CaSO_4$ can be regenerated to CaO that is recycled to the combustor for further removal of sulfur compounds.

This report presents information on: a 10-cycle combustion-regeneration experiment, an alternative regeneration process, preparation of synthetic SO_2-sorbents containing metal oxides, limestone characterization, studies of the enhancement of the sulfation of limestone by NaCl, and flue-gas particulate cleaning studies.

SUMMARY

Task A. Regeneration Process Development

Cyclic Combustion-Regeneration Experiments with Tymochtee Dolomite. The effect of repeated utilization cycles on the performance of Tymochtee dolomite as an SO_2-acceptor is being evaluated in a ten-cycle (combustion-regeneration) experiment. All ten cycles have been completed. Extent of regeneration remained at acceptable levels for all ten cycles, and SO_2 concentrations in the dry off-gas measured ~8 1/2% up to and including cycle 7. In the last three cycles, the SO_2 concentration upon regeneration was <7% because of the lower sulfur content of the sulfated sorbent fed to the regenerator. During sulfation, the sorbent exhibited a steady loss in reactivity with increasing utilization cycle.

After ten utilization cycles, ~13 g of coal ash had accumulated with the sorbent for every 100 g of starting virgin dolomite. Photomicrographs of sample particles from different cycles revealed the formation of shells (possibly coal ash) on the dolomite particles. Also, the porosity of regenerated dolomite decreased with cyclic use as did its capacity to act as an SO_2-acceptor during combustion. The loss of porosity and reactivity towards

SO_2 could be due to (1) the buildup of an ash layer around the particles or (2) high-temperature (1100°C) exposure during regeneration. Sintering, which begins to occur at the regeneration temperature, decreases the reactivity by decreasing the beneficial effect of porosity.

Over ten cycles, sorbent losses during each regeneration cycle have averaged a relatively low 2% of the material fed. The combined losses due to attrition and/or elutriation have been found to be ∿8% per complete cycle of combustion and regeneration. This is the minimum expected makeup rate for Tymochtee dolomite in an FBC process utilizing sorbent regeneration at the operating conditions used in these tests. A higher makeup rate may be required to maintain sufficient reactivity in the recycled sorbent.

The results of TGA sulfation experiments on samples of regenerated sorbent from the ten regeneration half-cycle experiments are presented. Except for an unexplained discrepancy in the TGA data for the fourth sulfation, both the rate of conversion and the extent of conversion decreased with sulfation cycle. There did appear to be a leveling-off of the data after the eighth cycle, however.

The carbonate level of sulfated and regenerated samples is also presented. It further indicates the decrease in reactivity of the sorbent during combustion. The extent of recarbonation steadily decreases as does the extent of sulfation with increasing utilization cycle.

An analysis is presented of the sorbent makeup requirements, the ratio of makeup to makeup plus recycle CaO, for a continuous combustion-regeneration cyclic process. It is estimated that a CaO/S makeup ratio as low as ∿0.2 may be sufficient to meet the EPA sulfur emission limit as compared with a CaO/S mole ratio of 0.93 estimated for once-through operation; recycle with 0.2 makeup would represent an estimated raw material (sorbent) savings of ∿78%.

Task B. Regeneration Process Alternatives

The objective of this task is to investigate various methods for the regeneration of sulfated limestone so that the stone can be reused for SO_2 sorption in FBC and the sulfur converted to either a useful or a nonpolluting product. The current work is directed toward the evaluation of the $CaSO_4$-CaS "solid-solid" regeneration method. In this method, sulfated limestone (or dolomite) is first partially reduced to give a mixture of $CaSO_4$ and CaS. This mixture is then heated to a higher temperature where a reaction to form CaO and SO_2 occurs. This method has the potential advantage over the single-step regeneration scheme (reported in Task A) of yielding a product gas containing a higher concentration of SO_2 and essentially no other reactive gases. This would reduce the cost of converting the SO_2 to either sulfur or sulfuric acid.

During this report period, the results for the first attempts to carry out the reduction in a laboratory-scale fixed-bed reactor (at 800°C) became available. Significant conversion of $CaSO_4$ to CaS was achieved. Good sulfur

and calcium material balances indicate that solid-solid reaction was negligible at this temperature.

Task C. Synthetic Sorbents for SO_2 Emission Control

Synthetic sorbents for the control of SO_2 emission from fluidized-bed combustors are being evaluated for use in place of naturally occurring limestone or dolomite. It is hoped that synthetic sorbents can be developed which can be used for a larger number of cycles in the combustor than can natural stones, thereby significantly reducing the quantity of sorbent waste. A reduction of the quantity of sorbent waste will reduce the environmental impact of both the quarrying and disposal of sorbent.

An estimate has been made of the probable energy cost of using synthetic sorbents for SO_2 emission control. The most important parameter is found to be the cost of the synthetic sorbent. It is shown that if the equivalent of twenty-five cycles in the combustor can be achieved, then a synthetic sorbent costing about $200 per ton is cost competitive with a process in which a natural stone is recycled. The environmental impact of the synthetic sorbent, as measured by the quantity of waste, would be about one-fifth that of natural stones. It is estimated that the synthetic sorbent currently available could be made for about $300 per ton. The energy cost for this sorbent would be about one mill/kWh greater than the cost for natural sorbent (with recycle).

Task D. Limestone Characterization

The objective of this task is to characterize the behavior of different limestones and dolomites as SO_2 sorbents for use in FBC. It is hoped that the physical and chemical properties of various stones can be correlated with their reactivity under FBC operating conditions. In addition to a cataloging of the results reported for various limestones, an attempt will be made to determine why stones behave as they do. This will be facilitated by a model for the process whereby the sulfur in the fuel is captured by the stone under fluidized-bed combustion conditions.

During the present report period, the effect of precalcination of a limestone on its capacity to sorb SO_2 has been under study, using a TGA apparatus. Tests with Greer limestone indicated that the SO_2 capacity (as measured on the TGA) was nearly doubled by precalcination and heat treatment. An estimate was made of the cost of introducing a precalcination-heat treatment step into a fluidized-bed combustion system. Costs of the order of 1 to 1.5 mills/kWh are indicated to reduce the quantity of waste to about 0.6 (*i.e.*, a 40% reduction).

Task E. Trace Elements and Combustion Emission Studies

Limestone SO_2 Reactivity Enhancement. The objective of these studies is to determine whether chemical additives can be used to enhance the SO_2 capacity of limestone in a practical fluidized-bed combustion system. The use of such

additives would decrease the quantity of waste sorbent and thereby decrease the environmental impact. It was discovered by Pope, Evans and Robbins that the addition of NaCl to a "spent" sulfated limestone bed renewed its ability to capture SO_2. The current work is directed toward an understanding of the mechanism whereby NaCl enhances the SO_2 capacity of limestone, the testing of other substances, and eventually to an evaluation of the energy cost of using chemical additives for limestone-SO_2 reactivity enhancement.

Results of qualitative experiments are presented which indicate that NaCl and other substances act to increase the SO_2 capacity of limestone by forming a fluid phase which facilitates diffusion and crystallization of the product ($CaSO_4$). Quantitative data are reported on the effect of NaCl on the SO_2 capacity of Greer limestone (as measured with a TGA apparatus).

The Determination of Inorganic Constituents in the Effluent Gas from Coal Combustion. The objective of these studies is to identify the compounds present in the hot combustion gas of coal, in either gaseous or particulate form, and their amounts. A laboratory-scale, batch-type, fixed-bed combustion system has been constructed for these studies. Results of shakedown experiments with the apparatus are reported. Corrosion of the cold condensate collector has been encountered which has made interpretation of the data uncertain. However, preliminary data indicate transport of only a small (less than 10%) fraction of sodium from a high-chlorine coal burned in the apparatus.

Task F. Flue-Gas Cleaning Studies

Evaluation of On-Line Light-Scattering Particle Analyzers. Two on-line, light-scattering particle analyzers will be evaluated in the ANL fluidized-bed combustion system. The instruments are manufactured by Spectron Development Laboratories and by Leeds and Northrup. The flue-gas lines of the PDU combustion system have been modified for these evaluations, and the Spectron particle analyzer has been installed.

Particle Filtration. Work is being initiated toward the evaluation of two promising techniques for high-temperature removal of particulate from the flue gas of fluidized-bed combustors. The first method is the use of a fixed-bed or moving-bed granular filter. The second method involves the use of sonic fields to condition the particulate matter (increase the mean size and reduce the number of the effluent particulates) for more efficient removal in cleaning devices. Design of fixed granular bed test equipment is under way, with initial testing anticipated to begin early next quarter. Visits are being planned to laboratories currently working on sonic agglomeration to provide the necessary background for selecting equipment and a system design for testing at ANL.

INTRODUCTION

In fluidized-bed combustion, coal is combusted in a fluidized bed of calcium-containing solids (limestone, dolomite, or synthetic stones) which react with the gaseous sulfur compound released in coal combustion, forming calcium sulfate. In another step, the calcium sulfate can be regenerated for reuse in the combustor.

Current objectives of the ANL fluidized-bed combustion-regeneration program are (1) to select and optimize a regeneration process, (2) to test the behavior of different limestones, dolomite, and synthetic additives during combustion and regeneration, and (3) to assess the behavior of biologically toxic trace elements and corrosive elements. Information is presented on cyclic combustion-regeneration using Tymochtee dolomite, alternate regeneration processes, synthetic sorbent preparation, limestone characterization, trace elements in combustion emissions, the effect of NaCl on the calcination and sulfation of $CaCO_3$ in limestone, and flue-gas particulate cleaning studies.

TASK A. REGENERATION PROCESS DEVELOPMENT

Cyclic Combustion/Regeneration Experiments with Tymochtee Dolomite

The feasibility of sorbent regeneration technology will depend on the ability to recycle the sorbent a sufficient number of times without loss of its reactivity for either sulfation or regeneration and without severe decrepitation. Unless both of these requirements are met, the sorbent makeup rate will be so high that regeneration may not be economically justified. The experimental work on a ten-cycle experiment with Tymochtee dolomite has been completed, and a thorough evaluation of the results is in progress.

Equipment. A flow diagram of the combustion system used in this work is illustrated in Fig. 1. The major items of the ANL pressurized, fluidized-bed combustion process development unit (PDU) are: coal and additive feeders, a preheater for the fluidizing gas, a 6-in.-dia combustor, cyclones and filters, and gas sampling and analyzing equipment. The combustor is capable of operation at pressures up to 10 atm. The temperature of the combustor is regulated by electrical heaters and cooling coils. The gas analysis system provides on-line continuous measurement of the flue-gas constituents, SO_2, NO, NO_x, CO_2, CO, O_2, CH_4, and total hydrocarbons.

Figure 2 is a schematic diagram of the regeneration system. The reactor ID is 10.8 cm (4.25 in.), and the bed height of the fluidized bed ($\sim$46 cm) is regulated by an overflow pipe that is external to the fluidized bed. The reactor is lined with a 4.8-cm-thick castable refractory. The coal and the sulfated sorbent are metered separately (for independent control) to a common pneumatic transport line which discharges into the fluidized bed above the gas distributor.

Other components of the experimental regeneration system are an electrically heated heat exchanger for preheating some of the fluidizing gas and for preheating air (used in startup only) to $\sim$400°C and a solids-cleanup

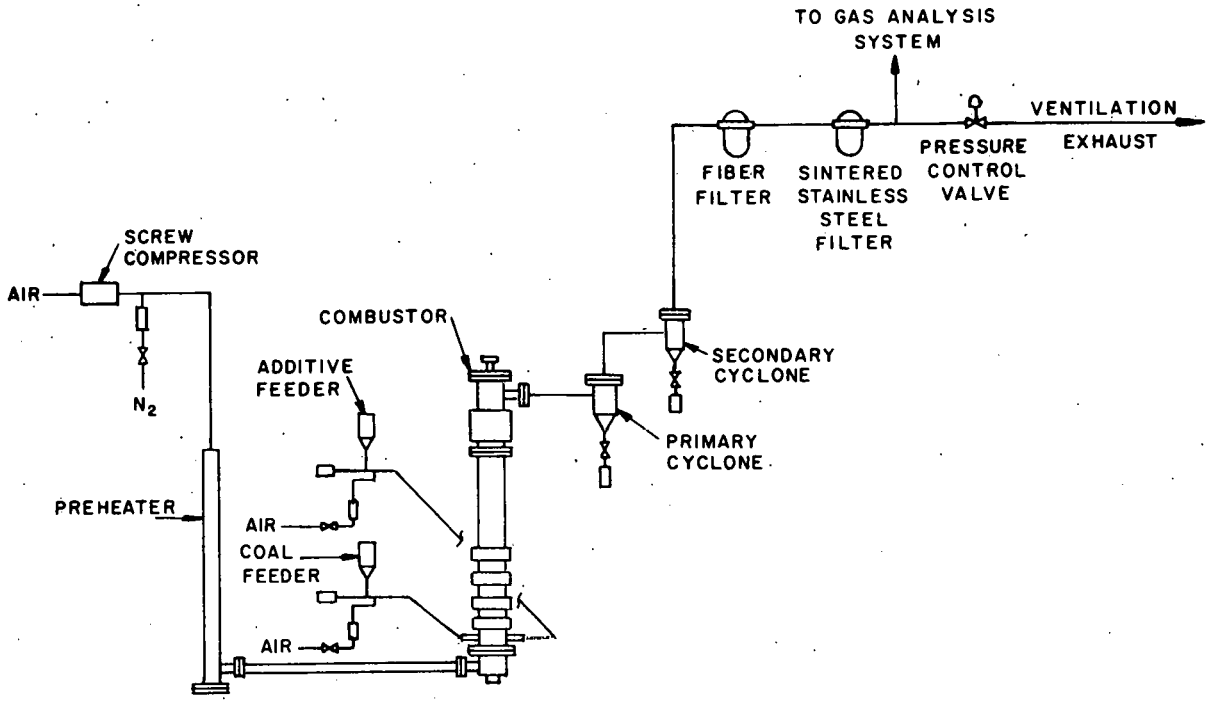

Fig. 1. Simplified Equipment Flowsheet of Fluidized-Bed Combustion Process Development Unit and Associated Equipment.

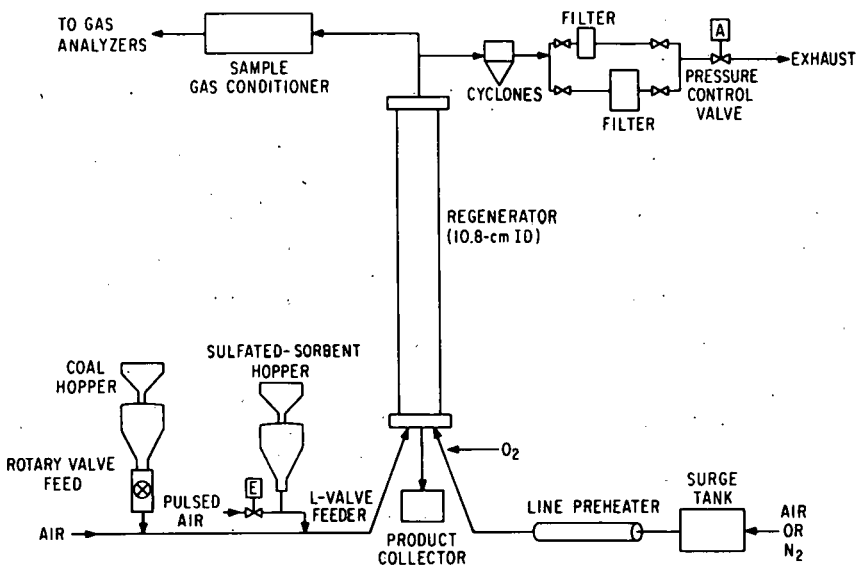

Fig. 2. Experimental Sorbent Regeneration System.

system for the off-gas. Continuous analyses of pertinent constituents (SO_2, O_2, CO, H_2, CH_4, and NO) in the off-gas were performed. Solids transport air constituted ∿40% of the total fluidizing gas in the reactor. The remaining fluidizing gas was a mixture of pure nitrogen and oxygen. Oxygen and nitrogen were metered separately and mixed to produce the required oxygen environment in the reactor. Hence, the experimental conditions for different oxygen requirements could be varied without changing the fluidizing-gas velocities (extent of off-gas dilution). Oxygen concentrations in excess of that in air were used in the feed gas for most of the reported regeneration experiments. Large amounts of heat (per unit capacity) were required to compensate for (1) the heat losses in the relatively small experimental system and (2) the heat load imposed by feeding cold, sulfated sorbent to the system. In a large-scale industrial regeneration system, such heat requirements would not be encountered and oxygen enrichment of the fluidizing air would not be needed.

Materials. The coal used in the combustion step of each cycle was a Pittsburgh seam coal obtained from the Consolidation Coal Company Arkwright mine. As received, the coal contained ∿2.8 wt % sulfur, ∿7.7 wt % ash, and ∿2.9 wt % moisture and had a heating value of 7,610 kcal/kg and an average particle size of 320 μm. In the first combustion cycle, unreacted -14 +30 mesh Tymochtee dolomite (∿50% $CaCO_3$, 39% $MgCO_3$ as received), obtained from C. E. Duff and Sons, Huntsville, Ohio, was fed to the combustor. In subsequent cycles, regenerated sorbent from the preceding cycle was fed, with no virgin sorbent makeup.

The Tymochtee dolomite that was regenerated contained ∿9 wt % S as $CaSO_4$ (no $MgSO_4$ present), 26 wt % Ca, 9.5 wt % $CO_3^=$, and a nominal size distribution of -14 +30 mesh before regeneration. Triangle coal, which was combusted under reducing conditions in the regeneration step, is a bituminous, low volatile coal that has a high ash fusion temperature (initial deformation at 1390°C under reducing conditions). As received, it contained 73.5 wt % C, 9.4 wt % ash, and 0.98 wt % S.

Regeneration Step Conditions and Results. The operating conditions during the regeneration step of each cycle were a nominal system pressure of 158 kPa and a bed temperature of 1100°C. The required heat and reductants for regeneration* are provided by incomplete combustion of coal in the fluidized bed of the regenerator reactor. The experimental conditions and results for a representative segment of the regeneration step for the eighth, ninth, and tenth cycles are given in Table 1, together with the regeneration results for the previously reported (ANL/ES-CEN-1017) regeneration cycles.

The extent of CaO regeneration (based on solids analyses) for these last three cycles remained as high (∿70%) as in previous cycles. In the ten regeneration experiments, solids residence times ranged from 6.8 to 8.1 min. The extent of CaO regeneration varied from 67 to 80% (based on solids analyses).

*See ANL/ES-CEN-1016, pp. 58 ff, for a discussion of the regeneration reactions.

Table 1. Experimental Conditions and Results for the Regeneration Step of the Ten Utilization Cycles with Tymochtee Dolomite.

Nominal Fluidized-Bed Height: 46 cm
Reactor ID: 10.8 cm
Pressure: 153 kPa
Temperature: 1100°C
Coal: Triangle (0.98 wt % S), ash fusion temperature (initial deformation under reducing conditions): 1390°C
Sorbent: -14 +30 mesh sulfated Tymochtee dolomite

Cycle No.	Expt. No.	Fluidizing-Gas Velocity (m/sec)	Solids Residence Time (min)	O_2 Conc in Feed Gas (%)	Reducing Gas Concentration in Off-Gas (%)	Sulfur Conc in Sulfated Sorbent (%)	CaO Regeneration (%)[a]/(%)[b]	Major Sulfur Compounds in Dry Off-Gas (%)			
								SO_2	H_2S	COS	CS_2
1	CCS-1	1.43	7	26.7	2.8	9.05	73/71	6.5	0.04	0.06	0.04
2	CCS-2	1.26	7.5	37.9	3.0	10.7	67/67	8.6	0.02	0.1	0.1
3	CCS-3	1.22	7.2	36.7	3.4	10.3	63/76	8.4	0.07	0.1	0.1
4	CCS-4	1.17	7.8	36.5	2.9	9.9	67/69	8.1	0.04	0.1	0.1
5	CCS-5	1.17	7.4	36.1	3.0	9.5	69/75	8.8	--[c]	--[c]	--[c]
6	CCS-6	1.18	7.8	41.8	2.6	9.3	66/75	8.7	0.03	0.2	0.1
7	CCS-7	1.16	7.3	38.2	2.9	8.5	69/77	8.2	0.07	0.1	0.1
8	CCS-8	1.18	8.1	35.9	3.0	7.8	64/80	6.3	0.06	0.07	0.07
9	CCS-9	1.09	7.3	36.4	3.0	7.9	53/67	6.1	0.1	0.1	0.1
10	CCS-10	1.24	6.8	38.0	3.0	7.1	63/68	6.7	0.05	0.08	0.09

[a] Based on off-gas analysis.
[b] Based on chemical analysis of dolomite samples.
[c] Analysis not performed.

The SO_2 concentration in the dry off-gas from the regenerator has varied from 8.8% to 6.1%. In the first cyclic regeneration experiment (CCS-1), the SO_2 concentration was diluted by gas used to obtain the fluidizing-gas velocity of 1.43 m/sec (other experiments were made at <1.26 m/sec). In the three final cyclic regeneration experiments, the lower SO_2 concentrations in the regeneration reactor off-gas were a result of the lower sulfur concentration in the sulfated sorbent (7.1-7.9 wt % S instead of ∿10% S). Although the combustion steps of these cyclic experiments were performed with a constant CaO/S mole ratio of ∿1.5 with no virgin sorbent makeup, the total sulfur content of the sulfated sorbent decreased with each cycle due to lowered sulfation reactivity of the sorbent.

Combustion Step Conditions and Results. The combustion experiments in each utilization cycle were performed at a 900°C bed temperature, 810 kPa (8 atm) pressure, 1.5 CaO/S mole ratio (ratio of unsulfated calcium in sorbent to sulfur in coal), ∿17% excess combustion air, 0.9 m/s fluidizing gas velocity, and a 0.9 m bed height. For continuity in the present discussion, the results reported previously (ANL/ES-CEN-1017) for the combustion experiments are reproduced here.

Representative steady state operating conditions and flue-gas composition data for the ten combustion cycle experiments were presented in ANL/ES-CEN-1017, Table 1. The level of sulfur dioxide in the flue gas and the corresponding sulfur retention based on the flue gas analysis for all ten combustion experiments were graphically presented in ANL/ES-CEN-1017, Fig. 2.

Sulfur dioxide levels in the gas increased from ∿300 ppm in cycle 1 to ∿950 ppm in cycle 10. This represents a decrease in sulfur retention from ∿88% in cycle 1 to ∿55% in cycle 10. Although there is some scatter in the data, it would appear that the reactivity of the sorbent for sulfur retention decreased linearly with combustion cycle over the 10-cycle experiment.

Coal Ash Buildup during Utilization Cycles. The extent of coal ash buildup in the fluidized bed during coal combustion is of particular importance in evaluating its effect on (1) the SO_2-accepting capability of the sorbent in the subsequent combustion step and (2) the ash-sorbent agglomerating tendency in the regenerator reactor.

The ash buildups during all ten sulfation and regeneration steps have been calculated from wet-chemical analyses (Si and Ca) of the sorbent product samples and are given in Table 2. As a basis for calculation, 100 g of virgin dolomite was used. The ash buildup was based on bulk silicon enrichment. The concentrations of silicon and the calculated coal ash buildups are plotted in Fig. 3. After ten utilization cycles with no fresh sorbent makeup, it has been found that for every 100 g of starting virgin dolomite, ∿13 g of coal ash accumulated in the sorbent. The silicon concentration increased from 2.1% in the virgin dolomite to 6.1% in the regenerated sorbent from the tenth cycle. The differences in the concentration of silicon in sulfated and regenerated samples are due to the weight loss of the sorbent during regeneration ($CaSO_4 \rightarrow CaO$). It is believed that most of the ash buildup occurred during the sulfation step because the feed rate of fresh ash (in the coal) was ∿1 kg for every 3 kg of regenerated sorbent feed. In contrast, during regeneration,

Table 2. Calculated Coal Ash Buildup during Sulfation and Regeneration of Tymochtee Dolomite, Based on Enrichment of Silicon.

Mass Basis: 100 g virgin Tymochtee dolomite (20.0 wt % Ca and 2.14 wt % Si)

Cycle No.	Cycle Step	Si Conc. (%)	Ash Buildup	
			wt %	g ash / 100 g virgin dolomite
1	S[a]	2.68	∿0	∿0
1	R[a]	3.64	∿0	∿0
2	S	2.88	2.4	2.1
2	R	3.98	4.0	2.7
3	S	3.19	3.3	2.8
3	R	4.35	7.7	4.8
4	S	3.43	4.1	3.4
4	R	4.51	7.0	4.9
5	S	3.70	6.0	5.2
5	R	4.6	7.4	5.2
6	S	3.68	5.9	5.1
6	R	5.38	11.5	8.1
7	S	4.19	8.2	7.0
7	R	5.39	11.2	7.8
8	S	4.72	11.0	9.6
8	R	6.41	17.0	12.5
9	S	4.69	11.0	9.7
9	R	6.05	15.8	12.2
10	S	5.42	14.7	13.3
10	R	6.13	16.3	12.7

[a]S = sulfation step, R = regeneration step.

the feed rate of fresh ash (in the coal) was ∿1 kg for every 70 kg of sulfated sorbent feed. The calculations for ash buildups do not identify in which of the two process steps (sulfation or regeneration) most of the ash buildup occurred.

The coal ash buildup was also evaluated as a function of particle diameter in a regenerated dolomite sample from the tenth cycle. The results are plotted in Fig. 4. It was found that ash accumulation increased with the particle diameter of the sorbent. The (nominal) 1700 μm particles (+14 mesh) are made up of agglomerates of smaller particles which are each coated with coal ash. Thus the larger (+14 mesh) particles had more ash-coated surface than did the smaller particles.

Sulfated and regenerated dolomite particles from the first, fifth, and tenth utilization cycles were examined for macrofeatures under a low-magnification microscope. Photomicrographs of these samples are given in Figs. 5

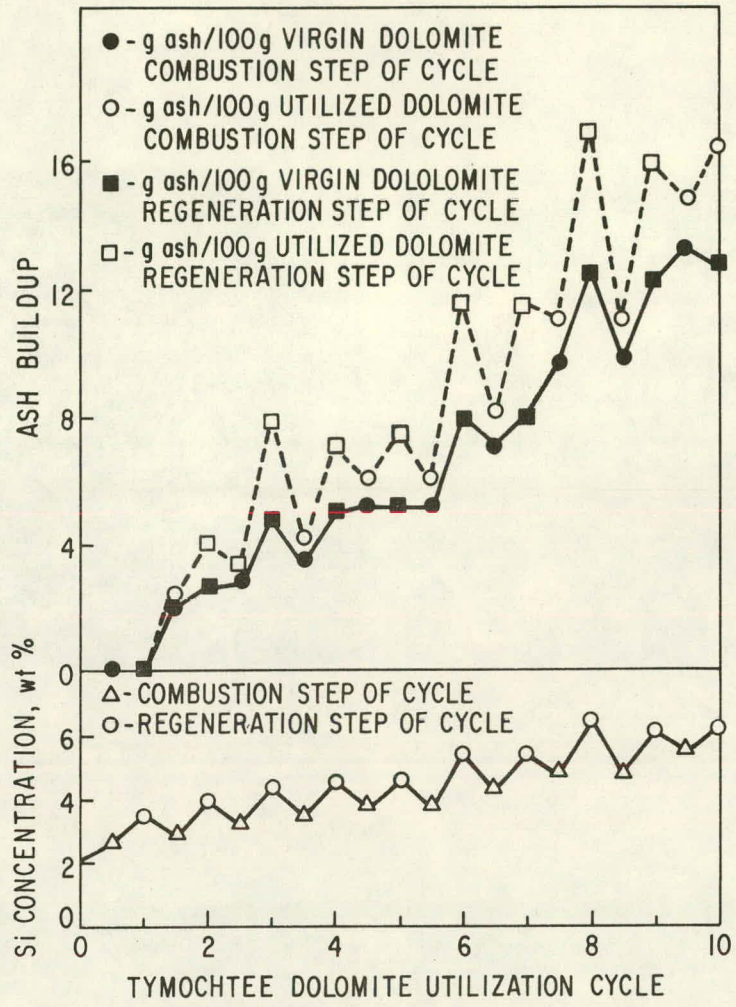

Fig. 3. Coal Ash Buildup as a Function of Utilization Cycle.

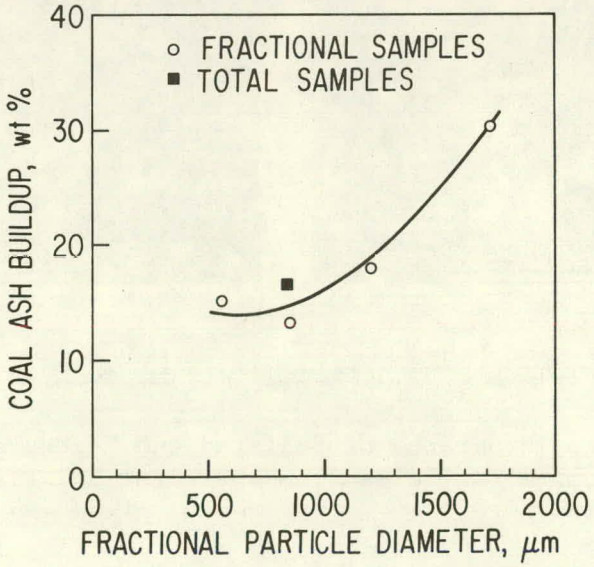

Fig. 4. Coal Ash Buildup as a Function of Particle Diameter in Tenth Cycle Regenerated Particles.

a. Cycle One, Sulfated (12.5 X)

b. Cycle One, Regenerated (12.5 X)

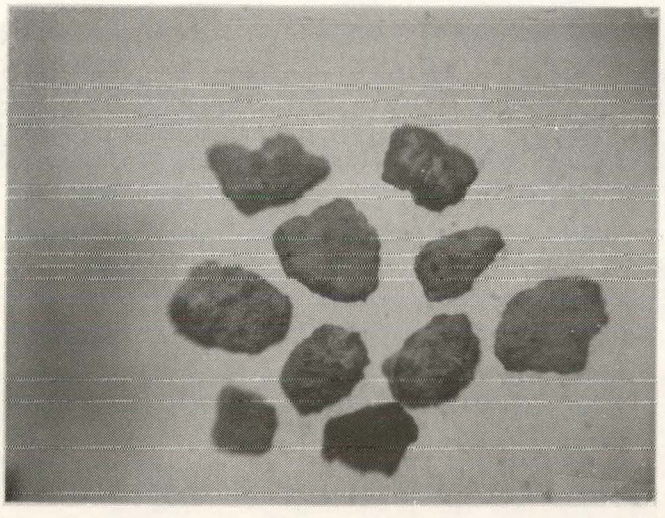

c. Cycle Five, Sulfated (12.5 X)

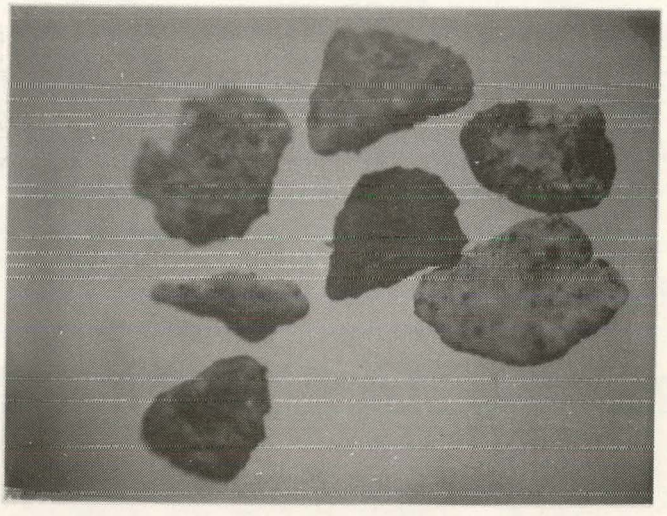

d. Cycle Five, Regenerated (12.5 X)

Fig. 5. Photomicrographs of Sulfated and Regenerated Tymochtee Dolomite Particles from the First and Fifth Utilization Cycles.

and 6. The photomicrographs reveal that even the once-sulfated stones were beginning to be coated with what is believed to be coal ash. Particles from the tenth cycle (Fig. 6) appear to be completely coated with ash. The coating can be more readily seen in color photographs. The cause of the ash blisters is uncertain; however, their presence is probably beneficial in that they expose reactive CaO in the particles.

A petrographic examination was also made of the unreacted dolomite and of samples of the dolomite after the first and tenth sulfation and regeneration half-cycles.* As in the above examination of the macrofeatures, the progressive buildup of a vitreous crust surrounding most of the particles is observed over the ten cycles. The spotty beginnings of crust formation during the first cycle are shown in Figs. 7 and 8. Representative encrusted particles from the tenth cycle are shown in Figs. 9 and 10.

Where the crust is well developed (as in Figs. 9 and 10), it is red with some black areas when viewed in ordinary light. Under the microscope, a polished section viewed in reflected light shows that the black parts have higher reflectivity and are magnetite (Fe_3O_4). The less reflective red parts resemble a silicate or silicate glass. The red coloration is probably due to finely dispersed hematite (Fe_2O_3) and is free of magnetite. The contrast between these two parts is indicated in Fig. 10.

X-ray diffraction analyses were made of the surfaces of particles from the first and tenth cycles. On the surface of first-cycle regenerated particles, the presence (very minor) of $Ca(Al_{0.7}Fe_{0.3})_2O_5$ was detected. On the surface of tenth-cycle regenerated particles, the evidence for the presence of this compound was more pronounced. The tenth-cycle sulfated particle surface contained a high concentration of α-Fe_2O_3.

Although the two predominant crystalline phases in the crust are magnetite and MgO, it is very likely that they are dispersed phases in a vitreous matrix (of unknown composition) as evidenced by the vesicular character shown in Fig. 11. In this respect, this material is similar to the fusion crust of stony meteorites. No silicon-based compound was found by X-ray diffraction (glassy silicate compounds would not be detected).

The iron and aluminum compounds on the surface of these particles are probably present in adhering coal ash. Specifically, the iron content of the crust is much greater than the iron content of the average dolomite particle. The unreacted dolomite particle shown in Fig. 12 contains the highest visible amount of iron oxide and iron sulfide of some 24 particles randomly selected and polished. Electron microprobe analyses are being performed on some of these samples to determine more definitely the composition of the shell which has built up on the dolomite particles.

---

*Analysis performed by L. H. Fuchs, Chemistry Division, Argonne National Laboratory.

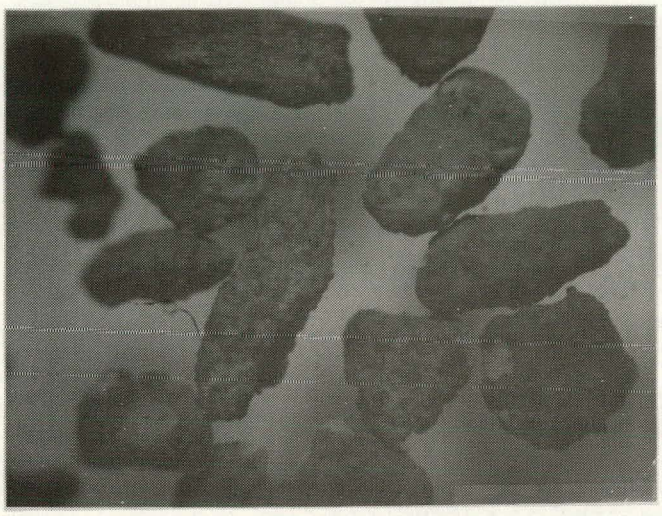

a. Sulfated (12.5 X)

b. Sulfated (38 X)

c. Regenerated (12.5 X)

d. Regenerated (38 X)

Fig. 6. Photomicrographs of Sulfated and Regenerated Tymochtee Dolomite Particles from the Tenth Utilization Cycle.

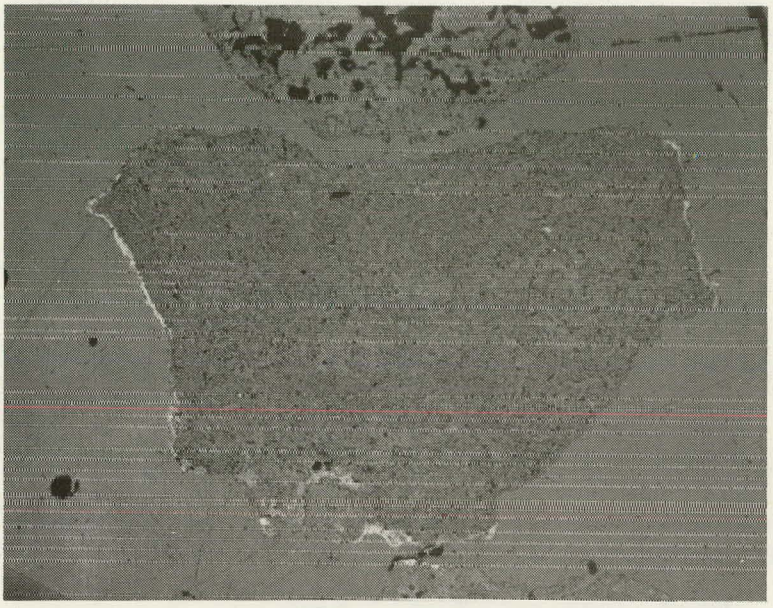

Fig. 7. Photomicrograph of Cross Section of a Tymochtee Dolomite Particle from the First Combustion Cycle. X75.

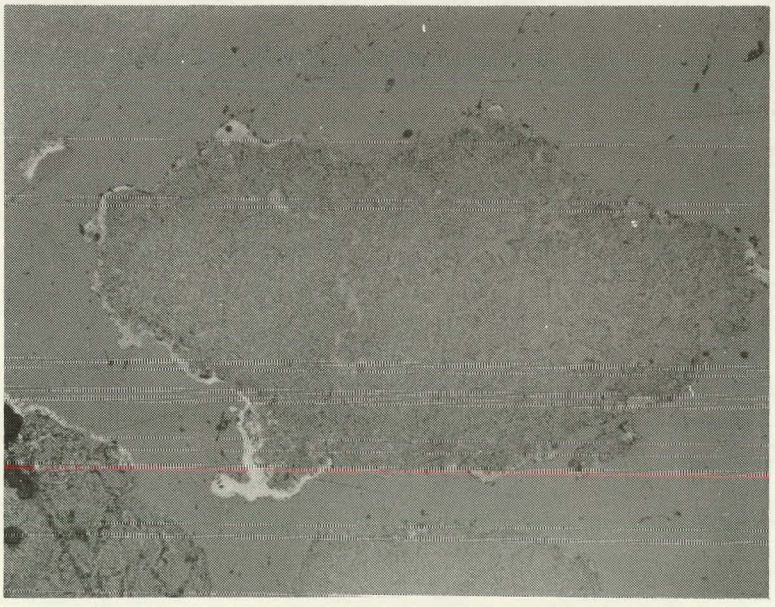

Fig. 8. Photomicrograph of Cross Section of a Tymochtee Dolomite Particle from the First Regeneration Cycle. X75.

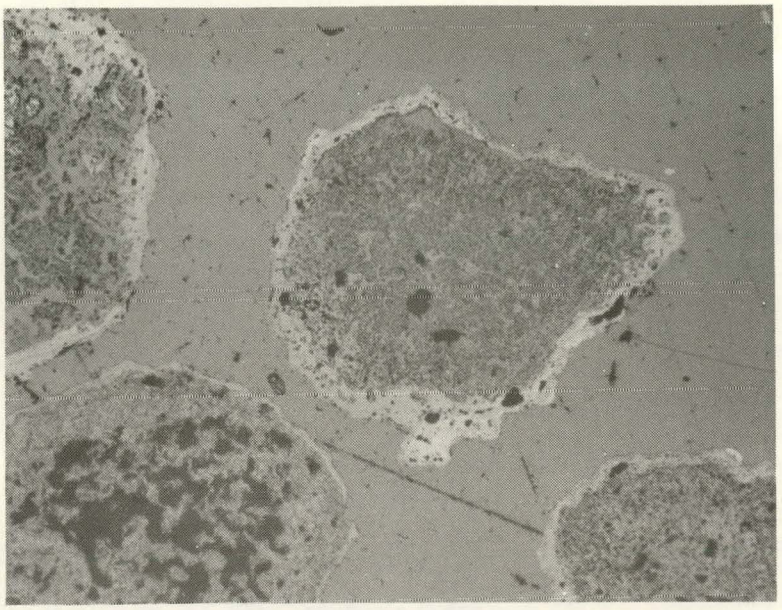

Fig. 9. Photomicrograph of a Cross Section of a Tymochtee Dolomite Particle from the Tenth Combustion Cycle. X75.

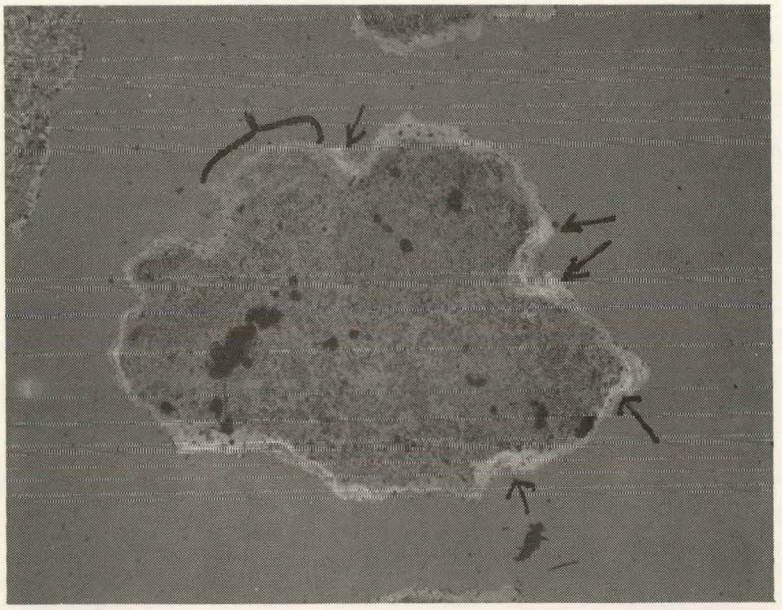

Fig. 10. Photomicrograph of Cross Section of a Tymochtee Dolomite Particle from the Tenth Regeneration Cycle. X75. Arrows indicate magnetite concentrations in crust; bracket = magnetite-free area.

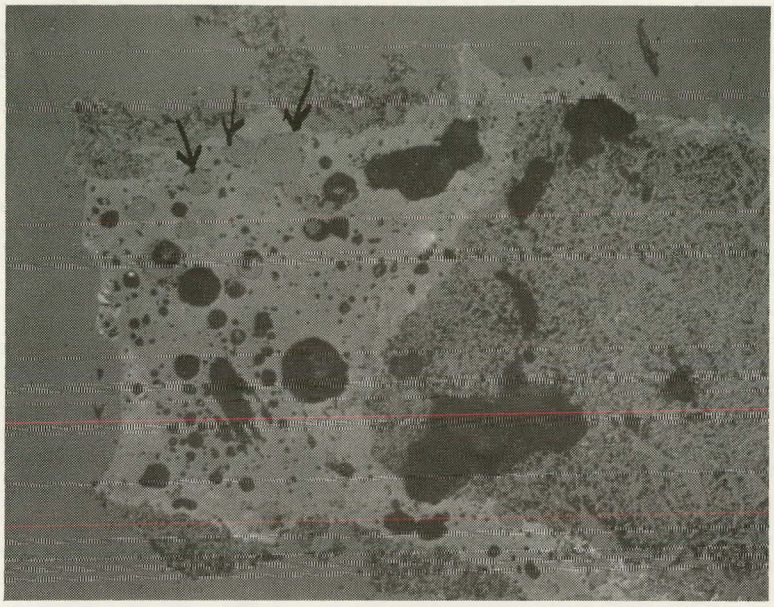

Fig. 11. Photomicrograph of a Tymochtee Dolomite Particle from the Tenth Regeneration Cycle. The arrows point to vesicles. X150.

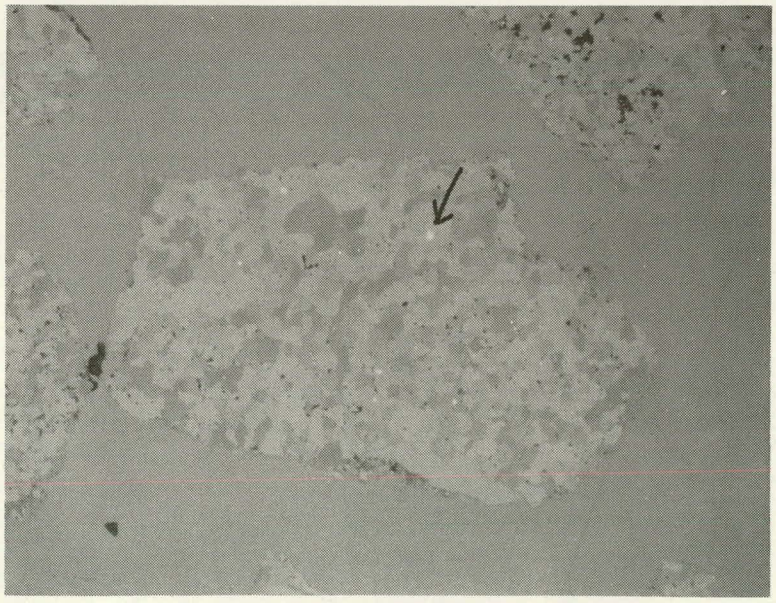

Fig. 12. Photomicrograph of Cross Sections of Unreacted Tymochtee Dolomite. The arrow points to a pyrite inclusion. X75.

It is reasonable to speculate that ash particles stick to the surface of dolomite particles during combustion. A glassy crust may form by fusion at the combustion temperatures in the combustor (there is evidence of crust formation during the first combustion cycle, Fig. 8) and later when the particles are regenerated at 1100°C.

The presence of coal ash shells on the dolomite particles did not cause routine defluidization during regeneration, although it is thought that in the regeneration reactor this shell is soft (at 1100°C under reducing conditions). The absence of agglomeration in the fluid bed during regeneration was probably due to the fluidizing velocity which was >1.0 m/sec and high enough to maintain stable fluidization for the -14 mesh particles used in these experiments. The beneficial effects of high fluidization velocities in "sticky" beds have been described by Gluckman *et al.*[1]

The following observation is evidence that the crust may be an effective sealant against gas diffusion: The observation pertains to samples from the tenth regeneration cycle which contain a few particles having no crust. (The crust was probably broken off prior to reduction.) An X-ray pattern of the interiors of these crust-free regenerated particles showed strong CaO and MgO and weak $Ca(OH)_2$, whereas a pattern of the interiors of encrusted particles in the same sample showed strong MgO, medium $CaSO_4$, and only weak CaO.

The ash layer appears to have a negligible effect on the activity of dolomite during regeneration. However, its effect on the reactivity of dolomite during sulfation may be detrimental--the ash layer appears to contribute to loss of porosity in the particles and thus slows down the already diffusion-limited sulfation reactions. Exposure to high temperature, causing sintering of the dolomite, could also be responsible for the loss of porosity.

Porosity of Dolomite as a Function of Utilization Cycle. The porosity of -25 +30 mesh particles was measured by the mercury penetration method. The pore distributions of samples from cycles 2 and 10 are given in Fig. 13. The cumulative pore volume for pores $\geq$0.4 μm and also for pores $\geq$0.04 μm in sulfated and regenerated Tymochtee dolomite are given in Table 3. It has been reported by Hartman and Coughlin[2] that most sulfation takes place in larger pores ($\geq$0.4 μm) and that pores smaller than 0.4 μm are relatively easy to plug. During sulfation of CaO, the pores shrink as a result of molecular volume changes.

The porosity of sulfated dolomite was relatively unaffected by utilization cycle, although the sulfur content decreased from ∿10 wt % to ∿7 wt % (Fig. 13). However, the porosity of the regenerated dolomite consistently decreased with utilization as did the sulfur content in the regenerated stones. The difference in porosity of the sulfated and regenerated samples decreased from ∿0.15 cm^3/g (pores $\geq$0.4 μm) after the first cycle to ∿0.07 cm^3/g after the tenth cycle. The porosity of regenerated dolomite decreased with cyclic use, and thus its effectiveness as an SO_2 acceptor decreased.

The loss of porosity in the dolomite could be due to (1) buildup of an ash layer around the particle or (2) high-temperature (1100°C) exposure during

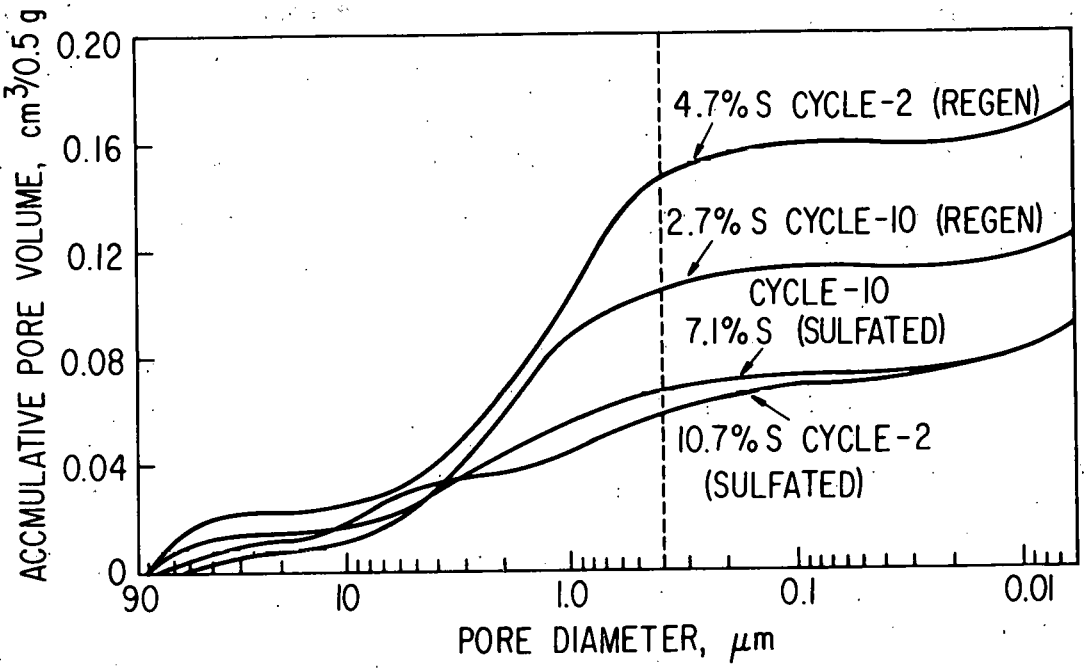

Fig. 13. Pore Distributions of Dolomite Samples from Cycles Two and Ten.

Table 3. Porosity (cm^3/g) of Tymochtee Dolomite as a Function of Utilization Cycle.

Cycle No.	Sulfated	Regenerated	Change (Δ)
1	0.120[a]/0.164[b]	0.268[a]/0.340[b]	0.148 /0.176
2	0.120 /0.212	0.288 /0.308	0.168 /0.096
4	0.120 /0.140	0.252 /0.276	0.132 /0.136
6	0.156 /0.164	0.244 /0.258	0.088 /0.094
8	0.144 /0.156	0.238 /0.260	0.094 /0.104
10	0.132 /0.140	0.204 /0.220	0.072 /0.080

[a]Pores ≥0.4 μm.
[b]Pores ≥0.04 μm.

regeneration. At the regeneration temperature, sintering begins, decreasing the reactivity by decreasing the beneficial porosity of the particles. This limits local diffusion and reaction of SO_2. The effect of porosity and reactivity of high-temperature exposure as a function of time is being evaluated for Tymochtee dolomite and will be reported.

Attrition and Elutriation Losses during Regeneration and Combustion. The extent of sorbent losses during the regeneration steps of the ten cycles has been determined. The losses were estimated using three different approaches, all based on the mass of calcium present in the particulate streams. In the first method, the sorbent loss for an entire regeneration step was calculated from the difference in calcium weight of the sulfated dolomite fed and the regenerated dolomite. In the second method, the sorbent losses were calculated for a steady-state segment of the experiment. The results obtained from both of these methods were inconclusive because the calcium balances were greater than 100% (generally <5% high) in most experiments. The high calcium balances may be explained by the accuracy of the calcium analysis being ∿5%. The calcium loss from the entire regenerated product stream is less than 5%.

In the third approach, the losses were predicted by evaluating the percentage of the calcium in the sulfated dolomite fed to the regeneration reactor that was elutriated and subsequently removed from the off-gas by the cyclones and filter. (The calcium contribution of the coal ash from the Triangle coal used for regeneration was found to be insignificant.) The losses, based on calcium content of particulates removed from the off-gas stream, averaged 2.0% (see Table 4). Because the off-gas particles were -30 mesh and the feed sulfated dolomite was normally -14 +30 mesh, it can be assumed that the off-gas particles were attrited fragments of the regenerated dolomite. No apparent trend in the extent of attrition was found for the ten cycles.

Table 4. Attrition and Elutriation Losses for Tymochtee Dolomite during Regeneration in the Cyclic Utilization Study.

S.D. = Ca in sulfated dolomite (feed), kg/hr
O.P. = Ca in particulate collected from off-gas, kg/hr

Regeneration Cycle CCS-	Loss for Steady-State Experiment Segment $\left(\frac{O.P.}{S.D.}\right) \times 100$
1	1.9
2	1.7
3	3.0
4	1.2
5	3.5
6	3.7
7	2.0
8	2.6
9	0.9
10	1.3
Avg.	2.2

The extent of sorbent losses by decrepitation and/or entrainment during the ten combustion half-cycles was also determined, based on the steady-state calcium material balances around the combustor, which accounted for the calcium in both the dolomite and the coal. The assumption was then made that all calcium entering the combustor in the coal was entrained in the flue gas as fly ash with no correction for ash buildup in the fluidized bed. (Based on the rates involved and the relatively small calcium concentration of the ash as compared with the calcium concentration of dolomite, such a correction would be very minor.) The sorbent loss by decrepitation and/or entrainment was then calculated as follows:

$$\text{Sorbent Loss (\%)} = \frac{\left(\begin{matrix}\text{Calcium in Entrained} \\ \text{Particulate Matter}\end{matrix} - \begin{matrix}\text{Calcium in} \\ \text{Coal Feed}\end{matrix}\right) \times (100\%)}{[\text{Calcium in Sorbent Feed}]} \qquad (1)$$

The results are presented in Table 5 along with the calcium material balances for the ten combustion experiments.

Table 5. Decrepitation and Entrainment Losses and Calcium Material Balances for the Ten Combustion Experiments in the Cyclic Sorbent Utilization Study.

Sulfation Cycle	Sorbent Loss by Decrepitation and Entrainment (%)	Calcium Material Balance (In/Out) x 100
REC-1	16	108
REC-2	4	94
REC-3	5	104
REC-4	3	96
REC-5	3	99
REC-6	6	102
REC-7	4	100
REC-8	7	101
REC-9	6	91
REC-10	4	96

The 16% loss reported for experiment REC-1 is a revision of the previously reported value of 20-25% (ANL/ES-CEN-1016). Although the first cycle loss was still quite large, losses during the remaining nine combustion cycles were reasonably small, averaging about 5% per cycle. It is quite likely that after the first combustion cycle, the resistance of the sorbent to decrepitation is increased by (1) residual sulfate in the sorbent following regeneration and (2) the presence of the vitreous crust on the particles. It is also possible that the rapid calcination of $MgCO_3$ during the first combustion cycle contributed to the large sorbent loss during that cycle. On the basis of these results, the loss of sorbent reactivity may be significant in affecting cyclic performance adversely than is the loss of sorbent by decrepitation.

Although the thermal cycling is more extreme and the regeneration reactions are more rapid (decomposition) during regeneration than during sulfation, the extent of attrition during regeneration was lower. The lower sorbent losses during regeneration can be attributed to the very short solids residence time (∿7.5 min) in the reactor in each regeneration step as compared with the much longer solids residence time (∿5 hr) in the combustor reactor for each sulfation step. The effect of introducing solids that were at room temperature into a hot reactor environment in each half-cycle cannot be estimated. In an industrial process, the solids would be cycled between the combustor and the regenerator reactor at the temperatures of the reactors, and hence the thermal shock would be lessened. It is believed that lower sorbent losses would be obtained with a continuous sorbent cycling system.

The combined losses due to attrition and/or elutriation per cycle (sulfation and regeneration) have been found to be ∿8%. In an FBC process utilizing sorbent regeneration, it is expected that the makeup rate for Tymochtee dolomite would have to be at least this high because of attrition. An even higher makeup rate may be required to maintain sufficient SO_2-sorption reactivity in the fluidized bed of the combustor.

TGA Sulfation Experiments. To further test the reactivity of the sorbent for sulfation, samples of the sorbent from each regeneration half-cycle experiment were sulfated in a TGA apparatus at 900°C, using a reactant gas containing 0.3% SO_2, 5% O_2, and the balance N_2. The results of the experiments are shown in Figs. 14 and 15. Figure 14 gives the percent of the CaO in the regenerated samples converted to $CaSO_4$ as a function of time (*i.e.*, the rate of conversion) for all ten regeneration half-cycles. The numbers of the curves (2 through 10) correspond to the numbers of the corresponding combustion half-cycles, and curve 11 represents sulfation of regenerated material from cycle 10. With the exception of the curve corresponding to the fourth combustion cycle, the rate of conversion decreased from the second through the eleventh sulfation. The calcium and sulfur analyses of the starting material for the fourth sulfation are being rechecked in an effort to explain the inconsistency of the data for that experiment.

An interesting observation is that after the eighth sulfation cycle, the loss in reactivity with succeeding sulfation cycles is quite small. This indicates that the reactivity of the sorbent may level off in the higher sulfation cycles. This potential leveling-off of reactivity was not detected in the cyclic combustion-regeneration experiments performed in the PDU.

Figure 15 plots the utilization of the stones for each sulfation cycle as a function of time for the TGA experiments--*i.e.*, the extent of conversion. The starting point for each sulfation experiment is determined by the extent of regeneration during the preceding regeneration half cycle. However, after sulfation for a period of several hours, the utilization of the stone decreases with sulfation cycle except for an unexplained inconsistency in the fourth-cycle sulfation data. Again, the attainable sorbent utilization appears to stabilize and become fairly constant at about the eighth combustion cycle.

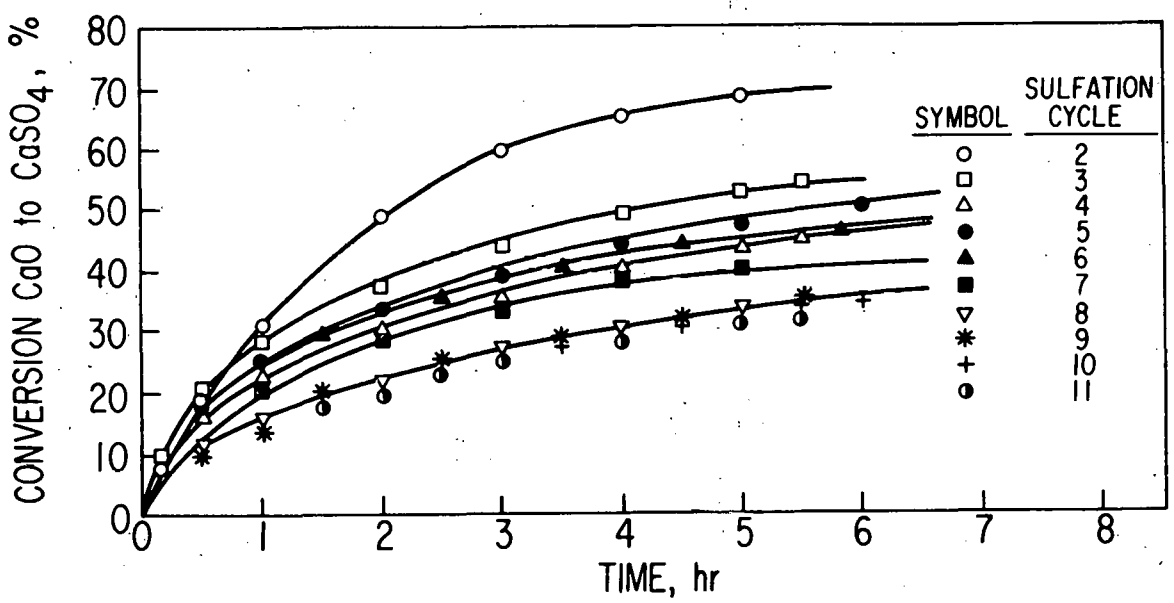

Fig. 14. Conversion of CaO to $CaSO_4$ as a Function of Time and Sulfation Cycle as Determined by TGA Sulfation Experiments. Temperature: 900°C; reaction gas: 0.3% S, 5.0% O_2, balance nitrogen.

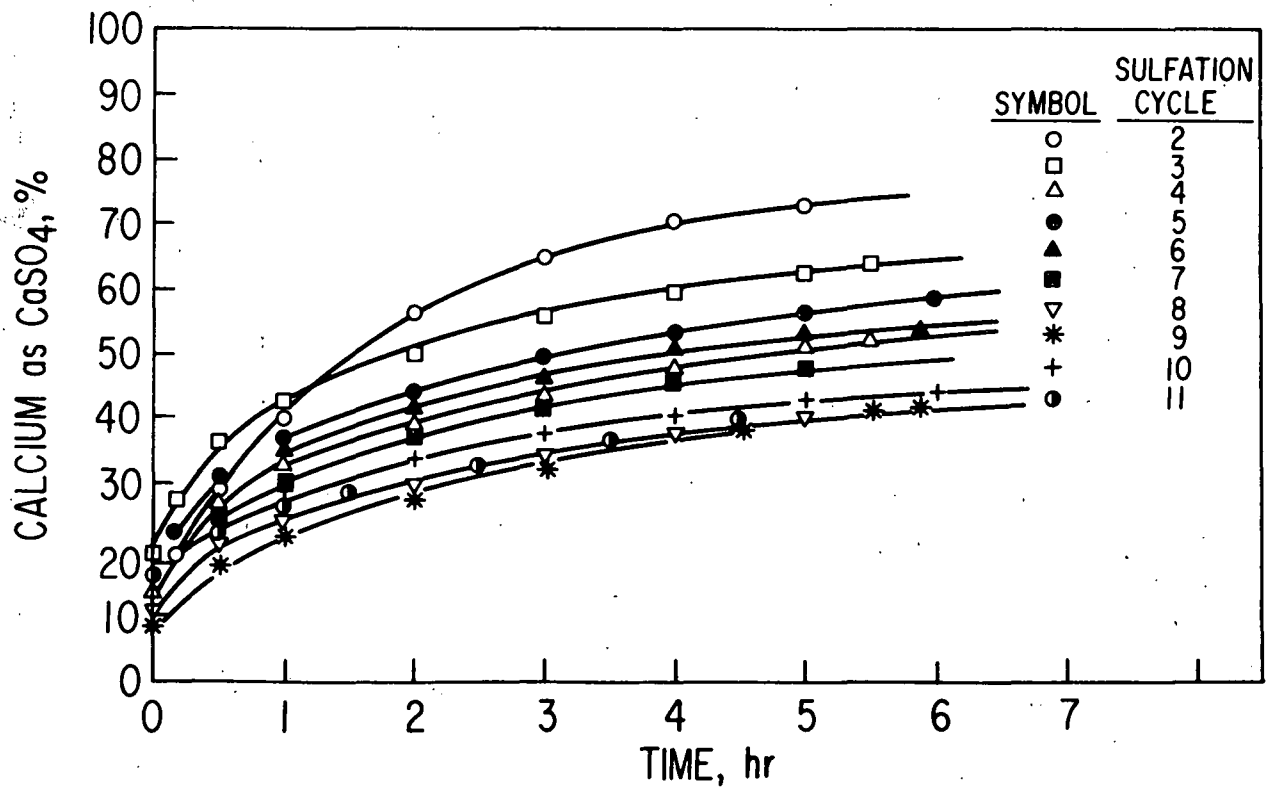

Fig. 15. Percent Calcium as $CaSO_4$ as a Function of Time and Sulfation Cycle. Determined by TGA Sulfation Experiments. Temperature: 900°C; reaction gas: 0.3% S, 5.0% O_2, balance nitrogen.

Carbonate Level of Sorbent Samples. The weight fraction of the unsulfated calcium present as calcium carbonate was derived for the sorbent at each half-cycle in the utilization study up to the end of the sixth full cycle. The results are shown in Fig. 16. Initially, all of the calcium was present as $CaCO_3$ in the virgin dolomite feed to the first combustion cycle. After the first combustion half-cycle, the unsulfated calcium was still predominantly ($\sim$68%) $CaCO_3$. Following the first regeneration, however, only 4% of the unsulfated calcium was present as $CaCO_3$. Although the carbonate fraction remained essentially constant during succeeding regeneration cycles, the carbonate fraction steadily decreased following successive combustion cycles. These results further emphasize the increasing blockage to gas penetration (for carbonation as well as sulfation) with increasing combustion cycle. Neither calcination nor regeneration appears to diminish or to be adversely affected with increasing utilization cycle, however.

Estimate of Sorbent Makeup Requirements to Meet EPA Sulfur Emission Limit. An attempt has been made to estimate the sorbent makeup rate which would be required in a continuous recycle operation to meet the EPA sulfur emission limit during combustion. The makeup rate is essentially determined by three factors: (1) the level of sulfur retention required, (2) the sorbent loss of reactivity with increasing number of utilization cycles, and (3) the sorbent recycle rate which establishes the total CaO/S mole ratio during the combustion cycle. In this discussion, the term CaO/S mole ratio is used to emphasize that the mole ratio refers to the ratio of the available (unsulfated) calcium in the sorbent feed to the sulfur in the coal feed.

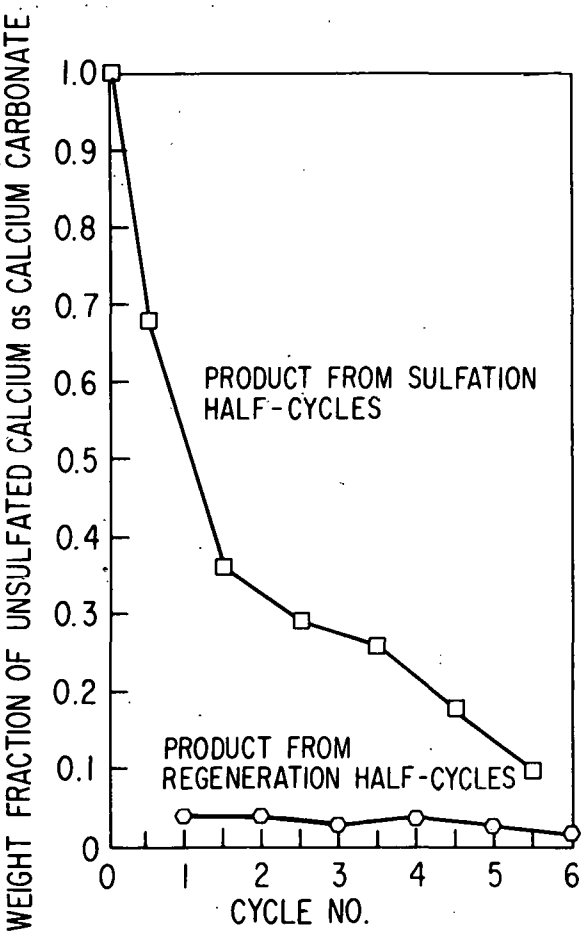

Fig. 16. Weight Fraction of Unsulfated Calcium as Calcium Carbonate in Sulfated and Regenerated Dolomite Samples as a Function of Utilization Cycle.

The analysis was based on the results obtained during the ten combustion experiments in the cyclic combustion-regeneration study. Conditions assumed for the analysis were, therefore, a 900°C bed temperature, 810 kPa pressure, and a 0.9 m/s fluidizing-gas velocity. The analysis was also based on maintaining a sulfur retention of 75%, which is slightly above the ∿70% required to meet the EPA sulfur emission limit.

The two requirements for the analysis were: (1) to determine the utilization ("activity") of the sorbent at 75% sulfur retention as a function of sulfation cycle and (2) to derive an analytical expression for the age distribution (that is, the cycle number distribution) of the reactor charge at steady state as a function of makeup rate.

In order to establish the first requirement in the analysis, it was first necessary to determine the CaO/S mole ratio required as a function of utilization cycle to maintain a constant sulfur retention of 75%. During two of the combustion experiments (REC-7 and REC-8) in the cyclic combustion-regeneration study, the CaO/S ratio was intentionally increased sufficiently above 1.5 near the end of each experiment to bring sulfur retention to ∿75%. With this additional data, it was possible to determine the required CaO/S ratio as a function of cycle to maintain a constant sulfur retention of 75%. These results are illustrated in Fig. 17.

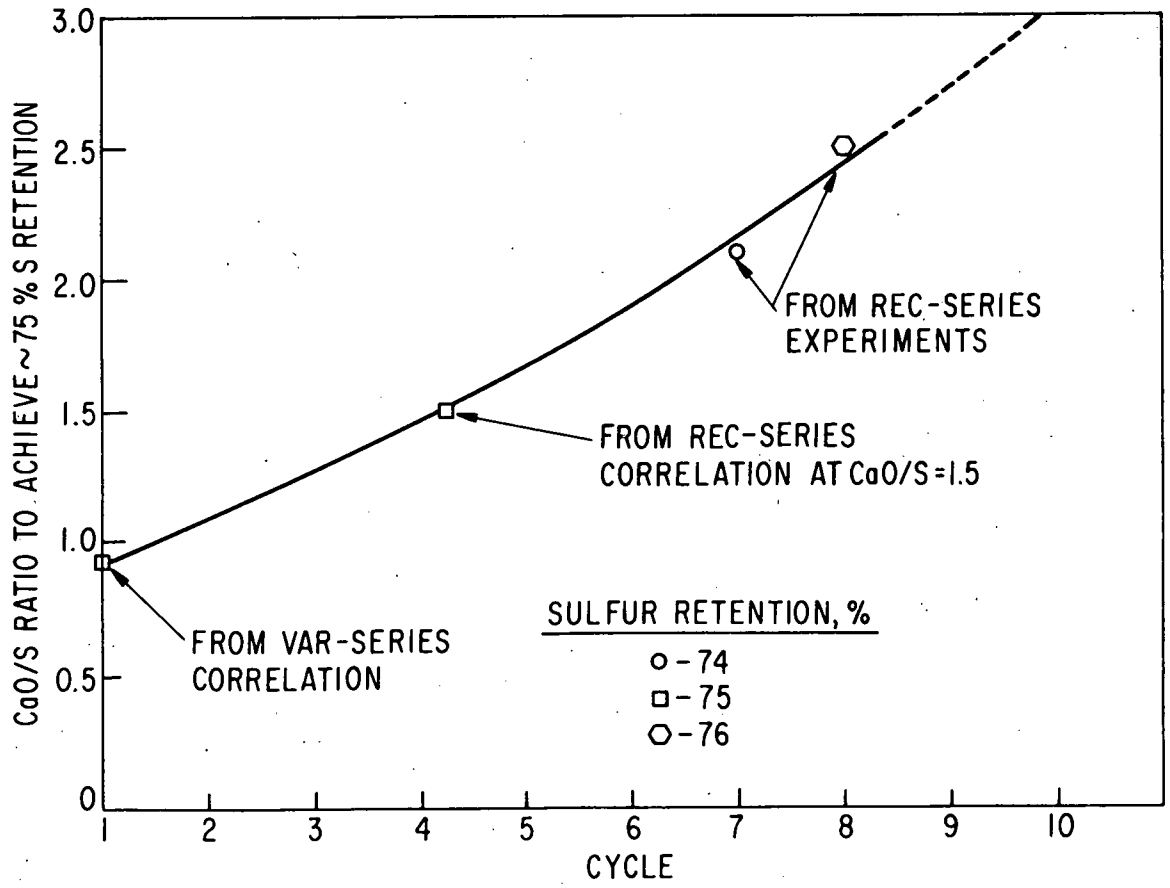

Fig. 17. CaO/S Ratio Required to Achieve 75% Sulfur Retention as a Function of Cycle.

From the correlation of VAR-series experimental results,[3] the CaO/S ratio which would be required to achieve ∿75% retention during the first combustion cycle was calculated to be 0.92. From the correlation of the REC-series cyclic combustion experiments at a CaO/S ratio of 1.5, a sulfur retention of 75% occurs during combustion cycle 4.2.* It was then experimentally determined that during combustion cycles 7 and 8, CaO/S ratios of 2.1 and 2.5 were required to achieve sulfur retentions of ∿74 and ∿76, respectively. The resulting curve indicates that the CaO/S ratio required in the eighth cycle to maintain a constant sulfur retention of 75% was approximately two and one-half times that in the first cycle.

Zielke *et al.*[4] performed a similar cyclic combustion-regeneration study using Tymochtee dolomite at ∿155 kPa. A comparison of the results of the two studies is given in Table 6. The results are obviously in very good agreement; CaO/S ratios reported by Zielke *et al.* to achieve ∿80% sulfur retention were slightly higher than the ANL values of CaO/S to achieve ∿75% retention.

Hammond and Skopp[5] also reported cyclic stone reactivity data for a series of batch sulfation/regeneration tests using a limestone. The CaO utilization at 80% SO_2 absorption was used as a relative measure of the cyclic stone reactivity. They reported that the CaO utilization decreased from ∿20% to 15% over seven cycles for stones with an average diameter of 930 μm.

By the use of the correlation of Fig. 17, it was then possible to calculate the utilization ("activity") of the sorbent at 75% sulfur retention as a function of sulfation cycle using the equation

$$U_n = \frac{0.75}{(CaO/S)_n} \tag{1}$$

where U_n = CaO utilization at 75% S retention for *nth* sulfation

$(CaO/S)_n$ = CaO/S mole ratio required for 75% sulfur retention during *nth* sulfation

The resulting correlation of the sorbent utilization at 75% sulfur retention with the sulfation cycle is graphically presented in Fig. 18. Utilization for a given sulfation cycle can be estimated from the equation for the straight line in Fig. 18,

$$U_n = 0.92e^{-0.139n} \tag{2}$$

where n is the sulfation cycle number.

The second requirement in the analysis was to develop an expression for the age distribution of the sorbent feed (recycle plus makeup) so that the fractional amount of the feed being sulfated for the *nth* time can be estimated. The approach taken was adapted from a procedure developed by Nagier[6] and is illustrated in Fig. 19.

*For purposes of correlation, a fractional combustion cycle such as 4.2 can be used to indicate a material which is less reactive than sorbent being sulfated for the fourth time and more reactive than sorbent being sulfated for the fifth time.

Table 6. Comparison of the Experimental Cyclic Sulfation Results Obtained at ANL with those reported by Zielke *et al.*[a] Tymochtee dolomite used in both studies.

Conditions	ANL	Zielke *et al.*[a]
Combustion		
Pressure, kPa	∿810	∿155
Temperature, °C	900	980
Excess Air, %	17	20
Gas Velocity, m/s	0.91	0.91
Sorbent Size, mesh	-14 +30	+14 +28
Solids Residence Time, hr	∿5	∿1.1
Regeneration		
Pressure, kPa	153	155
Temperature, °C	1100	1065
Gas Velocity, m/s	∿1.3	∿0.6
Solids Residence Time, min	∿7	108

Results	Cycle No. 1	2	3	4	5	6	7	8
ANL[b]								
Sulfur Retention, %	75	75	75	75	75	75	75	75
CaO/S Ratio	0.93	1.1	1.3	1.5	1.7	1.9	2.2	2.5
Zielke *et al.*[a]								
Sulfur Retention, %	79.3	80.4	80.2	78.7	77.6	79.3	80.6	N.D[c]
CaO/S Ratio	0.95	1.4	1.9	1.9	2.2	2.3	2.6	N.D

[a] Reference 4.
[b] Values obtained from Fig. 18.
[c] No data.

In Fig. 19,

w_o = constant CaO makeup charged to each cycle
w_n = total CaO charged to the n*th* cycle, n = 1,2,...n
α = constant fraction of total charge rejected after each cycle (includes decrepitation losses, incomplete regeneration, and sorbent drawdown)

Therefore, $(1 - \alpha)$ represents the fraction of the CaO charged to each stage which is recycled to the next stage. It can be easily shown that as $n \rightarrow \alpha$, w_n converges to

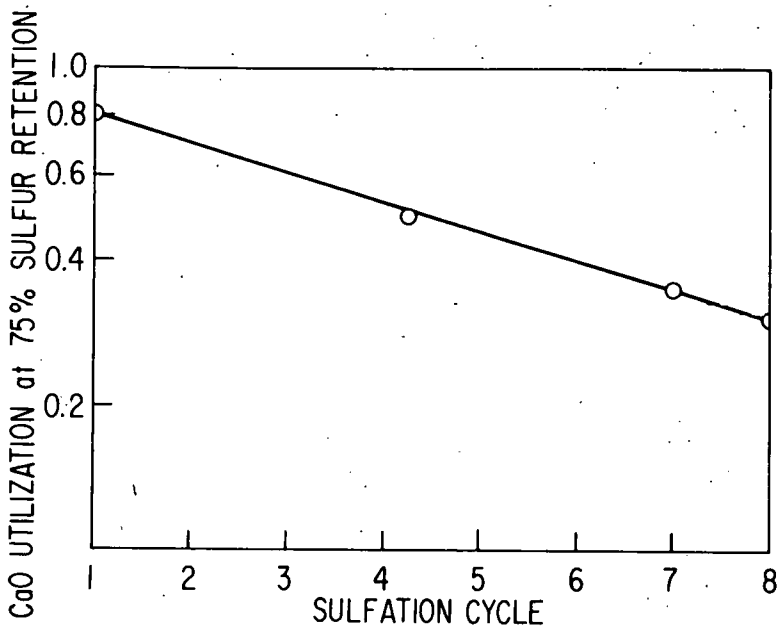

Fig. 18. CaO Utilization at 75% Sulfur Retention as a Function of Sulfation Cycle.

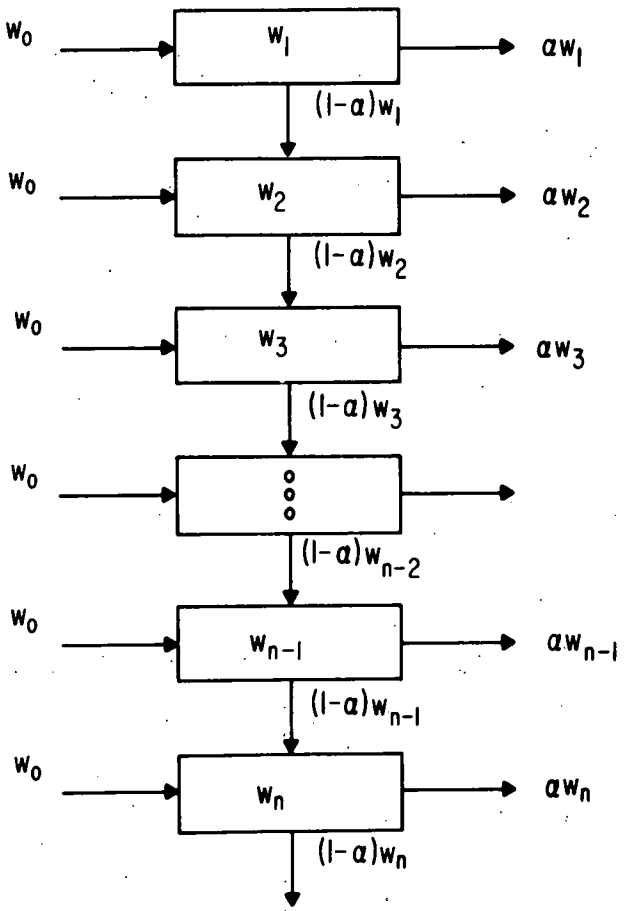

Fig. 19. Recycle Mechanism to Approximate the Steady-State Distribution of Sorbent for a Continuous Combustion-Regeneration Process.

$$w_n = [1 + (1 - \alpha) + (1-\alpha)^2 + ... + (1-\alpha)^{n-1}]w_o$$
$$= w_o/\alpha \quad (3)$$

where the fraction, g_n, of the total charge, w_n, being sulfated for the n*th* time is expressed as follows:

$$g_n = \alpha(1-\alpha)^{n-1}, \; n = 1, 2, ...,\infty \quad (4)$$

An equilibrium CaO utilization, U_{eq}, can then be calculated for 75% sulfur retention at steady state as

$$U_{eq} = \sum_{n=1}^{\infty} U_n g_n \quad (5)$$

From this result, the total CaO/S ratio at equilibrium can be calculated as

$$\text{Total CaO/S} = 0.75/U_{eq} \quad (6)$$

and the makeup CaO/S as

$$\text{Makeup CaO/S Ratio} = (\text{Total CaO/S})\cdot\alpha \quad (7)$$

The results of the analysis for U_n as given by Eq. 2 are presented in Fig. 20. As an example of using Fig. 20 for a total CaO/S ratio of 1.5, a makeup (makeup CaO/total CaO) of ∿18% and a makeup CaO/S ratio of ∿0.27 are indicated for a sulfur retention of 75%. It is difficult to assess the possible degree of error in making such estimates. However, the general form of the curves in Fig. 20 is still quite useful in demonstrating that low makeup rates and hence low CaO/S feed ratios should be obtainable with relatively minor increases in the recycle rate. For example, if the recycle rate is increased to maintain a total CaO/S ratio of 2 rather than 1.5, the estimated makeup CaO/S ratio drops from 0.27 to 0.20, a savings of ∿25% in the sorbent requirements. In comparison to the once-through CaO/S ratio of ∿0.93 for 75% sulfur retention, the makeup ratio of 0.2 for a cyclic process corresponds to an estimated savings of ∿78%.

The analysis further serves to illustrate that at a makeup of less than ∿10% (which is close to that required to overcome attrition losses), additional savings in the makeup CaO can be obtained only by large increases in the recycle rate.

Amount of Sorbent Processed Per Cycle. Table 7 utilizes the amounts of sorbent processed during each phase of the cyclic utilization study. It should be emphasized that losses of materials between cycles included handling losses (spills, *etc.*), sampling losses, and (in the case of combustion) losses during startup.

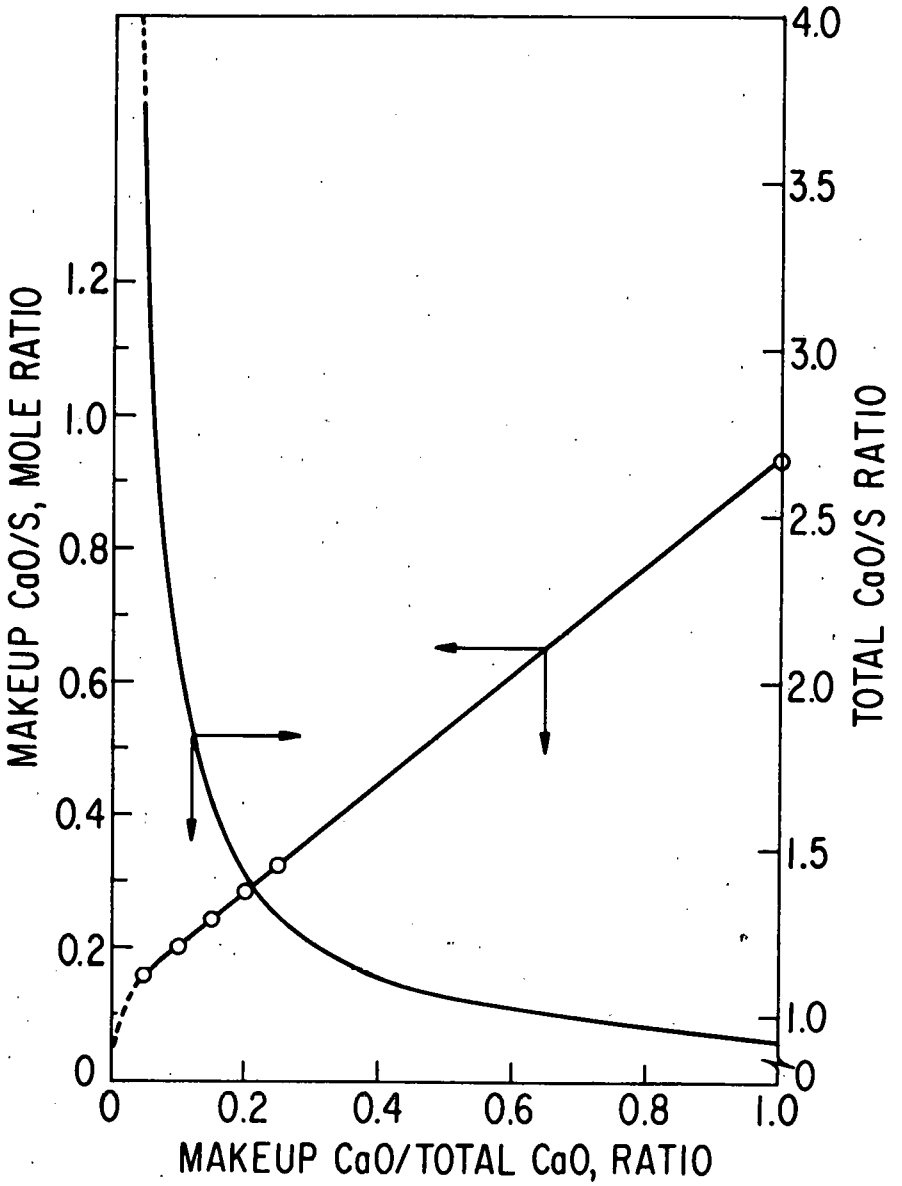

Fig. 20. Calculated Makeup and Total CaO/S Ratios Required to Achieve 75% Sulfur Retention as a Function of the Makeup CaO to Total CaO Ratio. Sulfation Conditions: Temp, 871°C; Pressure, 810 kPa, Sorbent, Tymochtee Dolomite; Sulfur Retention, 75%.

Table 7. Gross Amounts of Sorbent Processed and Calcium Balances for Each Half-Cycle in the Cyclic Combustion/Regeneration Study.

Cycle	Gross wt in (kg)	Ca (wt %)	Ca in (kg)	Gross wt out (kg)	Ca (wt %)	Ca out (kg)	Calcium Balance (%)
Combustion							
1	620	20.0	124	359	26.3	94.4	76
2	268	33.9	90.9	328	22.4	73.5	81
3	282	29.7	83.8	285	23.4	66.7	80
4	146	29.4	42.8	169	24.1	40.7	95
5	144	29.0	41.7	143	22.9	32.8	79
6	115	28.3	32.5	108	22.9	24.8	76
7	88.5	28.8	25.5	97.5	23.3	22.7	89
8	80.3	28.7	23.0	85.3	22.8	19.4	85
9	76.6	27.1	20.7	75.3	22.6	17.0	82
10	66.7	65.9	17.3	71.7	22.1	15.8	92
Regeneration							
1	359	26.3	94.4	268	33.9	90.9	96
2	328	22.3	73.5	282	29.7	83.8	114
3	181	23.4	42.5	146	29.4	42.8	101
4	169	24.1	40.7	144	29.0	41.7	102
5	143	22.9	32.8	115	28.3	32.5	99
6	108	22.9	24 8	88.5	28.8	25.5	103
7	97.5	23.3	22.7	80.3	28.7	23.0	102
8	85.3	22.8	19.4	76.6	27.1	20.7	107
9	75.3	22.6	17.0	66.7	25.9	17.3	102
10	71.7	22.1	15.8	62.1	25.6	15.9	101

TASK B. REGENERATION PROCESS ALTERNATIVES

A new investigation continues on a method for the regeneration of sulfated limestone that has the potential advantage over single-step regeneration reaction (as reported above in Task A) of yielding a product gas containing a higher concentration of SO_2 and essentially no other easily reducible gases. The cost of converting the SO_2 in such a product gas to either sulfur or sulfuric acid should be lower than for gas from single-step regeneration.

The current work is directed toward evaluation of the $CaSO_4$-CaS "solid-solid" regeneration method. This regeneration method comprises two-step regeneration reactions, which are represented by reduction reaction (Eq. 1) at about 800°C followed by "solid-solid" reaction (Eq. 2) at higher temperature (1000-1100°C):

$$CaSO_4 + 4\ H_2 \rightarrow CaS + 4\ H_2O \quad (1)$$

$$3\ CaSO_4 + CaS \rightarrow 4\ CaO + 4\ SO_2 \quad (2)$$

Experimental Apparatus

Figure 21 is a schematic diagram of the fixed-bed apparatus for measuring the rates of reduction reaction (1) and the "solid-solid" reaction (2). A sample of a fully calcined and sulfated dolomite can be held in a platinum basket (2.2 cm ID by 7.6 cm high with a platinum mesh bottom) in an alumina tube heated by a vertical tube furnace. The lower half of the alumina tube, packed with α-alumina beads, functions as a heat exchanger.

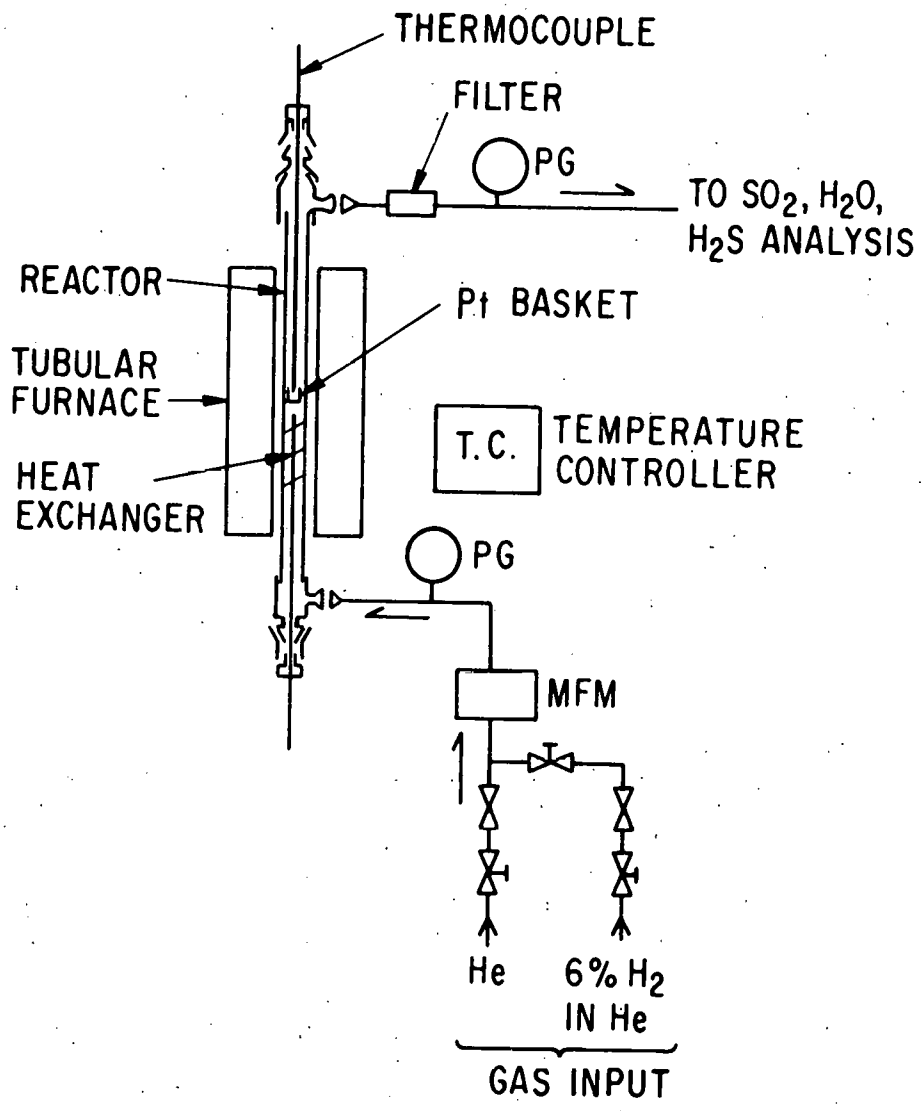

Fig. 21. Schematic Flow Diagram of the Reactor System.

Analytical Procedure

The following analytical procedure will be used. The effluent gas will be analyzed continuously for water and sulfur dioxide. Samples of the effluent gas will be taken for gas chromatographic analysis to check for the possible formation of hydrogen sulfide. The solids (reactant and product) will be chemically analyzed for calcium, total sulfur, and sulfide. The weight loss of the solid sample will be used to determine the extent of reaction.

Experimental Procedure

The experimental procedure employed for the first step of this regeneration method (reduction reaction) was as follows: A stock supply of half-calcined and sulfated Tymochtee dolomite from a PDU run (sulfated dolomite, PSI-4 bed, see ANL/ES-CEN-1016, pp. 89-94) was screened to obtain the desired fraction, -20 +35 mesh. Several batches of this screened stock supply were first fully calcined under a 20% CO_2/N_2 atmosphere at 900°C. Samples (8-24 g) of the fully calcined and sulfated Tymochtee dolomite were then reduced at 800°C under 6.32% H_2/He atmosphere. Results of the calcination and the reduction reaction are shown in Tables 8, 9, and 10.

Table 8. Weight Loss Results Under Calcination at 900°C and 1 Atm.

Calcination Batch No.	Half-Calcined Sulfated Samples (g)	Calcined and Sulfated Product (g)	Weight[a] Loss (%)
1	33.4	30.8	7.78
2	40.40	37.39	7.44

[a]The calculated theoretical percent weight loss is 8.45 wt %.

Table 9. Reduction of Calcined and Sulfated Dolomite at 800±4°C and 745±10 mm Hg under 6.32% H_2/He Atmosphere.

Expt. No.	Calcination Batch No.	Gas Flow Rate (liters/min)	Run Time (hr)	Initial Weight (g)	Final Weight (g)	Weight Loss (%)
Blank 1	1	4.71	1[a]	8.1023	8.0296	0.9
Blank 2	1	4.71	4[a]	8.0242	8.0183	0.1
Blank 3	1	4.71	2.5[a]	6.0378	5.9091	2.1
RED-I-1[c]	1	4.71	4[b]	8.0540	6.0314	25.1
RED-II-1	1	4.71	1[b]	8.1219	7.0161	13.6
RED-III-2	2	4.71	1[b]	24.2813	23.1667	4.6
RED-IV-1	1	1.54	1[b]	8.0873	7.1600	11.5
RED-V-2	2	4.71	1[b]	8.1353	6.9860	14.1

[a]He atmosphere with no hydrogen flowing.
[b]Reduction time. Follows 2.5 hr with He atmosphere and no hydrogen flowing.
[c]RED-I-1 means the first reduction experiment (I) from calcination batch No. 1.

Table 10. Analysis of Dolomite (Table 9).

Expt. No.	Weight Loss (%)	Sample[a] Analysis (mol)	Yield from Weight Loss (%)	Yield from Sulfide Analysis (%)
Blank 3	2.1	0.6412 Ca 0.3450 $S^=$ <0.0016 $S^=$ 0.0043 $CO_3^=$		
RED-V-2	14.1	0.6195 Ca 0.3362 $S^=$ 0.0499 $S^=$ 0.0060 $CO_3^=$	65.5	14.8
RED-I-1	25.1	0.6073 Ca 0.3512 $S^=$ 0.1160 $S^=$ 0.0023 $CO_3^=$	111.7	33.0

[a]Average: 0.623 ± 0.018 mol Ca (±2.9%)
0.344 ± 0.008 mol S (±2.4%)

Initial Results and Discussion--Reduction Step

Table 9 shows that the reaction with a 8 g initial sample was not H_2-limited. Table 10 shows that the extent of the reduction reaction computed from the weight change was significantly larger than that computed from the sulfide analysis of the solid product. The discrepancy is believed to be caused by air oxidation and hydrolysis of the sulfide in the sample when it was ground up for chemical analysis. Future samples for sulfide analysis will be ground in an inert atmosphere. Acceptable material balances on calcium and sulfur in the samples were obtained, indicating that "solid-solid" reaction had been negligible at 800°C and the other conditions of our experiments.

The next step is to carry out both reactions sequentially, using the chemical composition data obtained during the reduction reaction in experiment RED-V-2, which shows that after the first step (reduction reaction), the starting material for the second step ("solid-solid" reaction) contains an excess of CaS (65.5% of reduced form) compared to a stoichiometric 25% required by the "solid-solid" reaction. It is believed on the basis of previous experiments done by P. Cunningham (ANL/ES-CEN-1016, p. 140) that more than the stoichiometric quantity of the reduced form CaS is needed to force the solid-solid reaction toward completion.

After reaction to the desired percent of reduced form, solid-solid reaction will start under a helium atmosphere at a temperature higher

than 800°C, with the final equilibrium temperature in the range of 1000-1100°C.

Analysis of off-gases and a sample of the product will enable us to obtain an approximate value for the reaction rate for the "solid-solid" reaction (second step), which is expected to be slower than the reduction reaction (first step).

TASK C. SYNTHETIC SORBENTS FOR SO_2 EMISSION CONTROL

In fluidized-bed coal combustors, naturally occurring limestones are the predominant materials being considered as additives for removing SO_2 from the combustion gas. This is primarily due to the low cost of these calcium-bearing materials. However, disadvantages of using natural limestones are the environmental problems associated with quarrying and disposing of large quantities of solids. Possibly, regeneration can reduce the quantity of limestone required to meet EPA SO_2 standards. How much the feed rate of fresh limestone can be reduced by the use of regenerated limestone is limited by the loss of limestone reactivity under cyclic sulfation-regeneration operation and by decrepitation. Therefore, a synthetic SO_2 sorbent which would further reduce the environmental problems associated with disposal of SO_2 sorbent is desirable.

The major disadvantage of synthetic sorbents is their high cost. Therefore, a cost analysis (see also ANL/ES-CEN-1017) is presented below, along with initial results of the investigation of methods to prepare "low cost" synthetic sorbents.

The cost of synthetic sorbents such as CaO on alumina support materials (studied recently as part of this task) is estimated to range from about $200/ton to $2000/ton. Dolomite presently costs $10-20/ton. This information can be used to determine the incremental increase in power production cost (mills/kWh) if synthetic sorbents should be used in place of dolomite in pressurized fluidized-bed boilers (PFBB).

Westinghouse[7] determined the energy cost (mills/kWh) for PFBB using dolomite with a Ca/S ratio of 2. The cost analysis was performed for 17.5% and 100% excess air ("one pass-through" of the sorbent) and 100% excess air with sorbent regeneration. The fluidized-bed boilers were 600 MW, and the fuel was coal containing 3% sulfur. It was found that addition of the regeneration step adds approximately 3 mills/kWh to the cost of the PFBB (100% excess air), increasing the energy cost from 20 mills/kWh to 23 mills/kWh. The sorbent (120 tons/hr of dolomite) energy cost was 1.26 mills/kWh for the PFBB with a "once-through" SO_2-sorbent system.

Based on the above Westinghouse cost analyses, we calculated the electrical energy cost of using synthetic SO_2 sorbents. The estimated minimum cost of synthetic sorbents is approximately 20 times that of the natural sorbents or $200/ton. Thus, the energy cost for synthetic sorbents on a

once-through basis would be 25.2 mills/kWh,* increasing the total cost of PFBB from 20 mills/kWh to 45.2 mills/kWh. This is obviously prohibitive; therefore, the use of synthetic sorbents can be considered only if regeneration is part of the PFBB system. The minimum cost of the entire PFBB process is approximately 23 mills/kWh[7] (including the regeneration of dolomite). Since dolomite is inexpensive and has a minimal effect on cost, the effects on cost of the fresh feed rate and the feed rate of regenerated dolomite were not specified by Westinghouse. However, due to the higher cost of synthetic sorbents, the "makeup" rate of fresh synthetic sorbents is important.

Figure 22 shows PFBB energy costs, using a synthetic sorbent, as a function of sorbent material cost for various ratios of "fresh" sorbent feed rate (FF) to total feed rate (TF). A low value of FF/TF means that the sorbent has a low attrition rate and retains almost all of its reactivity during recycle. This graph clearly shows that if synthetic sorbents are to receive serious consideration, either the ratio of fresh feed to total feed (fresh plus regenerated sorbent feed), FF/TF, must be very low (<0.04) and/or the sorbent material cost must be low (<$500/ton).

For example, for a FF/TF of 0.1, a materials cost greater than $200/ton would be prohibitive. However, if the FF/TF value were 0.01, a materials cost of $1000/ton would add only 1.3 mills/kWh to plant energy cost. A 0.01 FF/TF value may be very difficult to realize, since it represents only 1% loss per cycle due to both attrition and reactivity loss (for example, from slag interaction).

These calculations assume a Ca/S ratio of 1 (instead of 2 as was used by Westinghouse) for a 10% Ca in α-Al_2O_3 sorbent. This Ca/S ratio of 1 with dolomite has been shown to be effective in meeting EPA SO_2 standards.

Since synthetic sorbents are expected to cost more than natural sorbents, it is important to estimate early in this program the probable cost-environmental tradeoff which will be introduced if synthetic sorbents are successfully introduced. The electrical energy cost for a PFBB can be estimated from Fig. 22 and then used to make the cost-environmental tradeoff calculation. If the fresh to total feed rate ratio is 0.1, it is estimated that the electrical energy cost for a synthetic sorbent costing $200/ton would be about 2 mills/kWh higher than that expected for dolomite with recycle. The amount of waste produced by the synthetic sorbent would be about one-half the amount produced with dolomite. Thus, for this case, halving the environmental impact costs about 2 mills/kWh. If a fresh feed to total feed ratio of 0.04 could be achieved (equivalent to 25 cycles), a sorbent with the cost of about $500/ton would add 2 mills/kWh to the cost of dolomite (with recycle), as would the $200/ton sorbent discussed above. In this case, the environmental impact of using the synthetic sorbent would be about one-tenth that produced using dolomite. These estimates are important in setting realistic cost and performance requirements for synthetic sorbents.

---

*Cost due to synthetic sorbent (once-through) = $1.26 \times \frac{(\$/\text{ton})}{10} = 1.26 \times \frac{200}{10}$ = 25.2 mills/kWh.

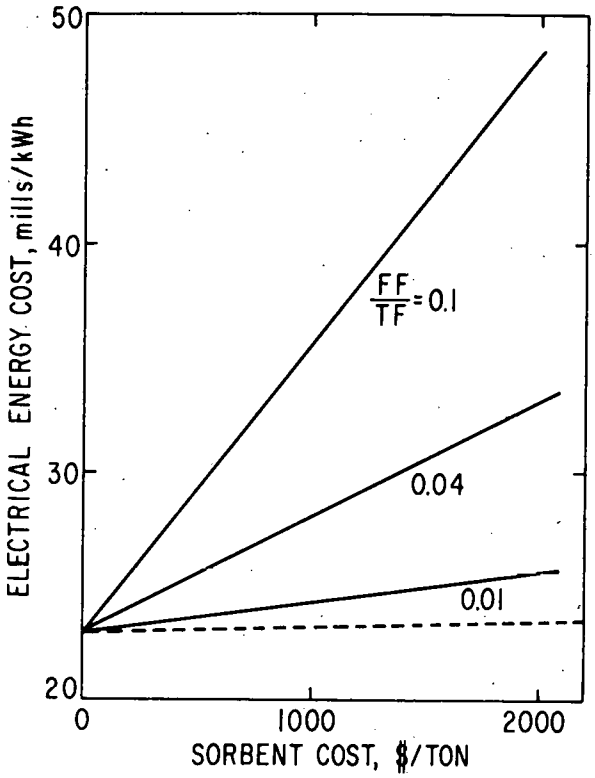

Fig. 22. Relationship of Electrical Energy Cost to Synthetic Sorbent Cost and Ratio of Fresh Feed (FF) to Total Feed (TF).

Due to the high capital cost of synthetic sorbents compared to that of naturally occurring limestones, an investigation has been initiated to determine the feasibility of producing "low cost" synthetic sorbents (costing approximately $200-400/ton). The use of calcined bauxite obtained from C. E. Minerals was tested as a support material for calcium oxide, in place of α-Al_2O_3. This material is approximately 70% Al_2O_3, 25% SiO_2, 3% TiO_2, and 2% Fe_2O_3. It has been calcined at approximately 1730°C and is very hard and attrition resistant.

Calcium oxide was impregnated into the calcined bauxite material, producing a 5.5% CaO sorbent. The sulfation rate in the TGA was very low; only 18% of the CaO was converted to $CaSO_4$ in 5 hr. Only 14 g of SO_3 can be captured per kg of sorbent in 5 hr, compared with 126 g/kg for CaO in α-Al_2O_3 and 230 g/kg for Tymochtee dolomite in 5 hr.

Since impregnation of the calcined bauxite with CaO was difficult, it is speculated that the material had a low porosity due to the high calcination temperature used. Bauxite calcined at lower temperatures will be tested in the future.

The studies performed on synthetic SO_2 sorbents by the Dow Chemical Company under a subcontract has been completed and a preliminary report (oral) has been made. In these studies they measured the SO_2 capacities of sorbents prepared by placing alkaline earth oxides or alkali metal oxides in supports of Al_2O_3 or TiO_2. From these tests they concluded that the CaO-Al_2O_3 system is the most promising in agreement with the results of the work done at Argonne. They also made a superficial cost analysis for the use of synthetic sorbents and concluded that it appeared very doubtful that synthetic sorbents could be made at a low enough cost to compete with the cheap natural sorbents such as limestone. Therefore, they recommended that the work on synthetic sorbents cease. The final report on this subcontract will be appended to the next quarterly report.

Our preliminary cost analysis also indicates that if synthetic sorbents are to be competative that the cost must be reduced and/or their performance (SO_2 capacity) improved. Therefore, before ending our studies we plan to briefly investigate the feasibility of using various low cost starting materials, such as bauxite, for the preparation of synthetic sorbents. On the completion of these studies the work will be terminated.

TASK D. LIMESTONE CHARACTERIZATION

A research program is under way to characterize limestone for fluidized-bed coal conversion plants. That is, the reactivity of limestone with SO_2 under various environmental conditions will be determined and correlated with the limestone's physical properties. Pretreatment (precalcination and heat treatment) will be investigated. The mechanism of SO_2 capture will be studied. Finally, the attrition rate of the various limestones will be determined. The compiled results will be used in designing a series of tests for limestones, the results of which will determine limestone performance characteristics. In this report, Greer limestone was tested for SO_2 reactivity with and without pretreatment.

In atmospheric fluidized-bed coal combustion, large quantities of limestone sorbent (Ca/S ratio of 4/1 to 6/1) may be required so that the flue gas will meet EPA SO_2 emission standards. Pretreatment of limestones to enhance their reactivity and their calcium utilization would reduce limestone requirements. Therefore, the effect of calcination-heat treatment on calcium utilization of Greer limestone has been studied and a preliminary economic-environmental impact assessment made.

Greer limestone was precalcined at 900°C in a 20-% CO_2-80% N_2 gas stream then heat-treated at 900°C for 0, 2, 6, and 22.2 hr. The pretreated Greer limestones were then sulfated at 900°C on a TGA, using 0.3% SO_2 - 5% O_2 in N_2.

In Fig. 23, the percent conversion of CaO to $CaSO_4$ is given as a function of sulfation time for the various pretreated limestones. Their CaO conversions are compared with that of Greer limestone, which was simultaneously calcined and sulfated with 0.3% SO_2 - 5% O_2 - 20% CO_2 in N_2 gas. The Greer limestone which was simultaneously calcined and sulfated had the poorest conversion--only 28% of the CaO was utilized to capture SO_2. This result is in excellent agreement with the data obtained on Greer limestone by Pope, Evans and Robbins[8] in the 9 ft^2 atmospheric combustor. They reported calcium utilizations of 25 to 28 percent with a limestone residence time of approximately 4 hr.

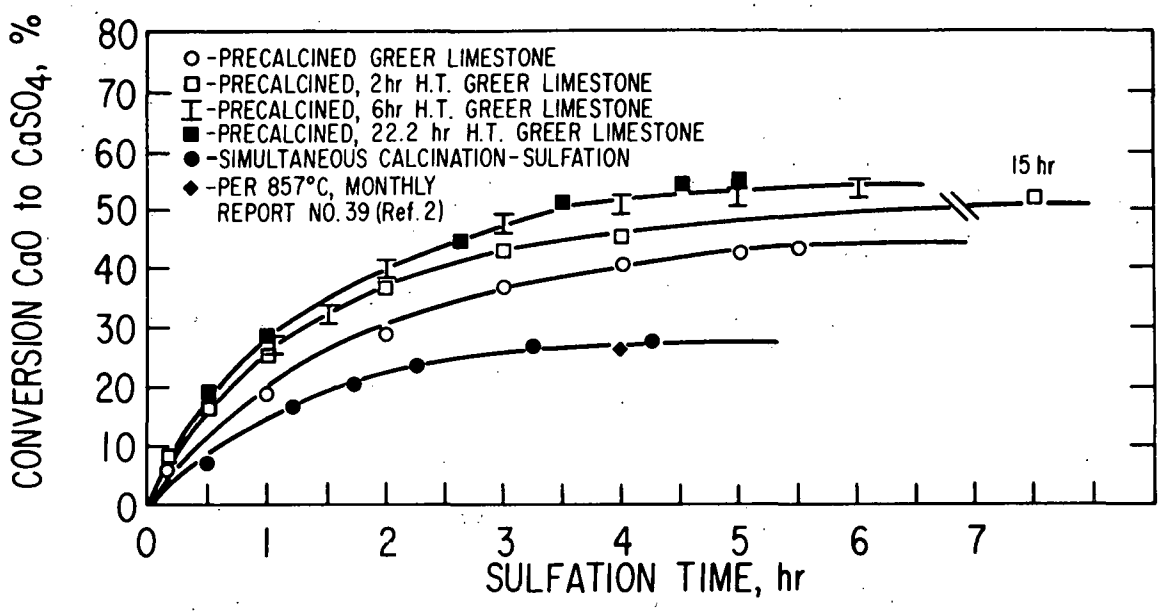

Fig. 23. Calcium Utilization as a Function of Various Pretreatments. Sulfation at 900°C with 0.3% SO_2 – 5% O_2 in N_2.

The Greer limestone tested in the TGA (Fig. 23) calcined completely in approximately 10 min. This was twice the calcination time for the limestone which had been simultaneously calcined and sulfated. The lower calcination rate during simultaneous calcination-sulfation probably produces a limestone having smaller pores and thereby results in less calcium utilization.

Precalcination increased the calcium utilization from 28% to 43% for a 5-hr sulfation time. Heat treating the limestone for 2 hr after a 5-min precalcination further increased the calcium utilization from 43% to 48% (a residence time of 15 hr gave a 51% calcium utilization). Heat treating for 6 hr and 22.2 hr gave calcium utilizations of 52 and 55% in 5 hr. The precalcination and heat treatments definitely increased the sulfation rate and calcium utilization. However, after heat treating for 6 hr, additional heat treatment gave a minimal change in sorbent performance.

To apply the results shown in Fig. 23 to a practical fluidized-bed combustion system, a preliminary economic analysis was performed to determine the cost of a precalcination-heat treatment step. The economic analysis was made for a 600-MW atmospheric fluidized-bed coal combustor.

The pretreatment costs were based on the costs quoted by the Kennedy Van Saun Corporation.[9] A kiln (calciner and heat treating unit) was estimated to cost $5 million/(1000 tons of calcined product per day). A limestone residence time of 178 min was assumed. This unit requires two operators per shift and also requires 5,000,000 Btu of energy per ton of product (calcined, heat-treated limestone). From this information, a first order economic analysis was performed to determine the cost of a pretreater for various limestone residence times and for various quantities of limestone per day.

Five costs were included in the analysis: capital, installation, operating, maintenance, and fuel costs. The capital cost was estimated to be a function of the limestone residence time and lime production rate to the 0.6 power. The installation cost was assumed to be twice the capital cost. On the basis of two men per shift, the operating cost was estimated to be 300,000 dollars per year. Maintenance cost and fuel cost are directly a function of the lime production rate. Limestone requirements were estimated to be 1720 tons/day for a plant using a Ca/S ratio of 4. Figure 24 shows the relative importance of the five costs on the energy cost for limestone precalcination and heat treatment for a 600-MW coal combustor. A Ca/S ratio of 4 and a 3% sulfur coal were assumed. For heat treatment times greater than 2 hr, the capital cost (installed) is the largest cost; the next largest is fuel cost.

Figure 25 shows the increase in energy cost due to the addition of a pretreater to a 600-MW plant as a function of limestone residence time in the kiln for three different Ca/S ratios. If a 2-hr residence time and a Ca/S ratio of 4 are assumed, the increased energy cost would be 0.85 mill/kWh. That is, it would cost 0.85 mill/kWh to decrease the environmental impact by 42 percent.

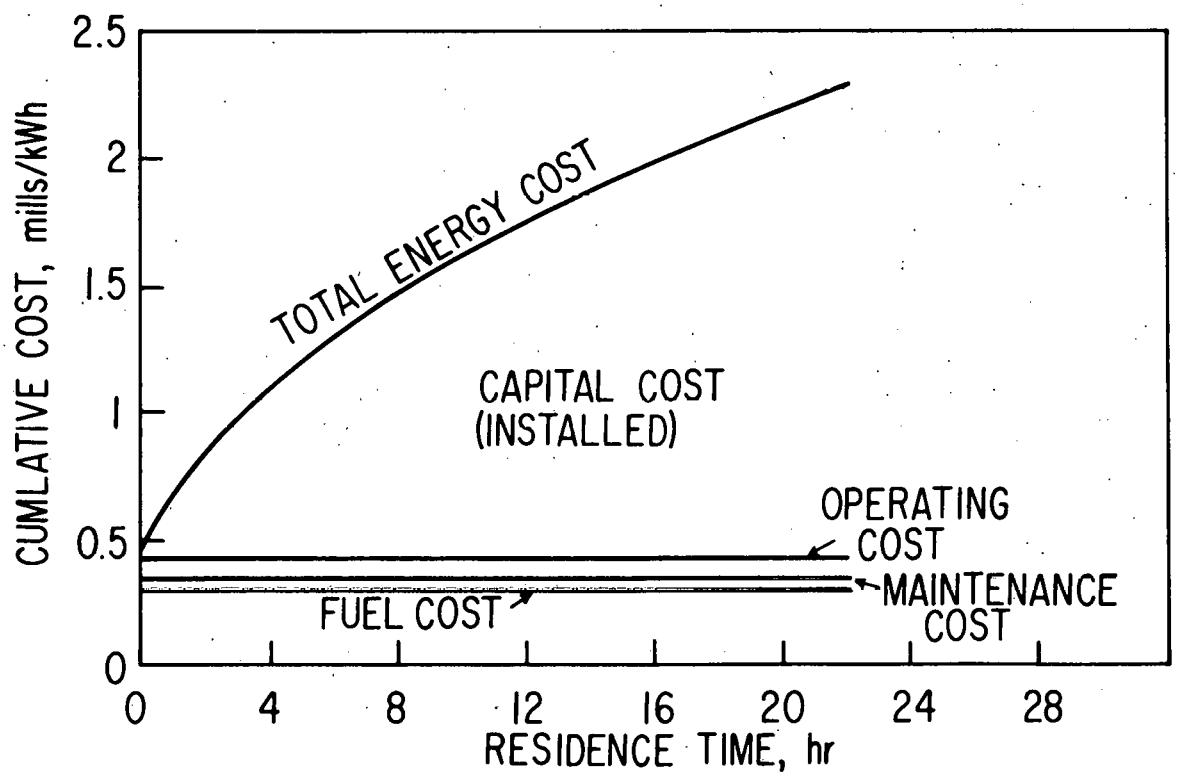

Fig. 24. Calcination of Limestone for 600-MW Plant Using Ca/S = 4.

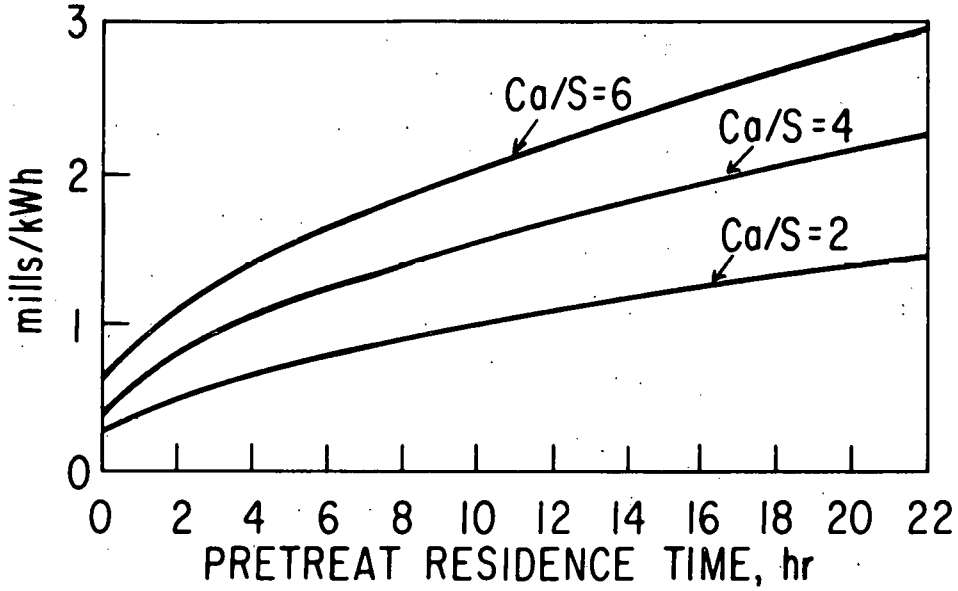

Fig. 25. Increased Energy Cost due to Limestone Pretreatment at 900°C.

Figure 26 illustrates the energy cost for reducing the environmental impact of Greer limestone. The environmental impact of Greer limestone with no precalcination treatment was arbitrarily set at 1.0. This can be converted to a given quantity of limestone that must be mined and disposed of. As shown in Fig. 26, the environmental impact can be reduced by increasing the energy cost (by means of pretreatment and thus greater calcium utilization). If the Ca/S ratio is 4, the quantity of limestone required can be reduced by 40% for an increased energy cost of 0.8 mill/kWh; however, decreasing the limestone requirements further would require a large increase in energy cost. In fact, however much is spent, the environmental imapct can not be reduced more than 50% by heat treating.

The above analysis is only for Greer limestone which has been tested at 900°C. Also, the cost analysis for pretreatment kilns is only a first approximation, and the effect of pretreatment on attrition has not yet been determined. Nevertheless, this is the type of cost *vs* environmental impact information needed for assessment of the viability of pretreatment.

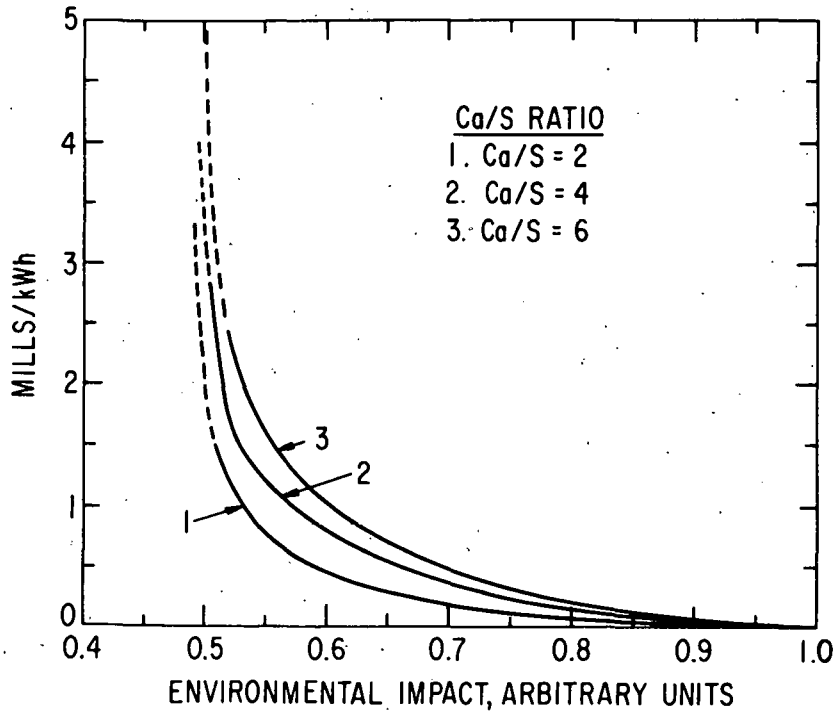

Fig. 26. Increased Energy Cost Required to Reduce the Environmental Impact of Mining and Disposal of Sorbents.

TASK E. TRACE ELEMENTS AND COMBUSTION EMISSION STUDIES

Enhancement of Limestone Sulfation

In a continuing study of the mechanism and the effect of mineralizing additives on the sulfation of limestone (see ANL/ES-CEN-1017, p. 38), preliminary experiments were performed using NaCl as the agent for enhancing the reactivity of limestone. These experiments were designed to provide qualitative assurance of the positive effect of common salt on the sulfur capacity of limestone. The suggestion that chemical additives to a fluidized-bed coal combustion system might enhance the SO_2 capacity of limestone is based in part on work done at Pope, Evans and Robbins,[8] who demonstrated that the addition of NaCl to a spent limestone sorbent renewed its SO_2 reactivity. This result is in agreement with a large amount of prior work on the use of various salt additives to facilitate the formation of highly reactive lime from the calcination of limestone.

Calcite spar crystals were used because of their low porosity and hence low reactivity and their high purity level (removing the possibility of side effects from included impurities). The low reactivity leads to a reaction

only on the surface of the crystal, which leads to a layering of reaction products, allowing the extent of reaction to be determined by visual examination. The $CaSO_4$ was formed as a highly crystalline layer surrounding an inner layer of CaO formed by calcination of the original $CaCO_3$.

Table 11 summarizes the observations made during a series of diagnostic experiments performed in a horizontal furnace, which lead to the design of thermogravimetric experiments to provide quantitative results. From the table, it can be seen that under simultaneous calcination and sulfation conditions, there is a marked decrease in the total amount of reacted material during a given period of time as compared with the amount of reaction under simple calcination conditions. The diffusional barrier of incoming SO_2 slows down the calcination of the $CaCO_3$. The addition of the mineralizer, NaCl, increases both the extent of calcination and the extent of sulfation by improving the porosity of the calcined stone. When simple calcination is performed under sufficient CO_2 pressure that calcination does not occur readily, the addition of NaCl vapor to this same system effectively overcomes the diffusional barriers, and calcination proceeds rapidly.

When a precalcined stone is reacted with SO_2, the amount of sulfation both with and without salt addition is increased relative to simultaneous calcination-sulfation. The addition of NaCl, however, increases the amount of sulfation and of interpenetration of CaO by the crystallizing $CaSO_4$, with a fluid phase following defects and grain boundaries within the crystal. This differs considerably from the sharply defined reaction front observed with no salt present.

Most workers agree that the reaction mechanisms of both calcination and sulfation have rate-controlling diffusion-limited steps so that any mineralizing effects in calcination may have similar results in sulfation. Many salts have been shown to be effective in the calcination of limestone and are used routinely to promote the formation of reactive limes. Table 12 summarizes the results of qualitative experiments in which NaCl and several other additives were used. The only salts comparable to NaCl (in terms of magnitude of effect) are $CaCl_2$ and $MgCl_2$; NaOH, Na_2CO_3, and Na_2SO_4 all behave similarly; the first two salts sulfate readily during reaction and then effectively behave as Na_2SO_4 in the system. One set of experiments was done using open boats of salt introduced into the furnace to supply a vapor to interact with the calcite. If a porous limestone instead of calcite spar crystals were used, the salts could be directly deposited within the stone and thus could perhaps avoid the difficulties associated with subsequent sulfation of the additive in an exposed situation.

The volatility of the Na_2SO_4 is low compared to that of NaCl and $CaCl_2$. Its melting point is fairly high compared to the reaction temperature, whereas NaCl and $CaCl_2$ are easily melted below 900°C. Sulfation with Na_2SO_4 and the other related salts (NaOH and Na_2CO_3) occurred only when the salts were placed directly on the calcite crystals. These effects support the view that a fluid phase is present during the reaction. The presence of low-melting eutectics of salt and matrix appears to open up the system to further sulfation. In porous stones, these salts may indeed have much greater effects due to more intimate surface contact of the salt with the stone.

Table 11. Effect of NaCl on Reactions of Calcite.

Experiment	Additive	NaCl Introduction Technique	Reaction Conditions[a]	Comments
NaCl-1a	None	-	Calcined at 900°C in air, 15 min	Reaction almost complete
NaCl-1b	NaCl	Vapor	Calcined at 900°C in air, 15 min	Complete reaction, salt gave a more porous product
NaCl-2a	None	-	Calcined at 900°C in high CO_2, 15 min	No reaction
NaCl-2b	NaCl	Vapor	Calcined at 900°C in high CO_2, 15 min	Almost complete reaction, porous product
NaCl-3b	None	-	Simultaneous 900°C calcination/sulfation, 15 min	Surficial reaction, white coating with thicker layer of CaO
NaCl-3B	NaCl	Vapor	Simultaneous 900°C calcination/sulfation, 15 min	Some $CaCO_3$ remains in center, a thick layer of CaO, outer thick layer of crystalline $CaSO_4$
NaCl-4a	None	-	Precalcined at 900°C 30 min, then exposed to SO_2 for 15 min	Thin layer of $CaSO_4$, flaky
NaCl-4b	NaCl	Vapor	Precalcined at 900°C 30 min, then exposed to SO_2 for 15 min	Thick layer of crystalline $CaSO_4$ intergrown with CaO
NaCl-5a	None	-	Partially sulfated stone further reacted, 15 min	No appreciable change
NaCl-5b	NaCl	Vapor	Partially sulfated stone further reacted, 15 min	Thicker shell developed having a more crystalline character

[a]Sulfation atmosphere was 20 vol % SO_2 in air.

Table 12. Effect of Additives on Simultaneous Calcination-Sulfation of Crystalline Calcite at 900°C.

Expt.	Additive	Salt Introduction Mode	Reaction Time (min)	% SO_2 in Air	Extent of Reaction	Comments
CS 1	None	None	30	25%	Minor	Surficial white deposit on $CaSO_4$ plus CaO
CS 2a	NaCl	Vapor[a]	30	25%	Major	Highly crystalline $CaSO_4$ over a thick layer of CaO
CS 2b	NaCl	Solid[b]	30	25%	Major	As in CS 2a, over entire crystal
CS 3a	$CaCl_2$	Vapor	30	25%	Major	Similar to NaCl though less CaO formed
CS 3b	$CaCl_2$	Solid	30	25%	Major	Similar to NaCl
CS 4a	Na_2CO_3	Vapor	30	25%	Minor	Some surficial reaction
CS 4b	Na_2CO_3	Solid	30	25%	Major	Reaction localized with small effects elsewhere
CS 5a	NaOH	Vapor	30	25%	Minor	Very little (NaOH appears to boil away and sulfate)
CS 5b	NaOH	Solid	30	25%	Major	Very localized (boils away)
CS 6a	Na_2SO_4	Vapor	30	25%	Minor	Small amount of surface reaction
CS 6b	Na_2SO_4	Solid	30	25%	Major	Entire crystal surface reacted
CS 7a	$MgCl_2$	Vapor	30	25%	Major	Similar to $CaCl_2$ though less extensive reaction
CS 7b	$MgCl_2$	Solid	30	25%	Major	Similar to $CaCl_2$

[a] Additive in a boat upstream.
[b] Additive on calcite surface as slurry.

These qualitative results indicate the desirability of pursuing quantitative experiments on a thermogravimetric apparatus to measure weight changes during sulfation and to deduce absolute values for sulfur capture when mineralizers are present. The effects on sulfur absorption of varying the concentration of the additives are reported below.

Figure 27 shows the effect of precalcination of Greer limestone (in the tube furnace) on sulfur retention and the enhancement by NaCl. The NaCl was introduced by immersion of the limestone in an aqueous solution. After it was soaked in a 20% NaCl solution, it was dried at 150°C, leaving approximately 1% NaCl by weight in the stone. The sample was then calcined in the furnace assembly at 900°C in an atmosphere of 20% CO_2 in N_2, reweighed to verify the completion of calcination, and then exposed to a gas mixture containing 4% SO_2. Despite the loss by evaporation of most of the salt, the effects upon sulfation can be seen, with the stones' capacity for SO_2 increased by approximately 50%. The effect of simultaneous calcination/sulfation can also be seen--a substantially lower reactivity--although within the time period the total amount of conversion eventually reaches the same level as does the precalcined stone at this concentration of SO_2. At lower concentrations of SO_2 (Fig. 28), as in a flue gas, the effect is much more apparent because the uncalcined stone does not reach the same level of sulfation as the precalcined stone in any reasonable time interval. Figure 28 shows experimental data points from the thermogravimetric analyzer with 0.4% SO_2.

Due to corrosion of the flow meters, the runs in the horizontal tube furnaces were inadvertently carried out at 4% SO_2. Future runs will be done at 0.4% SO_2 to allow comparisons with the TGA data and to conform to the flue gas composition.

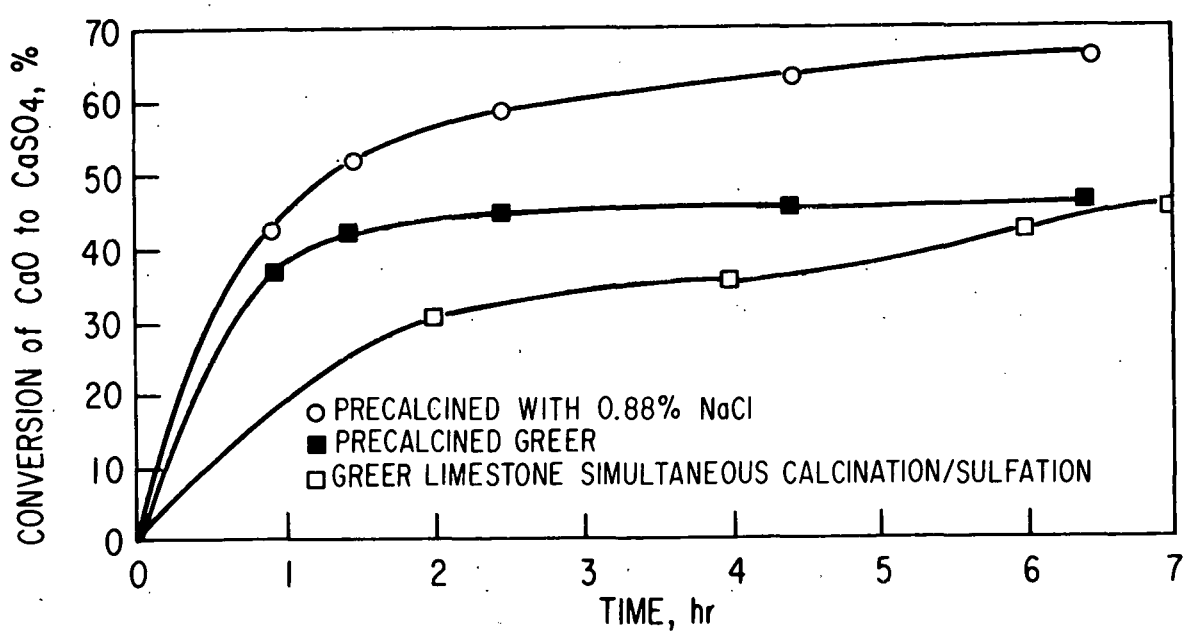

Fig. 27. Enhanced Sulfation in 4% SO_2 at 850°C of Greer Limestone by Pretreatment.

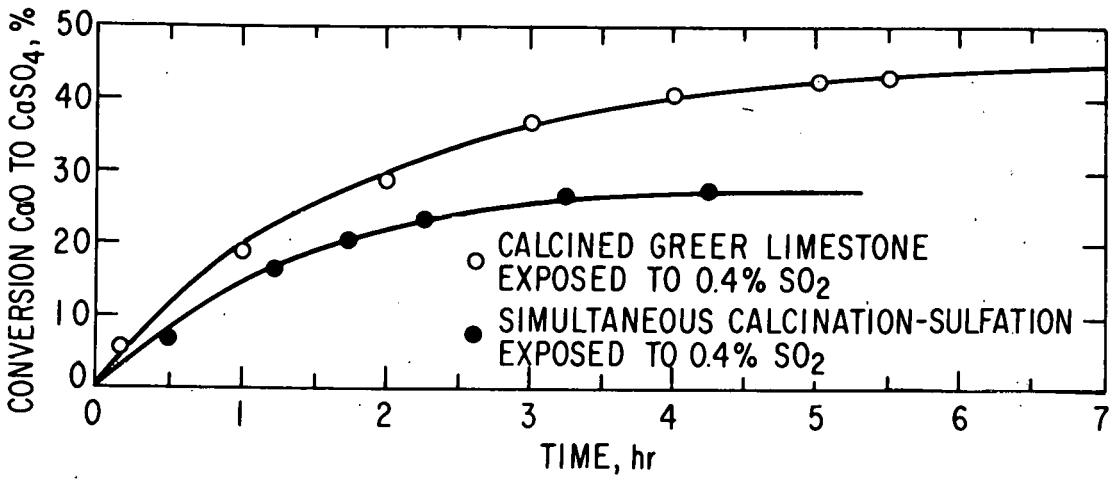

Fig. 28. Enhanced Sulfation in 0.4% SO_2 at 850°C of Greer Limestone by Precalcination.

Sulfation reactions of Greer limestone in the presence of various salts were carried out at 850°C in the horizontal tube furnaces. NaCl, Na_2CO_3, $CaCl_2$, and Na_2SO_4 were used at various concentrations with Greer limestone to study the effect of increasing the amount of mineralizer on the absorption of sulfur dioxide. Figures 29, 30, 31, and 32 show curves of time versus percentage conversion of the available CaO to $CaSO_4$, as measured by weight changes and sulfate analyses. In the experiments performed so far, NaCl enhances sulfation to the greatest extent. Higher concentrations of mineralizing salts will be used to complete the correlation of percent conversion with concentration of salt at lower SO_2 levels. At present, there is not enough data nor analyses of some of the sulfation products for complete understanding of the interaction between various salts and sulfur retention.

Future work will also include sulfation runs with a group of representative limestones and dolomites in order to gauge the effect of mineralizers on limestones of varying morphology and composition. NaCl will be used as the most effective mineralizer, and various stones and their sulfur absorption capabilities will be compared.

Porosity measurements will be made on limestone calcined in the presence of NaCl to evaluate any changes noted, as was found for Greer limestone

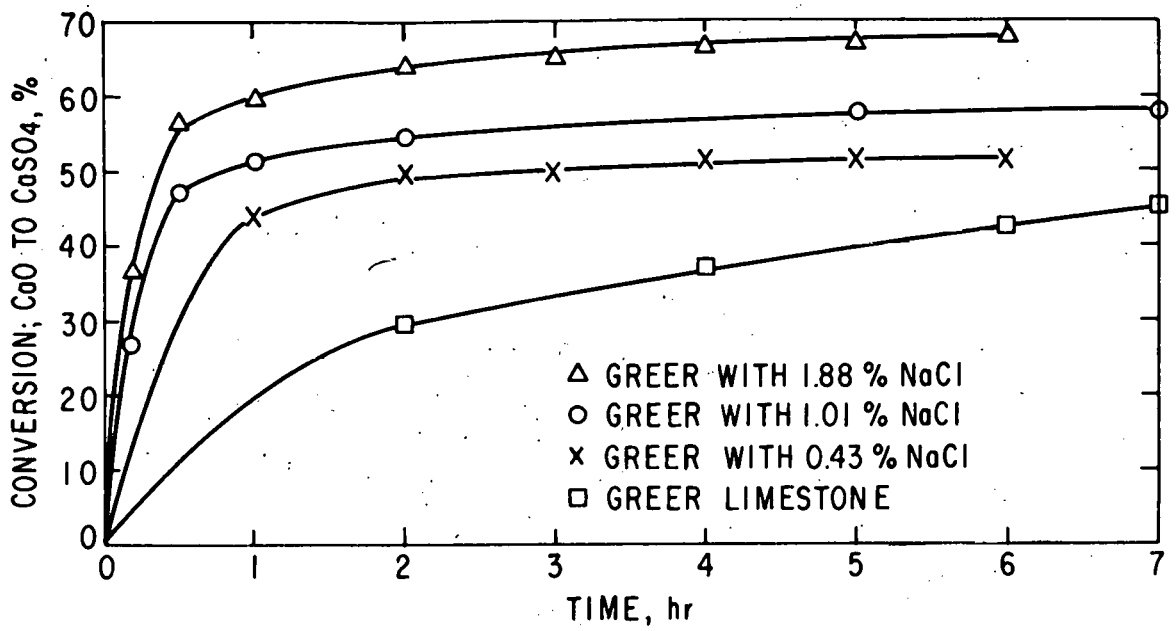

Fig. 29. Enhanced Sulfation of Greer Limestone with NaCl at 850°C, 4% SO_2.

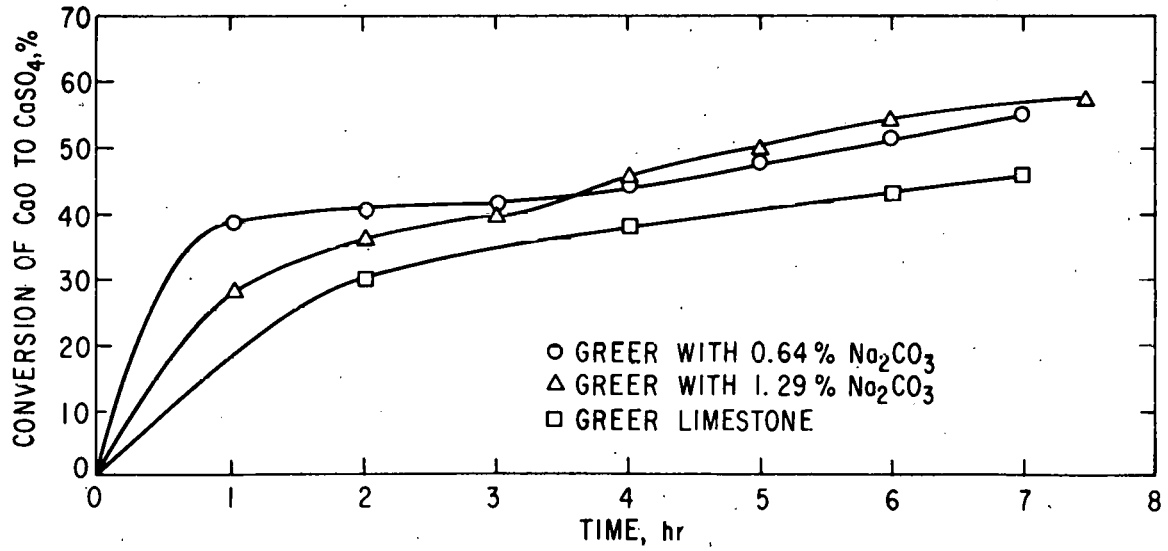

Fig. 30. Enhanced Sulfation of Greer Limestone with Na_2CO_3 at 850°C, 4% SO_2.

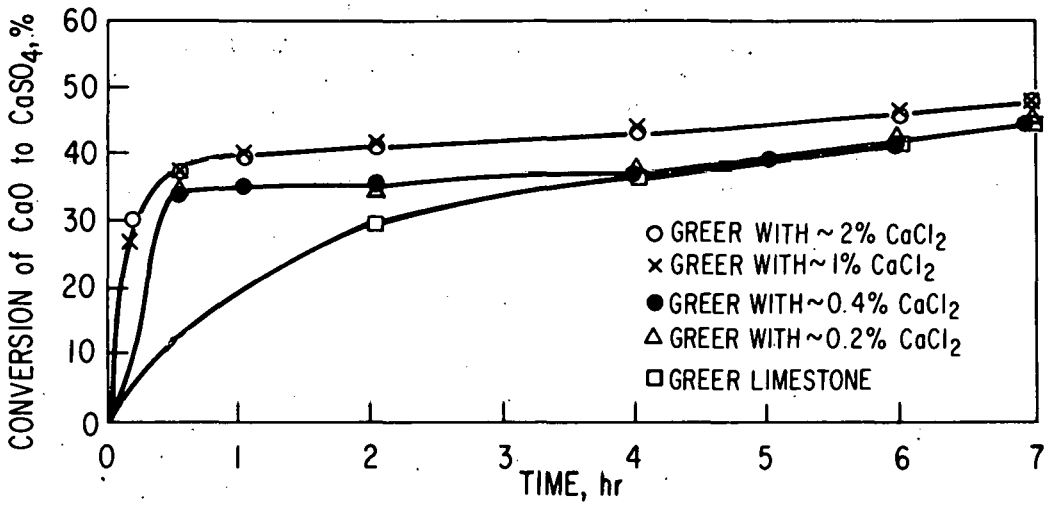

Fig. 31. Enhanced Sulfation of Greer Limestone with $CaCl_2$ at 850°C, 4% SO_2.

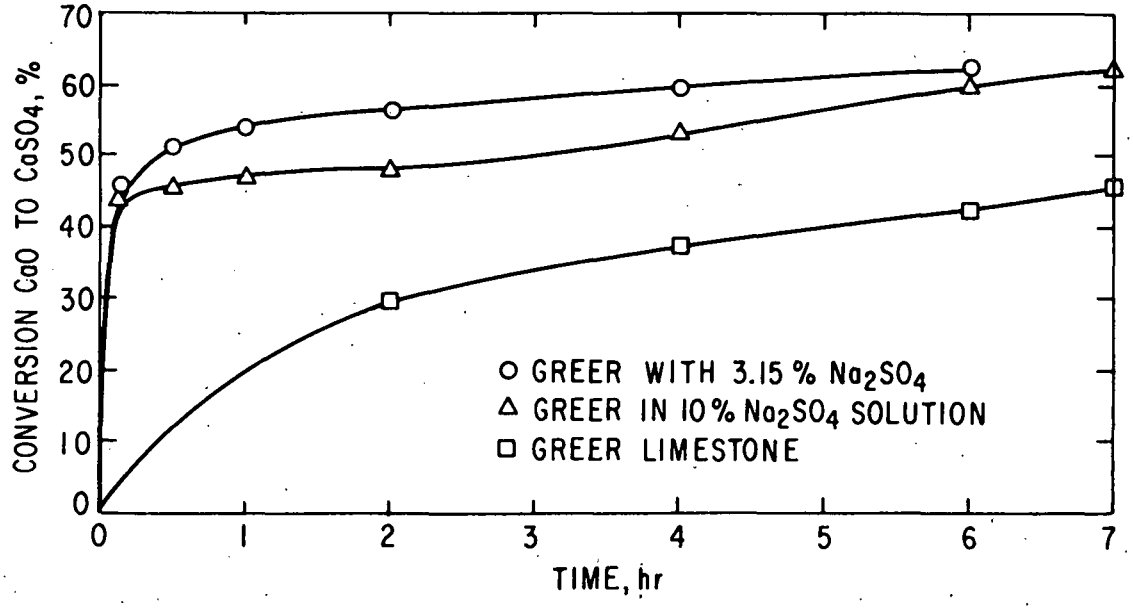

Fig. 32. Enhanced Sulfation of Greer Limestone with Na_2SO_4 at 850°C, 4% SO_2.

(ANL/ES-CEN-1017 p. 45 ff). Attrition studies also will be performed on treated stones, in order to evaluate the feasibility of using NaCl in fluidized-bed coal combustion where stone integrity is an important characteristic. In conjunction with the above, samples will be microscopically examined in an attempt to substantiate the proposed mechanism reported earlier (ANL/ES-CEN-1017, p. 38 ff) for the effect of mineralizers on the sulfation of limestone.

The Determination of Inorganic Constituents in the Effluent Gas from Coal Combustion

Some chemical elements in combustion gases are known to cause severe metal corrosion--for example, on turbine blades in a combined cycle system. The objectives of this study are to determine quantitatively which elements are present in the hot combustion gas of coal, in either volatile or particulate form. It is desirable to identify the compounds present as particulate species and their amounts, as well as the compounds present as condensable species and their amounts.

The laboratory-scale, batch-type, fixed-bed combustor system constructed for these studies was presented and described in the most recent annual report (ANL/ES-CEN-1016). The combustor contains a preheater section, the sample pan, a tubular filter and a cold trap. As mentioned in the previous report of this series (ANL/ES-CEN-1017, p. 34 ff.), shakedown coal-combustion experiments have demonstrated satisfactory performance of the combustor system. Several additional shakedown experiments were conducted during this report period to develop a control technique for burning coal without condensing tar and/or soot on the cold trap. This control technique was successfully achieved by introducing afterburning air downstream from the combustion section of the combustor. The purpose of the afterburning air was to facilitate combustion of volatile matter evolved during the early stage of the experiment. This control technique, which has been employed as a standard experimental procedure in all subsequent experiments, is as follows:

Prior to heatup of the combustion section, afterburning air was introduced into the combustor at a flow rate of 5.0 liters/min. The coal sample was then heated indirectly by induction heating (applied to the combustor pipe at the combustion section of the combustor). When, during heatup of the coal sample, CO_2 gas was detected in the effluent by the effluent gas analyzer, the inlet gas mixture of O_2 and N_2 was introduced into the combustion section to burn the coal. During initial feeding of the inlet gas mixture (65% O_2 in N_2 at a flow rate of 6.4 liters/min), volatile matter evolved during heatup of coal was completely combusted. This high-O_2-content gas mixture also burned coal at a high rate to heat the bed to the combustion temperatures rapidly. When the desired coal bed temperature was reached, the O_2 content of the inlet gas mixture was gradually reduced to 8%, and the afterburning air stream was shut off. The flow rate of the final inlet gas mixture was 6.0 liters/min. The combustion temperature of the coal bed was controlled at the desired level by regulating both the O_2 content of the inlet gas mixture and the induction heating energy input.

The success of the standard experimental procedures in eliminating the condensation of undesirable tar and/or soot on the cold trap was shown by a two-part test run designed to burn each of two batches of coal continuously under the same experimental conditions. This test run was also designed to test the capability of obtaining reproducible experimental conditions for the two batches by controlling the operational characteristics. This is a necessary capability because two or more batches of coal have to be burned under the same experimental conditions in order to collect enough condensates on the cold trap for analysis.

In each part of this test run, 50 g of -20 +40 mesh Herrin No. 6 coal from Montgomery County, Illinois, was burned. Neither the hot filter nor the cold trap was removed from the combustor during loading of the second batch of coal. The analyses of effluent gas compositions and the coal bed temperature for the entire course of the experiment are shown in Fig. 33 (batch 1) and Fig. 34 (batch 2). The experimental controls used for the two batches differed: a preheated inlet gas mixture was used in the batch 2 experiment but not in the batch 1 experiment, and the afterburning air was shut off earlier in the batch 2 experiment than in the batch 1 experiment. As shown in both figures, the first peak in the CO_2 concentration curve was a result of the sudden increase in flow rate caused by introduction of the inlet gas mixture. The second sharp peak in CO_2 curve (which ran over-scale on the graph) and the corresponding sharp drop in the O_2 curve showed that the volatile matter evolved during this stage burned rapidly. No carbon monoxide was detected, indicating that volatile matter was combusted completely. This rapid combustion of volatile matter also resulted in a rapid rise of the coal bed temperature. The bed temperature was controlled stably at 855°C (on the average) for both batches. The effluent gas compositions for both batches were also observed to be nearly identical, indicating that the rate of combustion of coal was the same for both batches.

This test run has demonstrated the capability of controlling the burning of coal under a single set of experimental conditions in this combustor system. The cold trap was stably controlled at 150°C in this test run. It was dry and completely free of tar and/or soot. Similarly to what was reported in the previous report of this series, significant amounts of bluish-green condensates mixed with a yellow substance were collected on the cold trap. By X-ray diffraction techniques, the bluish-green condensate was identified as ferrous sulfate. It is believed to be a corrosion product formed by attack on the stainless steel cold trap by sulfuric acid condensed on it. The yellow substance was identified as ferric sulfate. It is believed to have formed by the oxidation of ferrous sulfate by oxidizing flue gas.

Under experimental conditions similar to those mentioned above, another series of experiments (SL-1 series) has been carried out to burn the same Herrin No. 6 seam coal from Montgomery County, Illinois. The proximate analysis on a dry basis of this coal is 38.22% volatile matter, 45.13% fixed carbon, and 16.54% ash. It is a high-volatile bituminous B coal with 3.68% S, 0.18±0.01% Na, and about 0.1% Cl^{10} on a dry basis. In this series of experiments, five batches of -20 +40 mesh coal, impregnated with 0.5 wt % NaCl using water solution, were burned at the same experimental conditions. The NaCl was added to increase the chlorine content in the coal to about 0.4% and

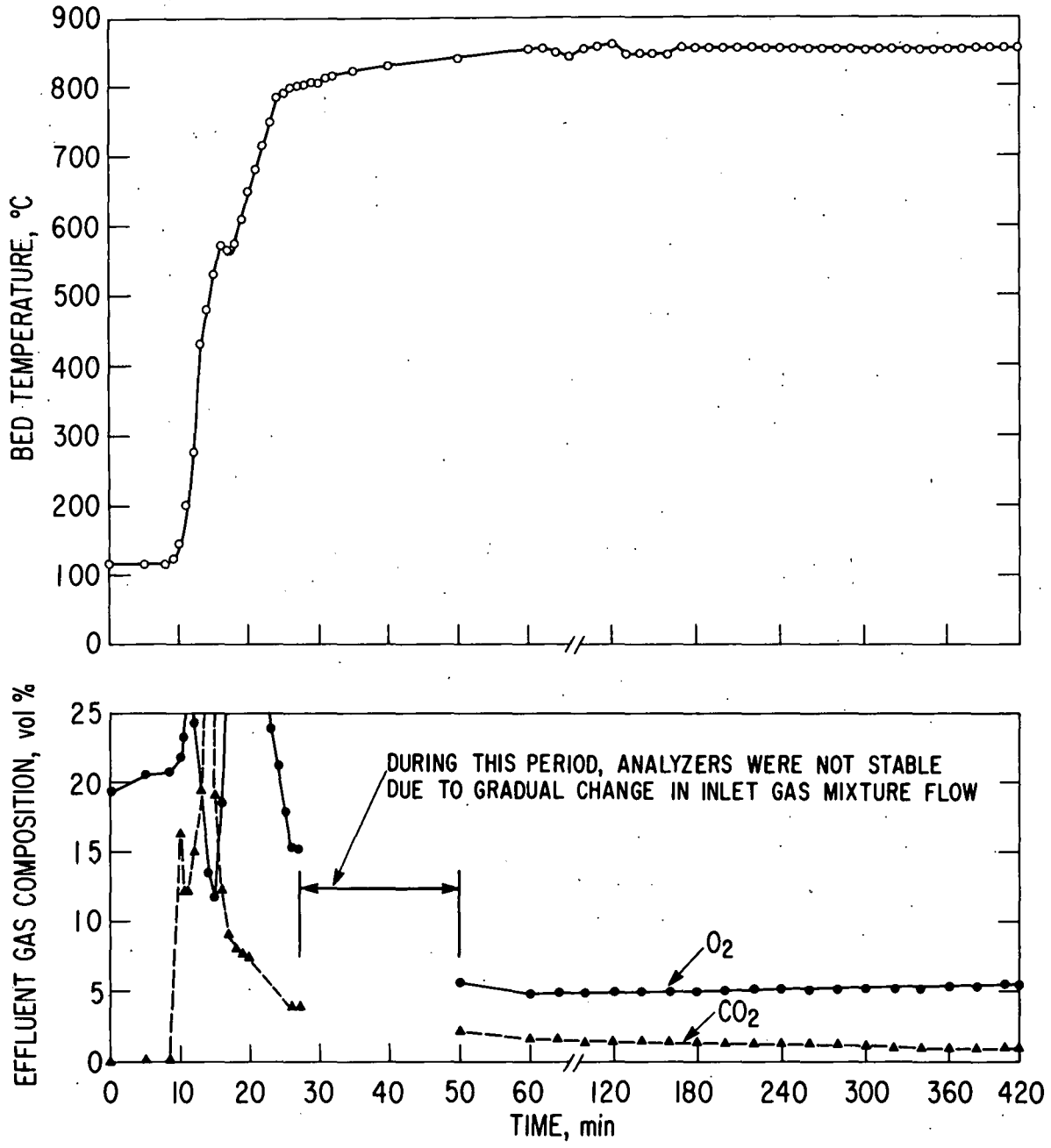

Fig. 33. Bed Temperature and Effluent Composition in a Typical Continuous Two-Batch Coal Combustion Experiment. Batch No. 1.

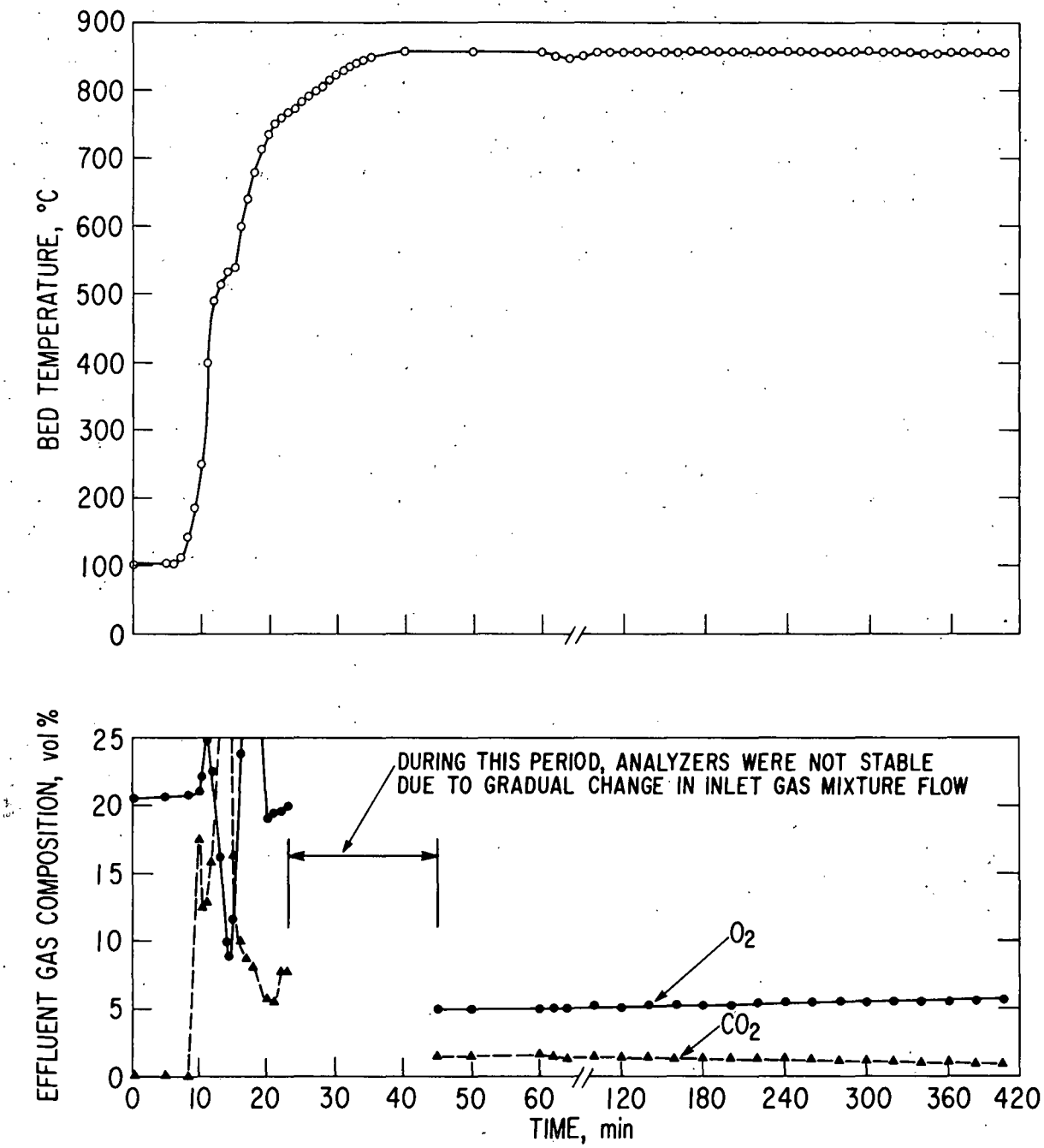

Fig. 34. Bed Temperature and Effluent Composition in a Typical Continuous Two-Batch Coal Combustion Experiment. Batch No. 2.

simulate high-chlorine coal. The chlorine content of coal has been found to be related to its fouling and corrosive effects on the fire-side of a boiler furnace. Data has been obtained showing that the rate of deposition in boiler furnaces does not become significant until the chlorine content exceeds about 0.3%;[11] therefore, the purpose of this series of experiments is to examine the transport of alkali metals and trace elements when a high-chlorine coal is burned. The choice of NaCl instead of other chlorine compounds to increase the chlorine content of the coal to the desired concentration is based on a general agreement that chlorine in coal is largely present as a chloride, especially as a sodium chloride.[10] The NaCl used was 99.5% purity A.C.S. reagent.

The effluent gas compositions for a typical batch run of this series of experiments are shown in Fig. 35. In this figure, zero time was the time when the inlet combustion mixture of O_2 and N_2 was introduced into the combustor. During the first 15 min, the inlet combustion mixture (containing 65% O_2) was used to facilitate rapid burning of the coal. The peaks noticed for this stage indicate the rapid burning of the volatile matter evolved during this early stage of the experiment. Then, coal was steadily burned in a flow of 8% O_2 in N_2 mixture. The flow rate was 6.0 liters/min. The ordinates in Fig. 35 apply only to the steady combustion stage. As shown in Fig. 35, no carbon monoxide was detected in the effluent gas, indicating that the coal was completely combusted. The SO_2 concentration was less than 100 ppm, as determined using gas chromatography equipped with a flame photometric detector. The bed temperature was steadily controlled at 850°C. The system pressure was 1 psig. In all, 215 g of coal was burned in this series of experiments.

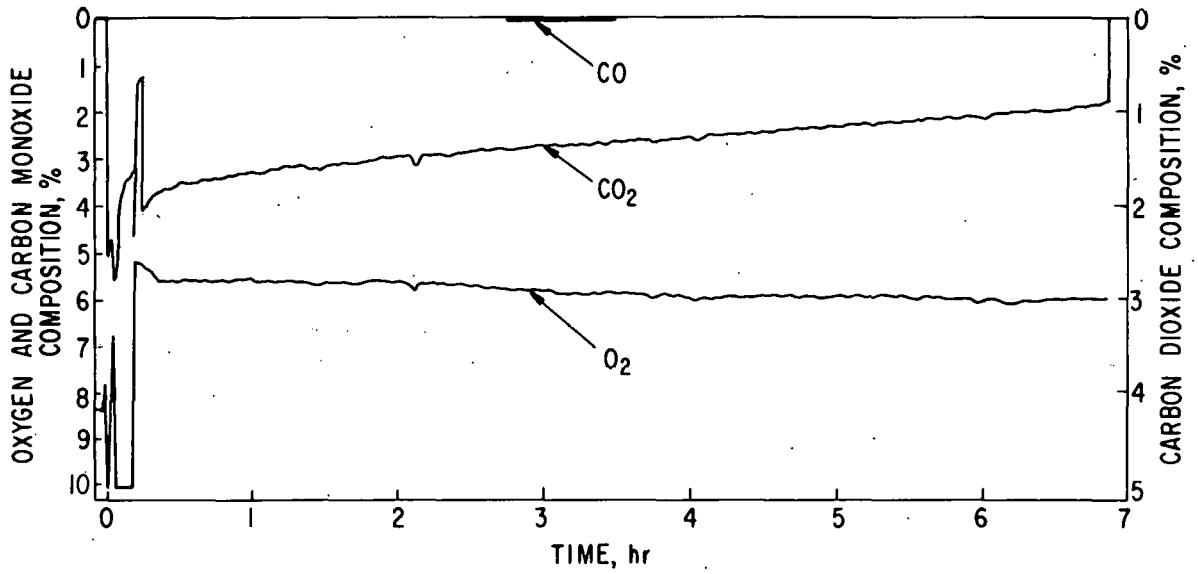

Fig. 35. Effluent Gas Compositions for a Typical Batch Run of the SL-1 Series of Experiments.

The cold trap and the Al_2O_3 filter were not removed until all five batches of coal had been burned. The cold trap used had been electroplated with a very thin layer of rhodium metal (about 0.00005 in.). No thicker layer was possible because, without special treatment, stress cracking would occur in an electroplated layer thicker than 0.00005 in. The choice of rhodium (instead of platinum) is based on its inertness (as compared with platinum) in corrosive environments, lower price, hardness (three times harder than platinum at room temperature), and its technical availability for electroplating.

Substantial amounts of bluish and light-yellow deposits were again collected on the cold trap. This was because the rhodium metal had peeled off the surface of the cold trap, so that again sulfuric acid attacked the cold trap. X-ray diffraction analysis of the deposits indicated the existence of pure nickel and Rh-Ni alloy containing 19% Ni. (Nickel was the base metal electroplated on the stainless steel surface of the cold trap before the rhodium metal was electroplated.) No NaCl or other alkali compounds were detected, either in the deposits collected on the cold trap or on the Al_2O_3 filter. Possibly, those compounds were not completely absent, for example, no detectable spectra pattern can be obtained if the quantity of a compound in the deposits is less than the detection limit of the X-ray diffraction technique (of the order of 10% of the sample).

To obtain quantitative information on sodium transport during combustion, the cold trap was carefully rinsed with distilled water to collect all deposits on the surface for analysis. The Al_2O_3 filter was leached, first with distilled water, and then with 5% HCl solution at a gentle boiling temperature for two hours. Both leaching solutions were collected for analysis. Before it was used in the combustor, this Al_2O_3 filter had been new and had been first treated as described above for 15 hr to remove both water- and acid-soluble salts, and then it had been heated in a muffle furnace at 900°C in an air flow to completely remove the absorbed HCl. The combustion residues left in the combustion boat after each experiment were also collected for analysis.

Table 13 shows the material balance for sodium element collected on the Al_2O_3 filter, collected on the cold trap, and retained in the ash bed. All analyses were made by atomic absorption.

It may be seen in Table 13 that the total sodium in the "output" is about 5% greater than that in the "input". The analytical error of the atomic absorption for the sodium determination is about $\pm$5%. It should be noted that sodium is an element that can be present everywhere during experimental handlings; therefore, the agreement in the material balance shown in Table 13 is within the experimental and analytical errors. Table 13 shows that the sodium is essentially retained in the ash bed, especially in compound forms that are not soluble in water. The reactions that cause NaCl to be retained in the ash may be very complicated. Possible chemical reactions are those in which NaCl, silica, and metal oxides (such as CaO, Al_2O_3, or Fe_2O_3) react to form end products with high melting points. Examples of these products are devitrite ($Na_2O \cdot 3CaO \cdot 6SiO_2$), Acmite ($Na_2O \cdot Fe_2O_3 \cdot 4SiO_2$), and sodium

Table 13. Material Balance of Sodium from Combustion of Illinois Herrin No. 6 Coal Impregnated with 0.5 wt % NaCl. Combustion was at 850°C and Atmospheric Pressure.

Input		mg
Na in Coal		450.00
Na added as NaCl		491.75
	Total	941.75
Output		
Na Condensed on Cold Trap		0.18
Na Captured by Al_2O_3 Filter		
(a) Water Leaching Solution		0.30
(b) Acid Leaching Solution		1.90
Na Left in the Combustion Residue		
(a) Water Leaching Solution		139.47
(b) Solid Residue after Leaching		848.79
	Total	990.64

aluminum silicates ($Na_2O \cdot Al_2O_3 \cdot 2SiO_2$). Some of the reactions involved are:

$$2\ NaCl + S + 1\ 1/2\ O_2 + H_2O \rightarrow Na_2SO_4 + 2\ HCl$$

$$Na_2SO_4 + 3\ SiO_2 \rightarrow Na_2O \cdot 3SiO_2 + SO_2 + 1/2\ O_2$$

$$2\ NaCl + 3\ SiO_2 + H_2O \rightarrow Na_2O \cdot 3SiO_2 + 2\ HCl$$

$$Na_2O \cdot 3SiO_2 + 3SiO_2 + 3\ CaO \rightarrow Na_2O \cdot 3CaO \cdot 6SiO_2$$

$$Na_2O \cdot 3SiO_2 + Fe_2O_3 + SiO_2 \rightarrow Na_2O \cdot Fe_2O_3 \cdot 4SiO_2$$

$$Na_2O \cdot 3SiO_2 + Al_2O_3 \rightarrow Na_2O \cdot Al_2O_3 \cdot 2SiO_2 + SiO_2$$

$$2\ NaCl + H_2O + Al_2O_3 \cdot 2SiO_2 \rightarrow Na_2O \cdot Al_2O_3 \cdot 2SiO_2 + 2\ HCl$$

Mineral matter in coal is the source of silica and metal oxides for all these reactions.

Table 13 also shows that only trace quantities of sodium were volatilized and transported downstream at the experimental conditions (1 psig system pressure and 850°C combustion temperature). The quantity of sodium captured by the Al_2O_3 filter, which had a nominal pore size of 10 μm, was observed to be more than ten times that captured on the cold trap, and most of the sodium retained on the Al_2O_3 filter was present in a form that was not soluble in

water. Further investigation will be conducted to obtain a better understanding of this data.

Sodium chloride has a significant vapor pressure at 850°C (1.55 mm Hg[12]). Significant amounts of NaCl would be expected to vaporize, if silica and metal oxides are not available or in inadequate quantity to fix NaCl by the reactions shown above. This appeared to be the case when a mixture of NaCl and coconut charcoal was combusted. A mixture of 20 g of 8 to 12 mesh activated charcoal and 1 g NaCl has been burned under the same experimental conditions as those of the SL-1 series. At the end of the experiment, substantial amounts of NaCl (which was identified by X-ray diffraction)* were collected on the cold trap, indicating that NaCl had vaporized at the experimental conditions and was condensed on the cold trap. Since the charcoal has low sulfur (0.4%) and ash (1.3%) contents for retaining the NaCl in the bed, NaCl vaporizes, as would be expected on the basis of its vapor pressure.

In the experiment with activated charcoal, the combustor pipe for the combustion and filtration sections was maintained at 800°C throughout the experiment. The purpose was to keep NaCl vapor from condensing on the pipe before it reached the cold trap. At the end of this experiment, all stainless steel sheaths of the thermocouples exposed to hot flue gases were noticed to be severely corroded, and substantial amounts of black scale had spalled off the combustion and filtration sections. These phenomena had not been observed when charcoal alone or coal was burned under similar experimental conditions. Apparently, the severe corrosion observed in this experiment resulted from attack of the NaCl vapor on the metal surfaces of the thermocouple sheaths and the combustor pipe. The corrosive property of NaCl vapor has also been reported in the technical literature.[13-15] Alexander[15] proposed that NaCl destroys the normally protective chromium-iron spinel oxide layer by the reaction:

$$24\ NaCl + 10\ Cr_2O_3 + 9\ O_2 \rightarrow 12\ Na_2CrO_4 + 8\ CrCl_3$$

In a fluidized-bed coal combustion system, the addition of a small amount of NaCl to the bed has been shown to improve the SO_2 absorption characteristics of limestones.[8] However, the experimental results reported above show that the use of NaCl may also dangerously increase the potential of the flue gases to corrode the metal surfaces of the components located downstream from the combustion system. The mechanism to explain the beneficial effect of NaCl on SO_2 absorption by the sorbent has been proposed and actively studied by John Shearer and Irving Johnson of Chemical Engineering Division, ANL (ANL/ES-CEN-1017). In our combustor system, the corrosive potential of NaCl in the presence of sorbent (limestone and/or dolomites) in coal combustion systems can be examined along with other work in this program.

Studies will be continued to evaluate the effect of operating variables on the evolution of inorganic species from the combustion of coal in the presence and absence of additives (limestones or dolomites). Among the

*Work done by B. Tani.

operating variables are combustion temperature, coal rank, ratio of coal to additive, and type of additives.

TASK F. FLUE-GAS CLEANING STUDIES

Specific objectives of the flue-gas cleaning study are to (1) evaluate methods for removing 2-10 μm particulate solids from the flue gas, (2) evaluate instruments for measuring sizes and numbers of particles in the gas, and (3) estimate concentrations and nature of alkali compounds in the gas. Information on instrument tests and program planning for particulate removal studies are presented. Information on the last item is being obtained.

Evaluation of On-Line Light-Scattering Particle Analyzers

In the development of fluidized-bed combustion systems, specifically in the pressurized system, a continuous on-line particle analyzer for the flue gas would be very useful (1) for measuring the efficiency of particulate-removing devices (cyclones and filters), (2) for evaluating particulate gas-loading characteristics and to establish corresponding gas turbine life performance, and (3) eventually to protect turbines in an industrial process. In a pressurized FBC system, the flue gas will be at ∿900°C and ∿1100 kPa (∿10 atm) between the boiler and the gas turbine. Without an on-line particle analyzer, mechanical sampling from the hot flue gas will be necessary on a routine basis, both during development of the process and afterward. Mechanical sampling from a pressurized hot-flue-gas environment is difficult, and it does not provide instant results. The time lag between sampling and analysis of samples is a major disadvantage.

Two on-line light-scattering particle analyzers (PA) will be evaluated in the ANL fluidized-bed combustion system under ERDA sponsorship. Both instruments use a laser light source. The first particle analyzer, which is presently being evaluated, is produced by Spectron Development Laboratories. The other particle analyzer, produced by Leeds and Northrup, will be evaluated within the next few months.

The flue gas system in the ANL fluidized bed combustion system has been modified for these evaluations, as shown in Fig. 36. Windows have been installed in two locations, one pair upstream from the primary cyclone. The other pair of windows has been installed near the system's outlet where flue gas from either upstream or downstream from the metal filters can be routed. With this arrangement, the coarse, entrained particles from the combustor, the smaller particles escaping the two cyclones, and the smallest particles leaving the metal filters (representative of particles that might enter turbines) will be sized. Downstream from each window location, sampling ports have been installed to allow parallel particle size analysis of representative samples with cascade impactors and a Coulter counter. Also, steady state particle samples will be obtained from the cyclones and test filter. These samples will be sized by sieve and Coulter counter analysis. The results obtained by the different independent techniques will be compared, and the performance of the light-scattering particle analyzers will be evaluated.

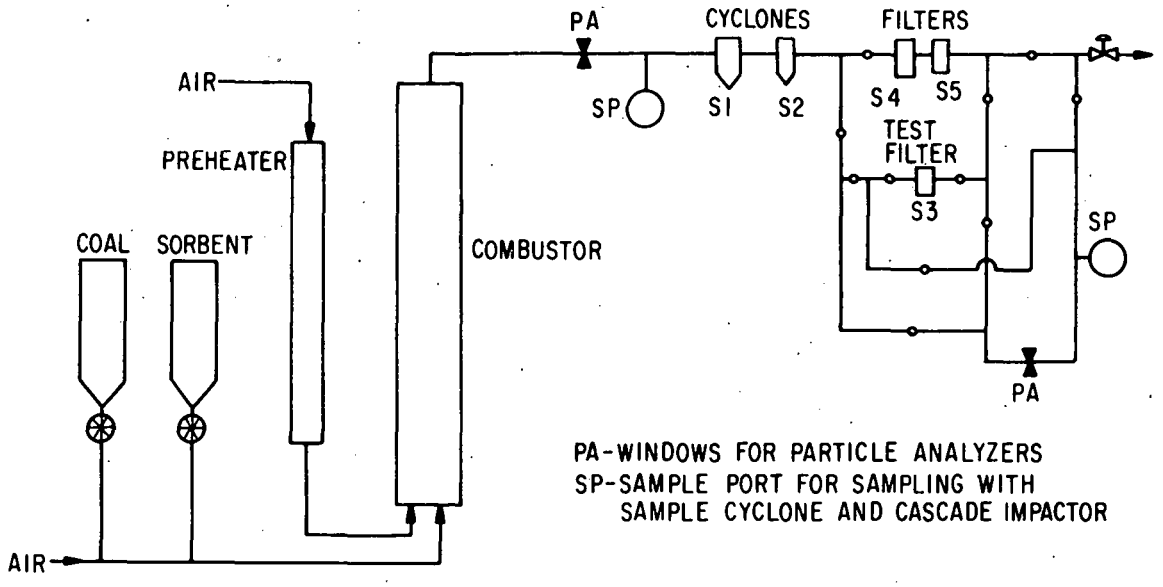

Fig. 36. Schematic of FBC System with Modified Flue-Gas System.

Particle Filtration

In pressurized fluidized-bed combustion, the hot flue gas from the combustor must be expanded through a gas turbine. It has been estimated that particulate solids in the flue gas (fly ash plus entrained sorbent) larger than about 2 μm in diameter would cause erosion of the turbine blade metal. Existing devices adaptable to high-temperature particulate removal (*e.g.*, conventional cyclones) are not very efficient below about 10 μm. Therefore, highly efficient methods need to be developed for removing from high-temperature flue gas particulate solids having diameters between 2 and 10 μm.

Work is being initiated at ANL to test and evaluate promising flue-gas cleaning methods for the off-gas system of the ANL, 6-in.-dia fluidized-bed combustor. The two methods currently being considered for testing are sonic agglomeration and granular-bed technology.

Granular bed collectors currently under active development can be generally classified as fixed-bed, moving-bed, and fluidized-bed devices. Our plans are to investigate the use of limestone or dolomite as the granular bed material for a fixed-bed and possibly a moving-bed type filtering device. Initially, tests will be done using a fixed-bed device. It the results obtained with the fixed bed are satisfactory, further testing would be done with a moving-bed filter. Design of the fixed-bed test filter is under way. Testing should begin early next quarter.

The second promising flue-gas cleaning method proposed for testing is sonic agglomeration. The general objective of this agglomerating technique

is to enhance the natural tendency of polydisperse particulate to impact upon each other. The acoustic conditioning of fine-particle emissions is a process by which the mean size of the effluent particulates is increased (and their number is decreased) by exposure to finite amplitude acoustical fields. Evaluations are being made to determine the proper acoustic field configuration for testing on the ANL, FBC system. Considerations include the selection of the acoustic field generator (progressive saw-tooth *vs* standing wave), the frequency range and intensity range of the acoustical wave form, and the appropriate physical location in the off-gas system (*i.e.*, upstream from the primary cyclone, the secondary cyclone, or the filter device). There are plans to visit other laboratories currently investigating applications of sonic agglomeration. These visits are expected to provide the necessary background for arriving at the proper test conditions for the ANL experimental program.

REFERENCES

1. M. J. Gluckman, J. Yerushalim, and A. M. Squires, "Defluidization Characteristics of Sticky or Agglomerating Beds," Proceedings of the International Fluidization Conference, Pacific Grove, California, June 15-20, 1975.

2. M. Hartman and R. W. Coughlin, "Reactions of Sulfur Dioxide with Limestone and the Influence of Pore Structure," Ind. Eng. Chem. 13(3), 248 (1974).

3. G. J. Vogel *et al.*, "Reduction of Atmospheric Pollution by the Application of Fluidized-Bed Combustion and Regeneration of Sulfur-Containing Additives," Annual Report, July 1, 1973 - June 30, 1974, Argonne National Laboratory Report No. ANL/ES-CEN-1007 (1975).

4. W. Zielke *et al.*, "Sulfur Removal during Combustion of Solid Fuels in a Fluidized Bed of Dolomite," J. Air Pollution Control Assoc. 20(3), 164-169 (1970).

5. G. A. Hammond and A. Skopp, "A Regeneration Limestone Process for Fluidized Bed Coal Combustion and Desulfurization," Final Report, Esso Research and Engineering Co., Gov. Res. Div., Linden, NJ (Feb. 1971).

6. M. F. Nagier, "The Theory of Recycle Processing in Chemical Engineering," Vol. 3, International Series of Monographs on Chemical Engineering, MacMillan, New York (1964).

7. D. L. Keairns *et al.*, "Fluidized Bed Combustion Process Evaluation, Phase II, Pressurized Fluidized Bed Coal Combustion Development," EPA-650/2-75-027-C, Prepared for USEPA by Westinghouse Research Laboratories, Pittsburgh, Penn. (September 1975).

8. Pope, Evans and Robbins, Inc., "Multicell Fluidized-Bed Boiler Design, Construction, and Test Program," Combustion Systems Division, Monthly Progress Status Report, No. 39, December, 1975.

9. Edward Bagdoyan, Kennedy Van Saun Corp., private communication, October 1976.

10. H. J. Gluskoter and O. W. Rees, "Chlorine in Illinois Coal," Circular 372, Illinois State Gelogical Survey, Urbana, Illinois, 1964.

11. W. T. Reid, *External Corrosion and Deposits - Boiler and Gas Turbines*, American Elsevier Publishing Company, N.Y., p. 140, 1971.

12. N. J. H. Small, H. Strawson, and A. Lewis, "Recent Advances in the Chemistry of Fuel Oil Ash," Proceedings of the Conference on Mechanism of Corrosion by Fuel Impurities, Butterworths, Scientific publications, London, p. 240, 1963.

13. P. D. Miller, H. H. Krause, J. Zupan, and W. K. Boyd, "Corrosive Effects of Various Salt Mixtures under Combustion Gas Atmospheres," Corrosion 28 (6), 222 (1972).

14. A. J. B. Cutler, W. D. Halstead, J. W. Laxton, and C. G. Stevens, "The Role of Chloride in the Corrosion Caused by Flue Gases and Their Deposits," Trans. ASME, J. Eng. Power 93, 37 (1971).

15. P. A. Alexander, "Laboratory Studies of the Effects of Sulfates and Chlorides on the Oxidation of Superheater Alloys," Proceedings of the Conference on Mechanism of Corrosion by Fuel Impurities, Butterworths, Scientific Publications, London, paper 40, p. 571, 1963.

APPENDIX A

SULFUR DIOXIDE REMOVAL FROM FLUIDIZED BED COMBUSTORS (The DOW Chemical Co.)

THE DOW CHEMICAL COMPANY
Texas Division
CONTRACT RESEARCH
Freeport, Texas 77541

SULFUR DIOXIDE REMOVAL FROM FLUIDIZED BED COMBUSTORS

Contract No. 31-109-38-3268
ARGONNE NATIONAL LABORATORY
Argonne, Illinois 60439

R. D. Daniels
T. A. Pearce

Progress Report No. 4
covering the period
May 1, 1976 through July 31, 1976

TABLE OF CONTENTS

LIST OF FIGURES

SUMMARY:

Experimental sulfation data were obtained for CaO, SrO, BaO, and Na_2O on TiO_2. In addition, cyclic sulfation regeneration tests were made with CaO and Na_2O on TiO_2 and CaO and Na_2O on Al_2O_3 supports. Attrition tests were conducted on Al_2O_3 and TiO_2 fluidizable granules with and without metal oxides impregnated on them. It was found that CaO strengthens Al_2O_3 and TiO_2 whereas Na_2O renders the support material less attrition resistant.

INTRODUCTION:

This program, sponsored by Argonne National Laboratory under a prime contract from the United States Energy Research and Development Administration, is concerned with a study of synthetic SO_2 sorbents for use in fluidized bed combustors. A program for screening several supported additives for SO_2 removal has been initiated. The work involves:

Preparation of the synthetic SO_2 sorbents from fluidizable "catalyst type" support materials.

Thermogravimetric analysis of the sorbents in simulated flue gas at combustion temperatures and in a regenerative mode at elevated temperatures in a reducing atmosphere.

This report presents new data on the rate of SO_2 sorption by $CaO \cdot TiO_2$, $SrO \cdot TiO_2$, $BaO \cdot TiO_2$, and $Na_2O \cdot TiO_2$. Attrition tests conducted under fluidizing conditions on several sorbents are reported as well as sulfation-regeneration TGA tests to investigate deactivation caused by cyclic operation.

EXPERIMENTAL HARDWARE AND PROCEDURE DEVELOPMENT:

The investigation of titanates for SO_2 removal, attrition testing of TiO_2 and Al_2O_3-based supports, and the use of cyclic sulfation-regeneration TGA experiments required procedure and hardware development as described below:

Cyclic Sulfation-Regeneration Experiments

The cyclic sulfation-regeneration experiments were made by modifying the TGA gas supply system to accommodate a one-liter cylinder of premixed reducing gases (1% CO, 1% CH_4, 1% H_2 in N_2) for the regeneration cycle. Regeneration in most cases was accomplished at the temperature of sulfation. The gain or loss of weight was monitored by the deflection of the quartz spring during both sulfation and regeneration.

Preparation of Titanate-Supported Sorbents

The laboratory-scale preparation of the titanate-supported metal oxides differed from the alumina support prepration method. The alumina support impregnation method involved coating particles of alumina in rinco flask-type apparatus with aqueous solutions of a metal nitrate.(1) The procedure for preparing the titanate-supported sorbents is as follows:

1. To 100 grams of powdered TiO_2 (2-micron size), add enough of the respective nitrate ($CaNO_3$, $BaNO_3$, etc.) to give the desired concentration of metal oxide on the TiO_2.

2. Add about 100 ml. of H_2O (amount not critical) and mix thoroughly.

3. Evaporate off moisture with low heat (i.e., on a hot plate).

4. Transfer slurry to crucibles; dry and calcine at 800°C for about 10 hours.

5. Grind solid particles to desired size and sieve to obtain a 20x50 mesh product.

5. Heat treat the product at 1100°C for 2 hours.

Attrition Testing Procedure

The cold test rig in Figure 1 was assembled to test the particles for attrition resistance. A standard test was developed as follows:

1. Weigh out 20 grams of sample to be tested.

2. Place particles in fluidizing tube with low flow rate of air to keep particles from falling through grid.

3. Place cyclone assembly on top of fluid bed tube.

4. Adjust air flow to desired fluidizing velocity. (A 2.0-foot-per-second fluidizing velocity produces a slugging bed and was deemed appropriate as a standard test.)

5. Weigh the particles remaining in the fluidizing tube after 24 hours of fluidizing.

6. Calculate attrition rate as percent of material lost per hour.

Figure 1

ATTRITION COLD TEST RIG

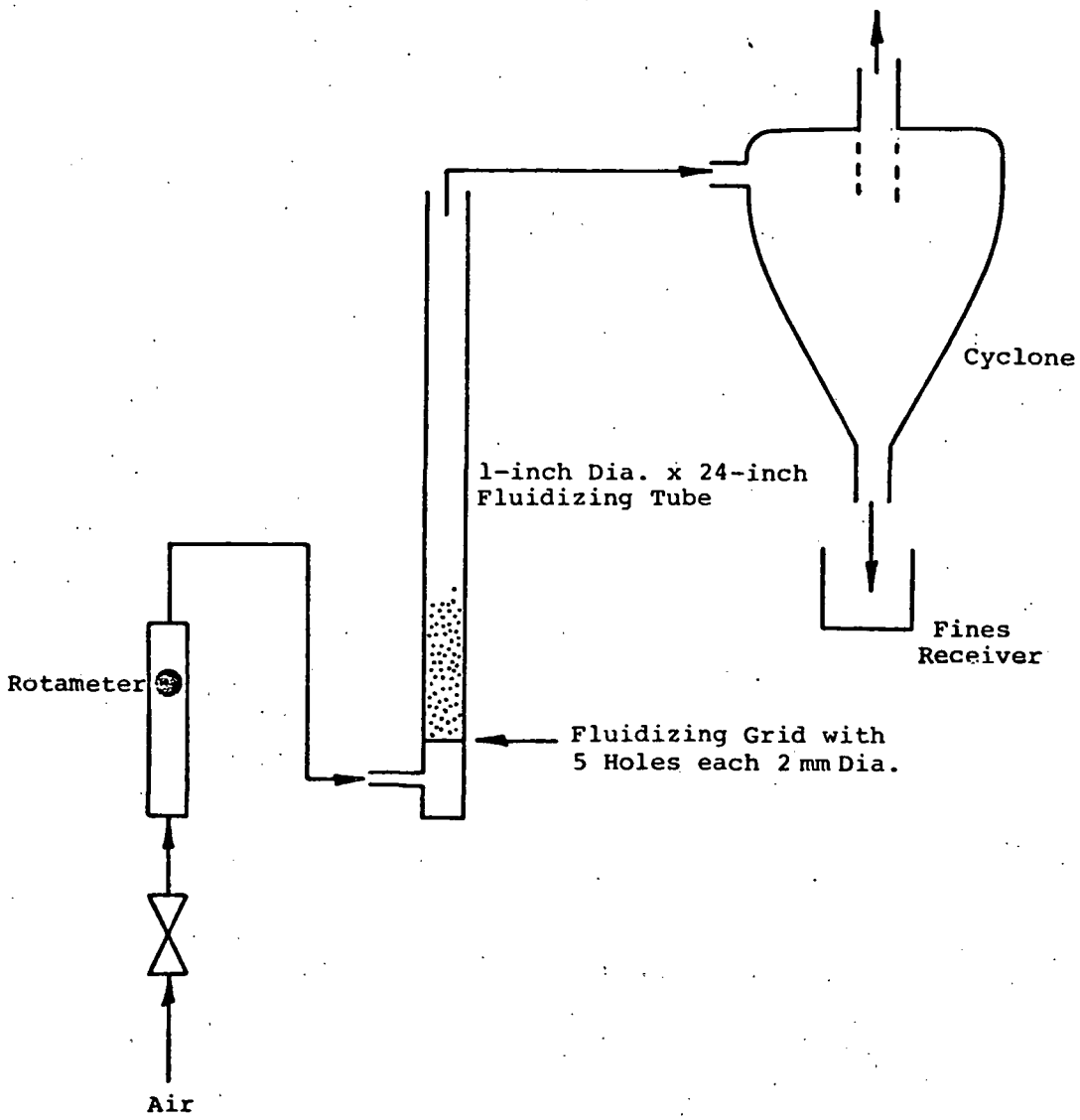

EXPERIMENTAL RESULTS:

Four titanates were tested for SO_2 sorption rate for the first time. In addition $CaO \cdot Al_2O_3$ and $Na_2O \cdot Al_2O_3$ were retested for cyclic deactivation and attrition resistance. The experimental results are as follows:

$CaO \cdot TiO_2$

Particles of $CaO \cdot TiO_2$ which were prepared as described previously were tested at 0.1%, 0.3%, and 0.5% S_2 levels as shown in Figures 2, 3, and 4, respectively. From these data, it appears that the equilibrium vapor pressure of SO_3 above the metal sulfate is great enough at 900°C to render the $CaO \cdot TiO_2$ inactive at SO_2 concentrations of about 0.3% SO_2 or less. This was somewhat unexpected because $CaO \cdot Al_2O_3$ can sorb SO_2 at temperatures over 950°C; evidently, the TiO_2 renders the CaO less available for SO_2 capture than does Al_2O_3. Attrition testing of the $CaO \cdot TiO_2$ indicated that the CaO made the titanate granules stronger. The attrition rate of the TiO_2 without CaO was found to be 0.65% per hour while for $CaO \cdot TiO_2$, the attrition rate dropped to 0.17% per hour.

$SrO \cdot TiO_2$

Particles of $SrO \cdot TiO_2$ were tested at various temperatures and SO_2 concentrations as shown in Figure 5. The predicted operating temperature range of 750°C to 920°C is supported by these data. The initial rates were found to be no faster than $SrO \cdot Al_2O_3$ which had been investigated earlier.

$BaO \cdot TiO_2$

Samples of $BaO \cdot TiO_2$ were tested at various SO_2 concentrations as shown in Figure 6. The $BaO \cdot TiO_2$ sulfated faster than the $SrO \cdot TiO_2$, the reverse of results obtained for the respective aluminates. However, the $BaO \cdot TiO_2$ was reported by Radian to be operable in the 750°-1000°C range which suggests that $BaSO_4 \cdot TiO_2$ may be more stable than $SrSO_4 \cdot TiO_2$ at temperatures around 900°C.

$Na_2O \cdot TiO_2$

As with the aluminates, $Na_2O \cdot TiO_2$ absorbs SO_3 faster than $CaO \cdot TiO_2$. Figure 7 shows the sulfation rate of $Na_2O \cdot TiO_2$ at various SO_2 concentrations. Cyclic sulfation-regeneration experiments showed that on the second and subsequent cycles, the sulfation rate was substantially greater as shown in Figure 8. However, the $Na_2O \cdot Al_2O_3$ was still faster than the titanate as shown in an analysis of the initial rates in Figure 9. An attrition test with $Na_2O \cdot TiO_2$ showed that the Na_2O caused the TiO_2 support to be less attrition resistant.

Figure 2

RATE OF SULFATION OF 20% CaO ON TiO_2
IN 0.5% SO_2 AT VARIOUS TEMPERATURES

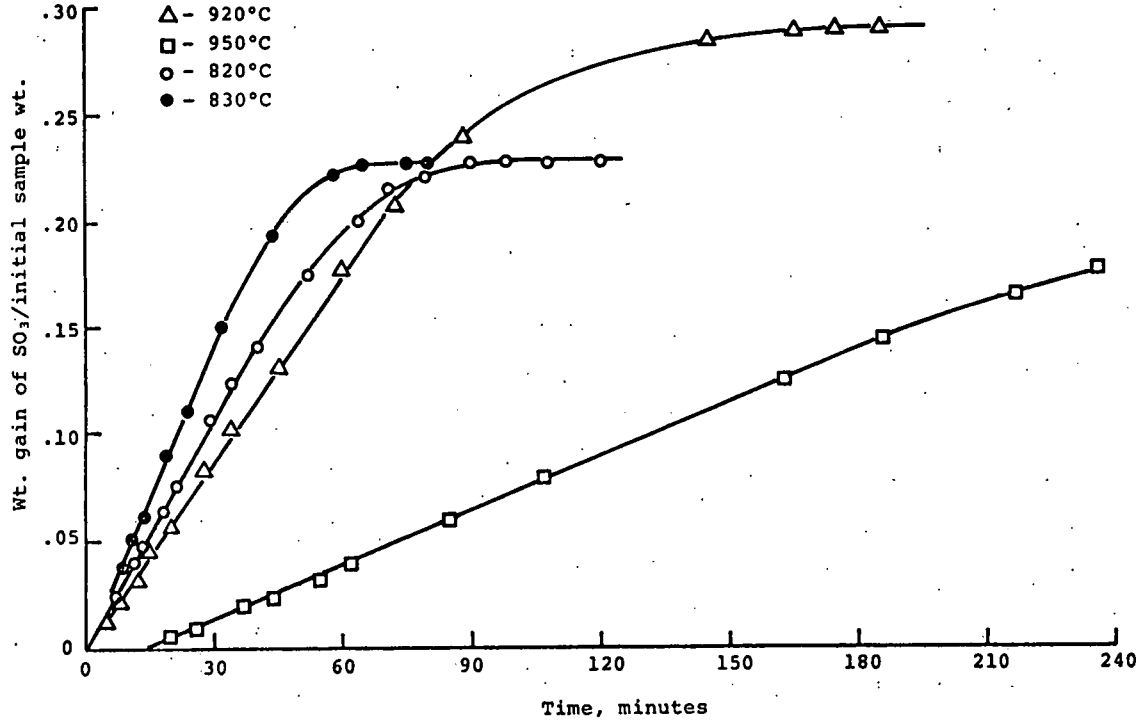

Figure 3

RATE OF SULFATION OF 20% CaO ON TiO_2
IN 0.3% SO_2 AT 810°C AND 920°C

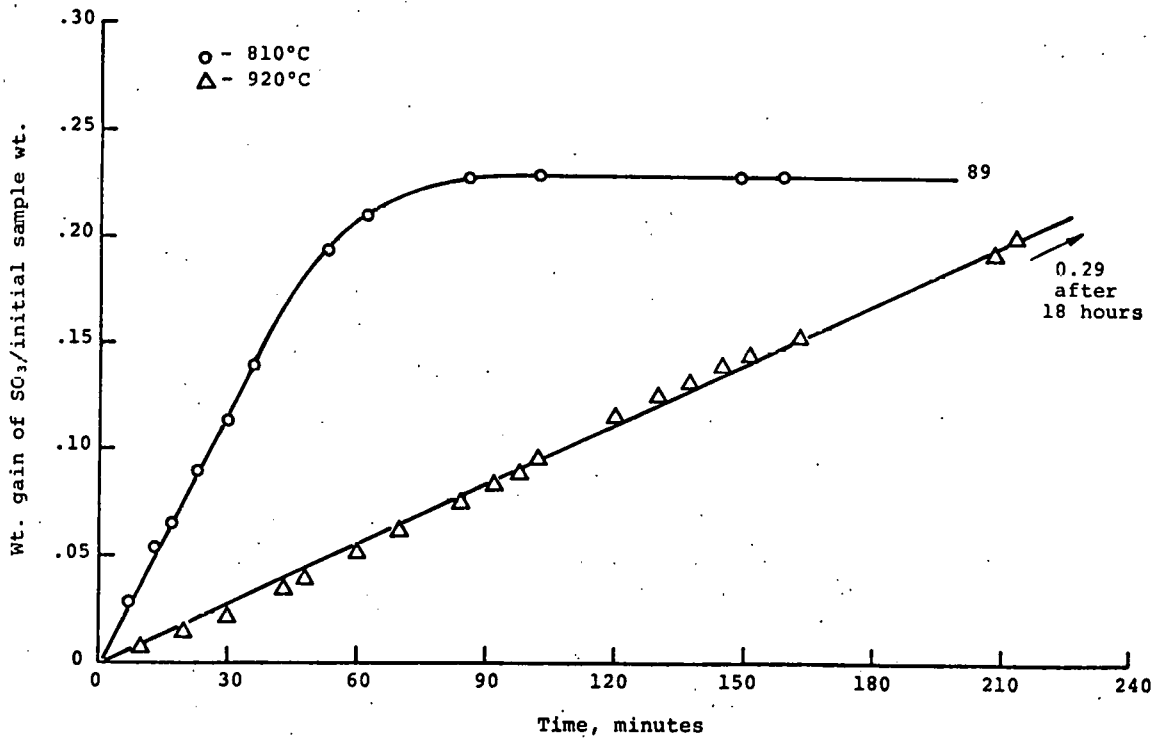

Figure 4

RATE OF SULFATION OF 20% CaO ON TiO_2
IN 0.1% SO_2 AT 840°C and 900°C

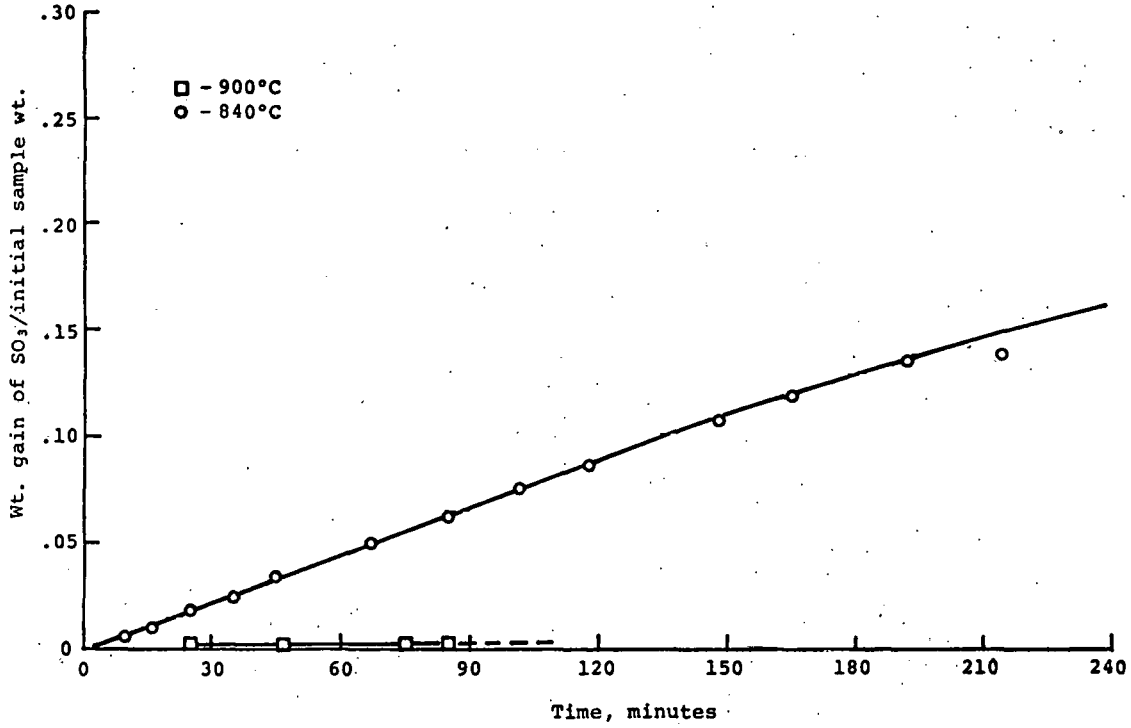

Figure 5

RATE OF SULFATION OF 20% SrO on TiO_2

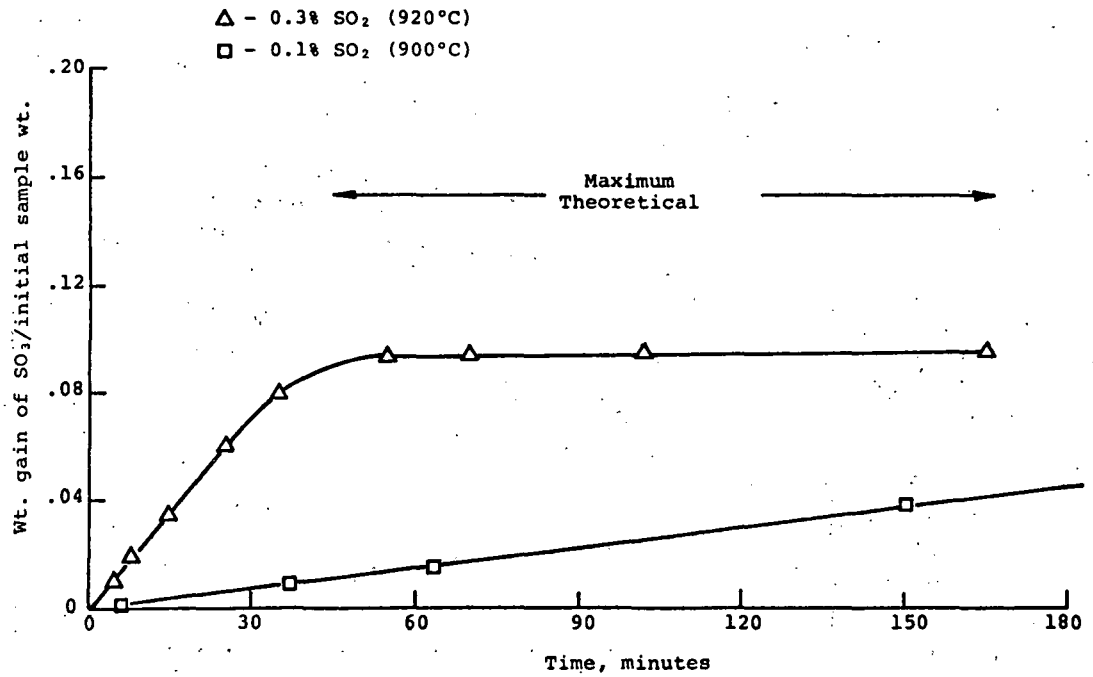

Figure 6

RATE OF SULFATION OF 20% BaO ON TiO_2

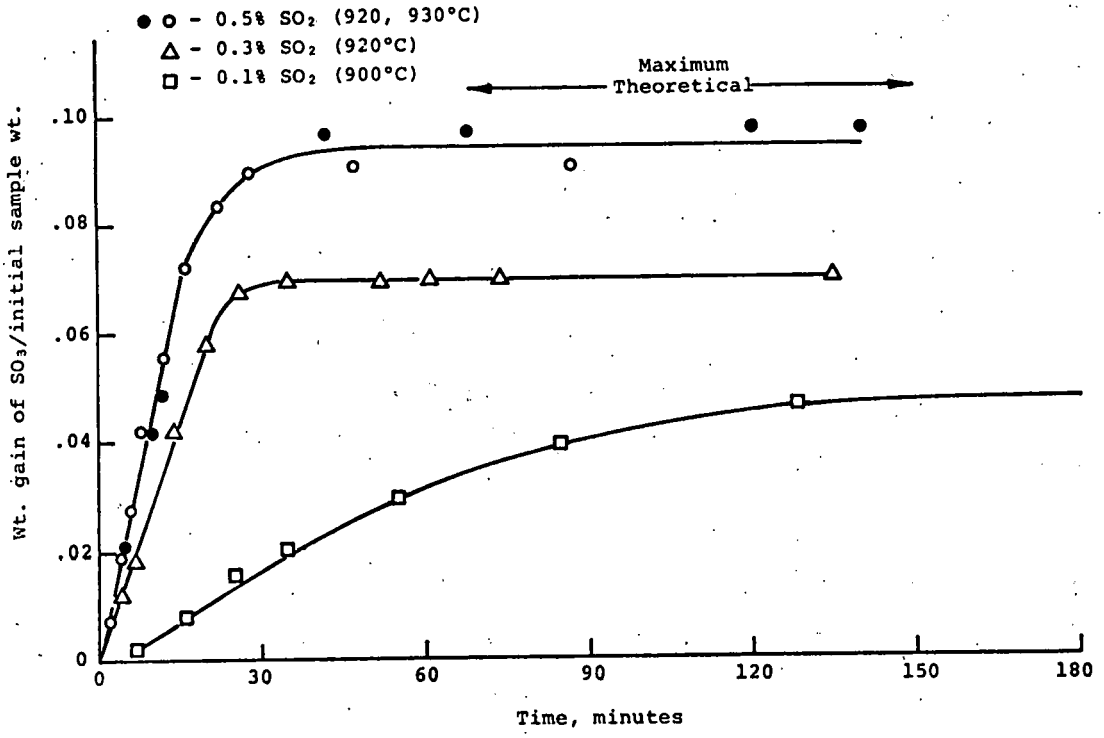

Figure 7

RATE OF SULFATION OF 20% Na_2O ON TiO_2 AT 900°C

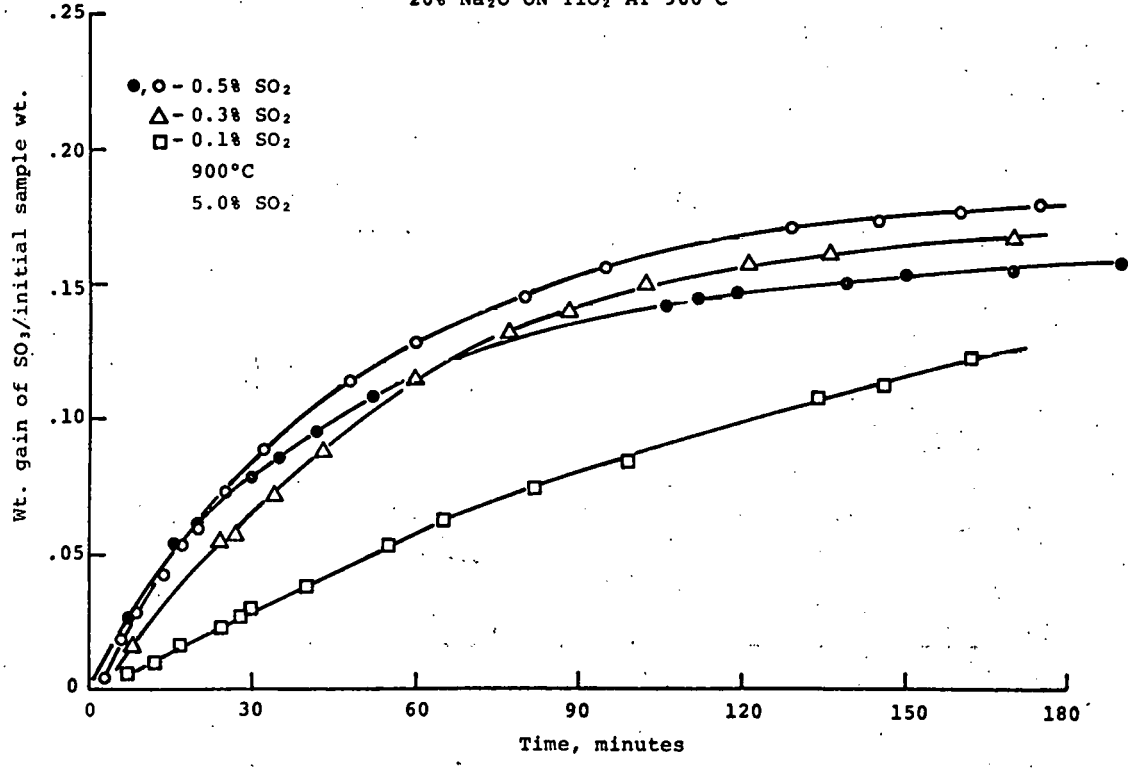

Figure 8

CYCLIC SULFATION CURVES
FOR 20% Na_2O ON TiO_2 AT 0.5% SO_2, 910°C

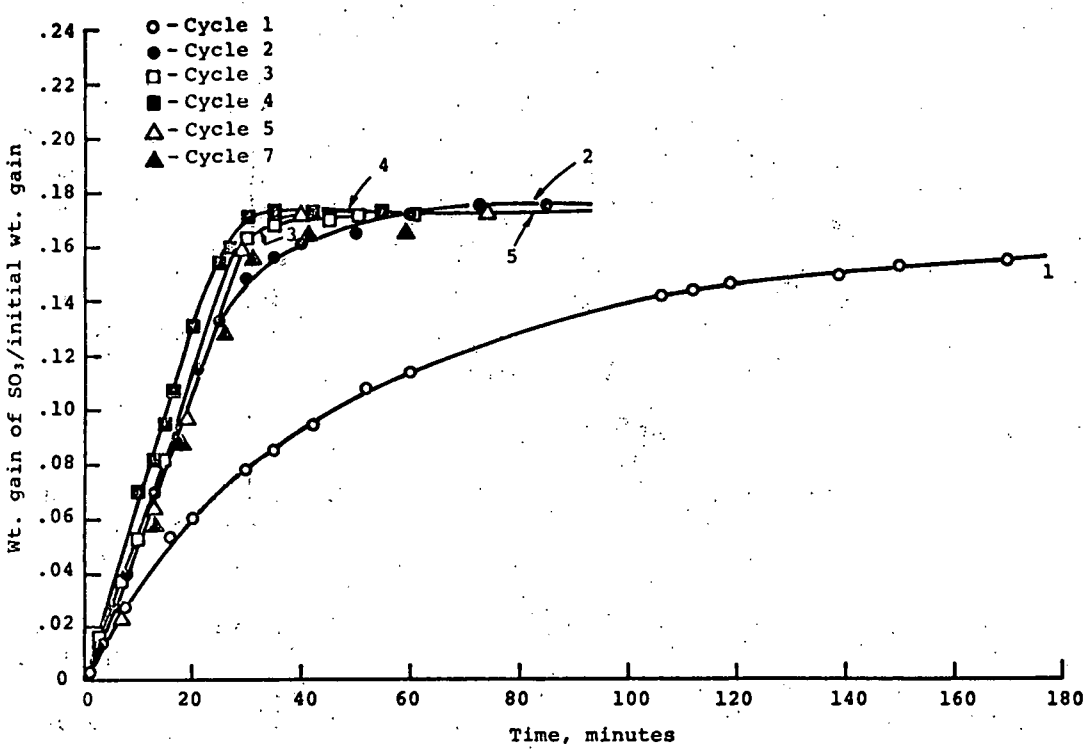

Figure 9

INITIAL SULFATION RATE VERSUS SO_2 CONCENTRATION
FOR ALUMINA AND TITANATE SUPPORTED Na_2O

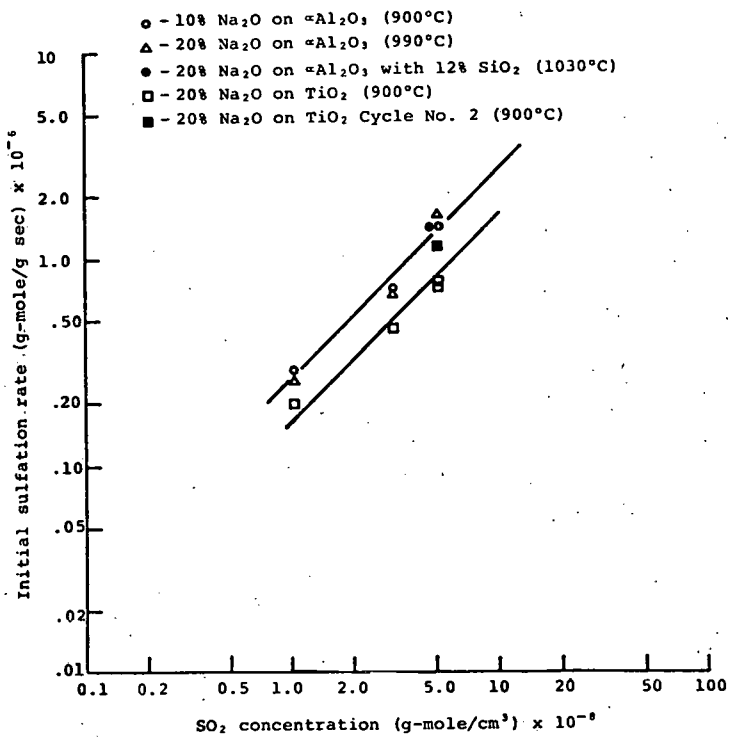

$CaO \cdot Al_2O_3$

Attrition testing of alumina with and without CaO showed that the presence of CaO on the support strengthens the particle in attrition tests. An attrition rate of 0.20% per hour was observed for a low porosity alumina with 12% SiO_2. The same support with 15% CaO and heat treated to 1100°C had an attrition rate of 0.025% per hour in identical tests of 24 hours at 2.0-feet-per-second fluidizing velocity. Cyclic test data with this particle, presented in Figure 10, show that the sulfation rate for the second cycle is faster than the first cycle. This is probably caused by additional surface area being produced during the first cycle. The loss in capacity of the particle may be attributed to silica binding of the CaO.

$Na_2O \cdot Al_2O_3$

Attrition testing of $Na_2O \cdot Al_2O_3$ showed that the presence of Na_2O on the particle rendered the particle less attrition resistant. The same alumina support described above, which contained 12% SiO_2, when impregnated with Na_2O yielded an attrition rate of 1.63% per hour. This is about eight times as fast as the same support without Na_2O. For high purity alumina, the Na_2O causes the support to crumble during preparation and handling. A cyclic sulfation-regeneration test conducted at 1030°C showed that the particle deactivated severely as shown in Figure 11. However, at a lower temperature of 895°C, this deactivation was not observed as shown in Figure 12.

Figure 10

CYCLIC SULFATION CURVES FOR CaO ON αAl_2O_3 AT 0.5% SO_2, 880°C

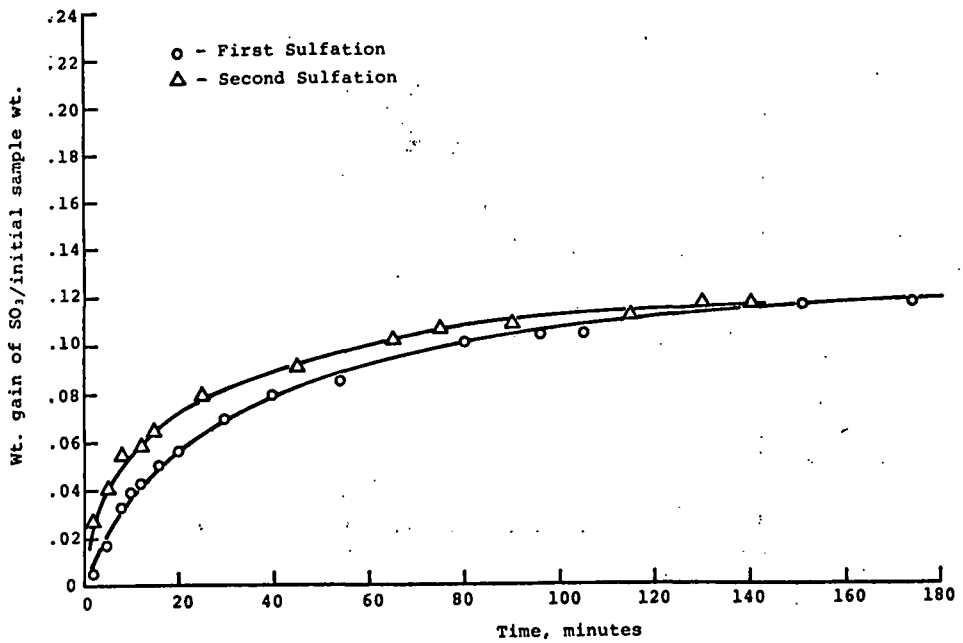

Figure 11

CYCLIC SULFATION CURVES FOR Na_2O
ON αAl_2O_3 at 0.5% SO_2, 1030°C

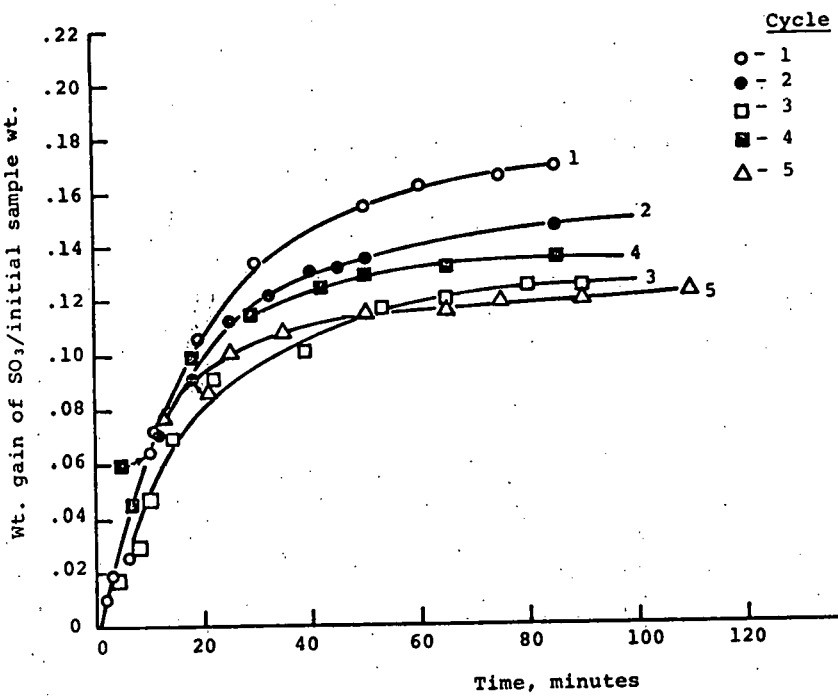

Figure 12

CYCLIC SULFATION CURVES FOR Na_2O
ON αAl_2O_3 AT 0.5% SO_2, 895°C

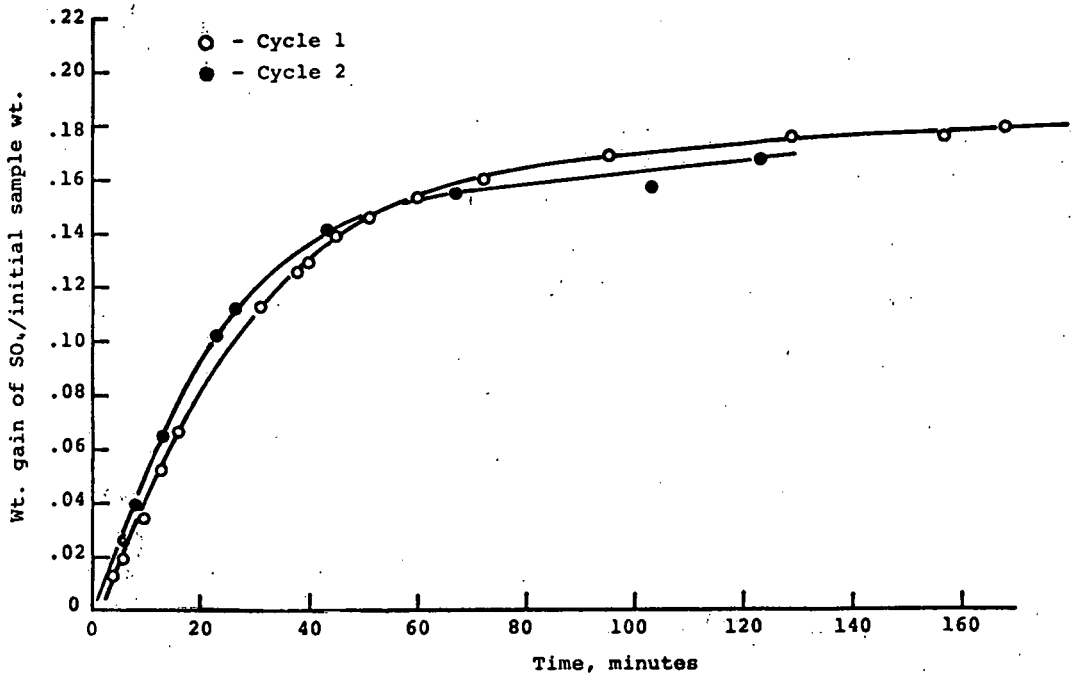

REFERENCES:

1. ANL Monthly Progress Report ANL/ES-CEN-FO85. "A Development Program on Pressurized Fluidized-Bed Combustion," November, 1975, Appendix A, page 5.

2. Lowell, Philip S., and Terry B. Parsons. Identification of Regenerable Metal Oxide SO_2 Sorbents for Fluidized Bed Coal Combustion. Radian Corporation. EPA Contract No. 68-02-1319, Task 10. p. 47 (June 1975).

Distribution of ANL/ES-CEN-1018 and FE-1780-6

Internal:

L. Burris
F. Cafasso
E. Carls
P. T. Cunningham
J. Fischer
H. Huang
B. R. Hubble
I. Johnson
A. A. Jonke
J. A. Kyger
R. V. Laney
S. Lawroski
S. H. Lee
J. F. Lenc
M. Sobczak (10)
E. G. Pewitt
R. N. Lo
J. Montagna
F. F. Nunes
W. Podolski
J. Royal
S. Siegel
J. W. Simmons
G. W. Smith
R. B. Snyder
W. M. Swift
G. F. Teats
A. D. Tevebaugh
G. J. Vogel (19)
S. Vogler
A. S. Lescarret
D. S. Webster
W. I. Wilson
J. Young
R. Bane
E. J. Croke
J. Gabor
K. Jensen
N. Sather
J. Shearer
E. Smyk
C. B. Turner
A. B. Krisciunas
ANL Contract File
ANL Libraries (5)
TIS Files (6)

External:

ERDA-TIC, for distribution per UC-90e (255)
Manager, Chicago Operations Office
Chief, Chicago Patent Group
V. H. Hummel, Chicago Operations Office
President, Argonne Universities Association
Chemical Engineering Division Review Committee:
R. C. Axtmann, Princeton Univ.
R. E. Balzhiser, Electric Power Research Institute
J. T. Banchero, Univ. Notre Dame
D. L. Douglas, Gould Inc.
P. W. Gilles, Univ. Kansas
R. I. Newman, Allied-General Nuclear Services
G. M. Rosenblatt, Pennsylvania State Univ.
S. Saxena, Univ. Illinois, Chicago
D. H. Archer, Westinghouse Research Labs.
E. C. Bailey, John Dolio and Associates
S. Beall, Oak Ridge National Laboratory
R. Bertrand, Exxon Research and Engineering (5)
R. D. Brooks, General Electric Co.
D. Clarke, Stearns-Rogers
N. Coates, The MITRE Corporation
A. L. Conn, Amoco Oil Company
G. G. Copeland, Copeland Systems, Inc.
R. C. Corey, U. S. Energy Research and Development Administration
G. Curran, Conoco Coal Development Co.
T. E. Dowdy, Babcock and Wilcox Company
S. Ehrlich, Electric Power Research Institute
M. Evans, Aerotherm Division of ACUREX Corporation
C. Fisher, Univ. Tennessee
J. F. Flagg, Universal Oil Products Co.
V. Forlenca, Englehard Industries

R. L. Gamble, Foster Wheeler Energy Corporation
D. E. Garrett, Garrett Energy Research and Engineering, Inc.
J. Geffken, U. S. Energy Research and Development Administration (5)
O. J. Hahn, Univ. Kentucky
M. J. Hargrove, Combustion Engineering, Inc.
R. D. Harvey, Illinois State Geological Survey
R. Helfenstein, Illinois State Geological Survey
G. Hill, Electric Power Research Institute
F. D. Hutchinson, Gibbs and Hill
D. L. Keairns, Westinghouse Research Laboratories
C. B. Leffert, Wayne State University
A. M. Leon, Dorr-Oliver Inc.
R. M. Lundberg, Commonwealth Edison Co.
A. Maimoni, Lawrence Livermore Laboratory
W. McCurdy, U. S. Energy Research and Development Administration
W. McGough, Jr., Tetra Tech, Inc.
J. Mesko, Pope, Evans and Robbins (2)
T. A. Milne, Midwest Research Institute
W. G. Moore, Dow Chemical, USA
S. Moskowitz, Curtiss-Wright Corporation
T. A. Pearce, Dow Chemical
W. A. Peters, Massachusetts Institute of Technology
A. F. Sarofim, Massachusetts Institute of Technology
W. K. Stair, Univ. Tennessee
W. Steen, U. S. Environmental Protection Agency (16)
M. Steinberg, Brookhaven National Laboratory
W. Strieder, Univ. Notre Dame
S. E. Tung, Massachusetts Institute of Technology
F. A. Walton, Combustion Power Co.
T. D. Wheelock, Iowa State University
R. E. Zoellner, Stearns-Rogers
J. Highley, U.K. National Coal Board, England
H. R. Hoy, BCURA Ltd., England
K. Janssen, Bergbau-Forschung GmbH, Germany
G. Moss, Esso Research Centre, England
B. A. Wiechula, Imperial Oil Enterprises, Canada